2013

Growth Plate Regeneration Using Polymer-Based Scaffolds Releasing Growth Factor

Amanda Clark

University of Kentucky, amandaclark06@gmail.com

STUDENT AGREEMENT:

I represent that my thesis or dissertation and abstract are my original work. Proper attribution has been given to all outside sources. I understand that I am solely responsible for obtaining any needed copyright permissions. I have obtained and attached hereto needed written permission statements(s) from the owner(s) of each third-party copyrighted matter to be included in my work, allowing electronic distribution (if such use is not permitted by the fair use doctrine).

I hereby grant to The University of Kentucky and its agents the non-exclusive license to archive and make accessible my work in whole or in part in all forms of media, now or hereafter known. I agree that the document mentioned above may be made available immediately for worldwide access unless a preapproved embargo applies.

I retain all other ownership rights to the copyright of my work. I also retain the right to use in future works (such as articles or books) all or part of my work. I understand that I am free to register the copyright to my work.

REVIEW, APPROVAL AND ACCEPTANCE

The document mentioned above has been reviewed and accepted by the student's advisor, on behalf of the advisory committee, and by the Director of Graduate Studies (DGS), on behalf of the program; we verify that this is the final, approved version of the student's dissertation including all changes required by the advisory committee. The undersigned agree to abide by the statements above.

Amanda Clark, Student

Dr. David Puleo, Major Professor

Dr. Abhijit R. Patwardhan, Director of Graduate Studies

GROWTH PLATE REGENERATION USING POLYMER-BASED SCAFFOLDS
RELEASING GROWTH FACTOR

_____

DISSERTATION

_____

A dissertation submitted in partial fulfillment of the
requirements for the degree of Doctor of Philosophy in the
College of Engineering
at the University of Kentucky

By
Amanda Rachel Clark

Lexington, Kentucky

Director: Dr. David Puleo, Professor of Biomedical Engineering

Lexington, Kentucky

2013

ABSTRACT OF DISSERTATION

GROWTH PLATE REGENERATION USING POLYMER- BASED SCAFFOLDS
RELEASING GROWTH FACTOR

Currently growth plate fractures account for nearly 18.5% of fractures in children and can lead to stunted bone growth or angular deformation. If the body is unable to heal itself a bony bar forms, preventing normal bone growth. Clinical treatment involves removing the bony bar and replacing it with a filler substance, which causes poor results 60% of the time.

Using primarily poly(lactic-co-glycolic acid) (PLGA) as the scaffold material, the goal was to develop an implant that would support to the implant site, allow for cell ingrowth, and degrade away over time. Porous scaffolds were fabricated from PLGA microspheres using the salt leaching method. The first part of this work investigated the effect of sintering the microspheres by studying the mechanical properties, degradation and morphology and their potential applications for hard and soft tissue implants. Growth factor or drugs can be encapsulated into PLGA microspheres, which was the second part of this work. Encapsulated insulin-like growth factor I (IGF-I) was able to withstand the scaffold fabrication process without compromising it's bioactivity and promoted cell proliferation.

The next part of this work experimented with the addition of a hydrogel porogen. Porogen particles were made using a quick degrading poly(beta-amino ester) (PBAE) hydrogel and loaded with ketoprofen. The addition of the porogen creates a dual drug-releasing scaffold with a localized delivery system.

The final step of this work involved animal studies to determine the effectiveness of the scaffolds in growth plate regeneration and how they compare to the current clinical treatment option. Gross observation, microCT analysis, angular measurement of bone growth and histological methods were employed to evaluate the scaffolds.

The goal was to develop a versatile scaffold that could be used for a wide range of tissue engineering applications. The mechanical properties, degradation profiles and drug delivery capabilities can be all tailored to meet the specific needs of an implant site. One specific application was regenerating the native growth plate that can also encourage the endogenous mesenchymal stem cells to follow the desire linage. By regenerating the native growth plate, angular deformation and stunted limb growth were greatly reduced.

KEYWORDS: Biodegradable polymers, biodegradable hydrogels, tissue engineering scaffolds, growth plate regeneration, controlled drug delivery

Amanda Rachel Clark

Student's Signature

December 1, 2013

Date

GROWTH PLATE REGENERATION USING POLYMER-BASED SCAFFOLDS
RELEASING GROWTH FACTOR

By

Amanda Rachel Clark

Dr. David Puleo
Director of Dissertation

Dr. Abhijit R. Patwardhan
Director of Graduate Studies

December 1, 2014

Table of Contents

List of Tables

List of Figures

Chapter 1 Introduction

Currently growth plate fractures account for nearly 18.5% of fractures in children (Mizuta et al., 1987). Depending on the type of growth plate fracture and the severity it can lead to stunted bone growth or bone growth deformation. The current treatment options for growth plate fracture are removal of the bony bar and replacing it with a filler substance, such as, bone cement or fat, but still yield poor results 60% of the time (Basener et al., 2009). In previous work, poly(lactic-co-glycolic acid) (PLGA) scaffolds were developed and studied *in vivo* for the purpose of growth plate regeneration. Based on the results of that study, it was thought that an increase in degradation time and mechanical properties would be an improvement (Ravi, 2009). Additional findings showed that PLGA scaffold loaded with insulin-like growth factor I (IGF-I) increased the formation of neocartilage, and therefore, more research was performed to enhance this effect (Sundararaj et al., 2012). In this dissertation, PLGA scaffolds of varying molecular weight, fusion temperature and a novel hybrid scaffold were fabricated, characterized and implemented for growth plate regeneration, along with several reported drug delivery options. This work not only shows how PLGA scaffolds can be used for the treatment of growth plate injuries but how they can also be used in other soft and hard tissue applications.

PLGA was chosen as the scaffold material since it has been shown to be biocompatible and biodegradable and is FDA approved for drug delivery devices. PLGA microspheres were fabricated using a double emulsion technique and then mixed with NaCl particles, compressed, heat sintered and leached to form a scaffold. The process of heat sintering was added in hopes of increasing the mechanical properties to be suitable for soft and hard tissue applications, which is discussed in chapter 1. Additionally, the effects of molecular weight on the morphology and degradation of the scaffold was evaluated. The scaffold also had the ability to incorporate chondrogenic growth factors (CGF) within the matrix. The growth factor helped to further promote and control desirable cell differentiation. Chapter 2 explored the drug delivery of IGF-I and the effects that scaffold fabrication had on the bioactivity.

A novel hybrid scaffold was fabricated by replacing the NaCl particles with hydrogel particles. The hydrogel porogen used was quick degrading, which ultimately result in a porous structure after a day, still allowing for cell ingrowth. They hydrogel system used a poly(β-amino ester) (PBAE), specifically the H6 system, based on the work of Anderson et al (Anderson et al., 2006). The effects that porogen loading had on the mechanical properties and morphology of the scaffold were investigated in chapter 3. Also in chapter 3, drug loading the scaffold while maintain bioactivity, and the results of the dual drug release study are discussed. This dual release may allow for enhanced treatment of a specific conditions or desired effect.

Completing this work was an animal study using the developed scaffolds for the application of growth plate regeneration. Chapter 4 gives the details of the New Zealand white rabbit model of growth plate arrest used in this study (Lee et al., 1998; Li et al., 2004), which mimics the problems seen clinically. The current treatment option involves resecting the bony bar and implanting a fat, silicon or bone cement as a space filler, in hopes of prevent bony bar regrowth (Lee et al., 1993). The problem with this approach is that it prevents the native growth plate from regenerating thereby preventing long bone growth. Other research groups have largely involved the use of mesenchymal stem cells (MSC), which requires an additional surgery to harvest the cells and additional time for culturing (Chen et al., 2003; Li et al., 2004; Planka et al., 2008; Tobita et al., 2002). The intention of this work was to regenerate the native growth plate, without the use of MSCs, resulting in restoration of normal bone growth better than the current clinical treatment options.

Chapter 2 Background and Significance

With the end goal in mind, a scaffold is developed from the ground up. First the polymer must be selected. Each polymer can be tailored through altering the inherent polymeric properties until the best combination is reached. With keeping the polymer selection in mind, the various scaffold fabrication methods can be explored. Along with the scaffold fabrication, the option for drug delivery potential must be considered. With the selection made will then dictate the possible applications of the scaffold based on the degradation and mechanical properties and drug delivery.

2.1 Biodegradable Polymers

Biodegradable polymers have become a major area of focus within tissue engineering research. A biodegradable polymer that is also biocompatible has the ability to degrade *in vivo* without eliciting an adverse effect, which can be advantageous for fabricating medical implants. Polymers can possess the mechanical properties necessary to withstand non-load bearing physiological environment yet over time they degrade away, avoiding the need for a retrieval or replacement surgery. Depending on the fabrication methods, most degradable polymers can be used as a drug delivery carrier. The success of polymers as an implant material relies on understanding the benefits and limitations each specific polymer has in regards to the degradation and mechanical properties and drug delivery application. The most common polymers are polyanhydrides, polyorthoesters, polycaprolactone and polyesters.

2.1.1 Polyanhydride

Polyanhydrides are characterized into three different classes based on the type of molecule used to connect the polymer backbone. Aliphatic, unsaturated and aromatic polyanhydrides offer variation in degradation and mechanical properties. Aliphatic polyanhydrides degraded within days as compared to the aromatic polyanhydrides that can take years to degrade (Agrawal et al., 2001; Uhrich et al., 1999). Regardless of the class, polyanhydrides degrades by surface erosion. Even though it degrades through hydrolytic cleavage the hydrophobic nature of the polymer prevents bulk degradation (Uhrich et al., 1999). Having the surface erosion, allows for a near zero-order drug

3

release (depending on the geometry) and a tailorable release time by altering the polymer composition (Rosen et al., 1983). In order to make polyanhydrides more applicable for orthopedic implants poly(anhydrides-co-imides) and crosslinked polyanhydrides have been developed to increase the mechanical properties (Attawia et al., 1995; Gunatillake et al., 2003; Muggli et al., 1998).

2.1.2 Polyorthoester

Polyorthoesters (POE) have been divided into four families, which differ by the polymer backbone, reflected in the degradation (Heller et al., 2002). POE I uses ortho ester linkages that degrade through hydrolysis, increased by the autocatalyst of the degradation products (Heller et al., 2002; Uhrich et al., 1999). POE II has an additional diol in the structure that eliminates the autocatalyst and depending on the diol used, the mechanical and thermal properties can be adjusted (Heller et al., 2002). POE III has a more flexible backbone and offers the advantage of being able to load drug into the polymer at room temperature without the use of solvents (Heller et al., 2002). The most versatile of the POEs is family IV. It is a variation of POE II but it yields easily reproducible degradation and release results that can be varied from days to months (Heller et al., 2002).

2.1.3 Polyester

Polyesters are the most widely research and well-characterized polymers used for implants. Poly(lactic acid) (PLA) and poly(glycolic acid) (PGA) are both used on their own to fabrication scaffolds, but can also be combined to make poly(lactic-co-glycolic acid) (PLGA). These materials are already patented for surgical sutures or FDA approved drug delivery systems, such as, Lupron Depot®, Zoladex®, and Atridox®, for the treatment of prostate cancer, endometriosis, and fibroids (Schmitt et al., 1967). Ester linkages of lactic and glycolic acid units build the structure of PLGA. When the polymer is exposed to water these ester linkages undergo hydrolysis and the chains begin breaking down into shorter polymers until eventually it is broken down into lactic and glycolic acid units producing an alcohol and a carboxylic acid as the end groups (Houchin et al., 2008). The degradation creates an acidic environment most concentrated at center of the

scaffold (or at places where the water cannot yet flow freely) and results in autocatalysis effect, which, further break down the ester links (Fu et al., 2000).

In order to tailor the mechanical and degradation properties of a scaffold there are a few polymer properties that can be altered. The molecular weight can be adjusted, altering the length of the polymer chains (Clark et al., 2013). However, after the initial degradation, the longer chains can result in a larger build up of the acidic monomers, acting as an autocatalyst. This also reduces the pH in the center of the scaffold, which could cause degradation of any protein that might be loaded in the microspheres or potentially cause aseptic cysts (Fu et al., 2000; Meyer et al., 2012). Also, the ratio of lactic to glycolic units can be used to control the hydrophobicity since glycolic is slightly more hydrophilic and therefore increasing the degradation rate (Anderson et al., 1997; Lu et al., 1999; Tracy et al., 1999). Lastly, the end groups (methyl ester or carboxylic acid terminated) can be selected to alter the degradation since the carboxylic acid ended is more hydrophilic than the methyl ester ended, therefore increasing the degradation rate (Anderson et al., 1997; Tracy et al., 1999).

2.1.4 Poly(β-amino ester)

Poly(β-amino ester) (PBAE) is hydrogel biodegradable system. A large library of diacrylate and amines can be used to fabricate these polymers (Anderson et al., 2006). The macromer is synthesized through a step-wise reaction between the diacrylate and amine, which then undergoes free radical polymerization. Polymerization can be achieves using a chemical initiator or photopolymerization (Anderson et al., 2006). With photopolymerization a mask and laser technique can be used, adding spatial control to the areas that become polymerized. The molecular weight of the macromer can also be altered, changing the degradation and mechanical properties (Brey et al., 2008; Hawkins et al., 2011). Degradation occurs via hydrolysis of the ester linkages, therefore, the more crosslinks, the longer it will take to degrade.

2.2 Scaffold Fabrication

Polymer scaffolds can be tailored to meet the needs for specific tissue engineering applications. Regardless of the application, there are several characteristics that the scaffolds most possess. First, the scaffolds must be biodegradable, ideally having a

degradation rate equal to the rate of tissue regrowth (Dhandayuthapani et al., 2011; Hutmacher, 2000). Tissue growth into the scaffold requires a porous structure that allows for cell to migrate into, where the cells can proliferation and remain active (Hutmacher, 2000; Van Tienen et al., 2002). This porosity must be balanced with maintenance of the necessary mechanical properties to withstand the physiological conditions at the site of implantation (Hutmacher, 2000; Ikeda et al., 2009).

2.2.1 Particle Leaching

During the fabrication process the polymer can be mixed with a particle that will act as a temporary porogen until removal, resulting in a porous scaffold. The polymer itself is commonly in the form of microspheres, while the temporary porogen may be NaCl (salt) crystals, sucrose or hydrogel particles (Dorati et al., 2010; Hawkins et al., 2013; Hou et al., 2003; Kim et al., 2009). Tailoring the size and amount of the porogen particles controls the overall pore size and porosity of the scaffold (Hou et al., 2003). Once the polymer is mixed with the porogen particle the polymer must be solidified around the particles using one of several methods. One method is using solvent casting, where the polymer and salt are mixed with a solvent to create a lower viscosity solution (Mikos et al., 1994). Common solvents are methanol, acetone, chloroform, tetrahydrofuran, and dichloromethane that will evaporate over time and leave a solid polymer matrix (Liao et al., 2002; Mikos et al., 1993). A second option is using a sintering technique that fuses the polymer around the porogen microspheres together. Using temperatures above the glass transition temperature allows for the polymer chains to entangle with neighboring chains and solidify upon cooling (Brown et al., 2008; Clark et al., 2013). A third method is gas foaming, which saturates the polymer with CO_2 using high pressure and then rapidly reducing the pressure (Harris et al., 1998; Mooney et al., 1996; Nof et al., 2002; Park et al., 1998), thus making the gas instable and causes the polymer to expand and create a continuous matrix around the particles (Harris et al., 1998; Mooney et al., 1996; Nof et al., 2002; Park et al., 1998). Gas foaming eliminates the use of solvents or high temperatures, which is advantageous when consider the effect they may have on drugs or proteins that would be used for drug delivery. However, this method lacks pore interconnectivity and requires the addition of salt-leaching to gain a more homogenous pore distribution (Liu et al., 2004). Lastly, the polymer can be

6

compressed around the porogen (Nof et al., 2002). Regardless of the method used to mold the polymer around the particle, the particle is removed by leaching the scaffold in water, yielding a porous structure (Liao et al., 2002).

2.2.2 Emulsion Freeze Drying

Emulsion freeze-drying creates a homogenous solution of polymer mixed with solvent and water. This solution is molded into the desired shape, frozen and freeze dried, removing the water and creating a porous structure (Liu et al., 2004; Whang et al., 1995). A highly porous structure can be fabricated using this method, but lacks pore interconnectivity (Liu et al., 2004).

2.2.3 Phase Separation

Phase separation involves mixing the polymer with a solvent at high temperatures to create a homogenous solution. The temperature is then reduced, the polymer becomes a solid and the solvent is either extracted or evaporates, leaving pores in the polymer structure (Liu et al., 2004; Schugens et al., 1996; Van de Witte et al., 1996). The advantage of this method is the high mechanical properties, reported to be up to 20 times greater than salt leaching technique (Liu et al., 2004). The disadvantage is the variability of the pore structure because it depends on many factors, such as, the polymer, solvent, polymer concentration and phase temperature (Liu et al., 2004).

2.2.4 Solid Freeform Fabrication

Solid freeform fabrication (SFF) technology is a more recent development that is crossing over into biomedical applications in the past couple decades. This technology builds a 3-D structure in a computer aided design (CAD) software program and then constructs the scaffold layer by layer using one of several methods (Sachlos et al., 2003). The layers can be printed using a 3-D printer where a binding agent is printed onto powder, dissolving and adjoining the powder as directed by the CAD program (Bredt et al., 1998; Sachlos et al., 2003). Stereolithography uses a laser to selectively polymerize areas of each layer (Hull, 1990; Sachlos et al., 2003). Fused deposition modeling extrudes polymeric fibers to match the designated design of that layer (Scott, 1991), while 3-D plotting melts the polymer and uses compressed air to deposit a thin layer of material that cools upon contact with the previous layer (Landers et al., 2000; Sachlos et al., 2003).

The advantage to SFF methods is the precious it has to create varying pore sizes, distribution and concentration. SFF can also construct complex internal structures and easily reproducible. However, depending on the method used, solvents and/or high temperatures are required, which can be damaging to drugs or proteins loaded with the polymer. The mechanical properties of SFF constructs are usually poor due to lack of interconnectivity between the layers.

2.3 Growth Factors

Growth factors can be used to interact with specific signaling cascades that create a favorable reaction. Growth factors can be used to regrow tissue by increasing cell proliferation and decrease apoptosis (Baserga et al., 1998; Rotello et al., 1991). Additionally, growth factors can be used to direct cells toward a desired cell lineage in order to generate a specific tissue type (Baserga et al., 1998). Growth factors even play a role in tissue repair and overall homeostasis (Li et al., 2008). Utilizing these mechanisms growth factors can be used for bone and cartilage regeneration (Nishida et al., 2004; Schmid, 1995). Combining the use of two growth factors has been researched as well to create multiple outcomes or to create a synergistic effect. For example, one study showed that using IGF-I with transforming growth factor β1 (TGF- β1) created a 20% increase in cartilage production over IGF or TGF alone (Fukumoto et al., 2003).

2.3.1 Insulin-like Growth Factor

The family of insulin, insulin-like growth factor I and II are common found in every organ system in the body (Flier et al., 1997). Insulin most commonly works in the liver, muscle, and adipose tissue, while IGF I and II act in all organ systems and embryotic development, however IGF-II is not well understood and isn't as dominant as IGF-I (Flier et al., 1997). Extensive knowledge exists on IGF-I (Flier et al., 1997), a growth factor used to increase cell proliferation and has been tested in vivo (Baxter, 1994). It has been shown to stimulate the synthesis of proteoglycan and type-II collagen while enhancing chondrocyte matrix synthesis (Fortier et al., 1999; Schmid, 1995). In rat studies it was found to widen the tibial epiphysis, while increasing the levels of endogenous IGF-I (Schoenle et al., 1985).

IGF utilizes the phosphatidyl inositol 3-kinase (PI3 kinase) signaling pathway through binding a tyrosine kinase receptor and activates PI3 kinase intracellularly (Heng et al., 2004). This leads to the generation of second messengers Ins(1, 4, 5)P$_3$ (IP$_3$) and diacylglycerol (DAG) that can take several different actions. They can activate Ark signaling, shown to inhibit apoptosis, which further aids the cell survival of chondrocytes (Andres, 2010). The second messenger IP3 can diffuse into the endoplasmic reticulum where it triggers calcium release. This calcium release allows for DAG to bind protein kinase C (PKC) (Andres, 2010). PKC influences cell differentiation and has been shown to influese chondrogensis (Chang et al., 1998). IGF has also been shown to activate the mitogen-activated protein kinase (MAPK) pathway to increase cell proliferation (Choi et al., 2008; Weng et al., 2009).

In studies performed by Fukumoto et al. IGF-I at low concentrations (5-10 ng/mL) IGF-I did not cause a chondrogenic response (measured as % yield cartilage). Increasing the dosage to 100-500 ng/mL concentration a 25-30% yield cartilage increase was seen over the control (Fukumoto et al., 2003).

2.3.2 Transforming Growth Factor β

TGF-β is presented in literature to promote chondrogenesis (Shen et al.). An additional increase in chondrogenesis was seen when TGF-β was used in combination with IGF-I. IGF-I signaling has crosstalk with the pathways initiated by TGF-β (Sakimura et al., 2006). It is the SMAD signaling cascade that is initiated by TGF-β when the ligand binds to the TGF-β type II receptor and becomes activated. The receptor then recruits the type I receptor and goes through a series of phosphorylation and conformational changes until a tetramer is formed. The tetramer translocates into the nucleus and binds to the DNA directly or interacts with other transcription factors, such as, the Smad 3 transcription factor that inhibits cell maturation (Dennler et al., 2002; Ferguson et al., 2000; Pateder et al., 2001). Interaction with the transcription factors leads to increased presences of sox-9 and collagen type II and aggrecan production (Zeiter et al., 2009).

TGF-β has been shown to cause an effect in as little as 2 days at a concentration of 10 ng/mL, resulting in an increase of 20% cartilage growth compared to no TGF-β treatment at all (Fukumoto et al., 2003). However, this study also showed that IGF-I (at

9

100 ng/mL) was just as effective as TGF-β (10 ng/mL) at the 6 week time point (Fukumoto et al., 2003). Overall, TGF-β and IGF-I have found to be equally as effective at inducing chondrogensis (Longobardi et al., 2006).

2.3.3 Bone Morphogenetic Protein

BMPs belongs to the TGF- β super family and have been shown to play a role in heart, neural and cartilage development but they are best recognized in bone formation (Chen et al., 2004). BMP-2 is already being used clinically in products such as Osigraft™, InFUSE™ and InductOs™, for the treatment of nonunions, degenerative disc disease, sinus augmentation and localized alveolar ridge augmentation (Cornell et al., 1991; Inai et al., 2008; Martina et al., 2007; Pond et al., 1984; Ratner et al., 1996). Cell growth, differentiation and apoptosis can all be affected through the SMAD signaling pathway, activated by BMP-2 protein binding BMP-receptor type I and II (Nohe et al., 2002). BMP-2 induces protein DLX3, which activates the transcription of *Runx2*, osteocalcin and alkaline phosphatase genes, which have all been shown to be a marker for osteoblastic activity (Hassan et al., 2006; Nohe et al., 2002; Wang et al., 2011). Osteocalcin can also be a marker for the presence of hypertrophic chondrocytes (Hanada et al., 2001). The effect of BMP-2 is also dose dependent over a very wide range (Kuhn et al., 2013; Laurencin et al., 2001; Patel et al., 2008; Riew et al., 1998; Whang et al., 1998). Wang et al. saw a 2.8 and 60-fold increase in bone formation after 7 days over no BMP-2 treatment with a dose of 1.2 and 115.3 μg of BMP-2 (Wang et al., 1990).

BMP has also been found to play a role in chondrogenesis (Hanada et al., 2001). While, BMP-2, -4 and -6 have all been shown to increase chondrogenic differentiation, BMP-2 is the most effective (Sekiya et al., 2005). Studies have shown that cells treated with BMP-2 induces the expression of aggrecan core protein and type II collagen (Hanada et al., 2001). A cellular response to BMP-2 has been seen (as measured by the overall Sox-9 expression) at concentrations as low as 10 ng/mL resulting in a 1.5 fold increase over the control. Up to a 4-fold increase was seen at a higher concentrations of 200 ng/mL (Brown et al., 2008).

2.3.4 Alternative drugs - Glucocorticoids

Another option for promoting chondrogenesis is the use of steroids, more specifically glucocorticoids (GCs). There are many types of GCs on the market already, including dexamethasone (DEX), used as an anti-inflammatory for arthritis patients and for allergic reactions (Ballock et al., 2003). Dex is already FDA approved by the brand names of Decadron or Ozurdex. It is known that GCs are required for chondrogenic differentiation of stem cells in vitro and was demonstrated using DEX (Derfoul et al., 2006). It was further shown that using DEX along with TGF upregulate the production of collagen type II and cartilage oligomeric matrix protein. However, GCs can be inhibitory when given in high doses and cause apoptosis and gastrointestinal bleeding, so the dosage will need to be tightly regulated (Behrens et al., 1975; Cabre et al., 1998; Satterwhite et al., 1992).

2.4 Applications of Polymeric Scaffolds in Medicine

Polymeric scaffolds offer the biocompatibility and biodegradability properties that are desirable for soft and hard tissue implants, and they are a potential alternative to autografts, allografts or metal implants. Autografts and allografts can introduce infection, while metal implants can loosen, cause systemic problems, and/or require replacement surgery (Burg et al., 2000; Hallab et al., 2009; Törmälä et al., 1998). The tunable system of polymer systems makes it easy to meet the desired degradation and mechanical properties for soft and hard tissue implants. Some of the polymers have already been FDA approved for the use of drug delivery and sutures.

Extensive research has been published on the many applications of biodegradable polymers. Studies have shown that polymers can be used for soft tissue, such as vascular grafts (Liao et al., 2007), skin grafts (Kim et al., 2005; Wake et al., 1996) and cartilage regeneration (Chen et al., 2004; Hutmacher, 2000), more specifically articular cartilage (Sherwood et al., 2002; Temenoff et al., 2000), fibrocartilage (Kang et al., 2006; Klompmaker et al., 1991), and hyaline cartilage (Chen et al., 2003; Freed et al., 1994; Lee et al., 1998; Sundararaj et al., 2012). Hard tissue applications are also a possibility for polymers in bone regeneration (Fujihara et al., 2005; Laurencin et al., 1996; Solheim et al., 1992; Thomson et al., 1996), specifically trabecular bone (Forcino et al., 2007) and cortical bone regeneration, both loading bearing (Ibim et al., 1998) and non-load bearing

placement (Hollinger et al., 1987).

2.5 Specific Aims

The work in this dissertation was guided by these specific aims:

- Develop and characterize PLGA scaffolds with tuned structural and mechanical properties
- Incorporate a growth factor into the scaffold and determine the bioactivity and efficacy in vitro
- Develop a hybrid scaffold capable of releasing two drugs
- Tailor the scaffolds to be suitable for cartilage (growth plate) regeneration and evaluate the *in vivo* response
- Compare the results to current clinical treatment options and offer possible improvements for the future.

Chapter 3 Tailoring Properties of Microsphere-Based Poly(lactic-co-glycolic acid) Scaffolds

3.1 Introduction

Polymeric materials are commonly used to develop implantable scaffolds exhibiting a wide range of properties with varying applications. Biodegradable scaffolds are advantageous to the patient because there will be neither long-term foreign materials in their body nor additional retrieval surgeries required. Polymeric biodegradable scaffolds offer a beneficial scenario by providing the initial mechanical support needed at the site of implantation and then degrading away as the tissue regrows, allowing the body to heal naturally by creating an environment for cell proliferation and differentiation (Agrawal et al., 2001). The porous nature of the scaffolds further promotes tissue growth by allowing cell infiltration. Depending on the intended application, many polymeric scaffolds are loaded with proteins and/or drugs to enhance the overall effect. For example, the regeneration of bone or cartilage can be enhance with the addition of bone morphogenetic protein or insulin-like growth factor, respectively (DiCarlo et al., 2009; Govender et al., 2002; Madry et al., 2005; Nielsen et al., 1994; Stein et al., 2005; Wang et al., 1990). Fabrication methods may be limited, however, based on the processing steps used to make the scaffold, such as elevated temperatures, compression, or solvents used, that can be harmful to the encapsulated molecules (Arakawa et al., 1991; Fernández‑Martín et al., 2000; Hofmann et al., 1995).

Poly(lactic-co-glycolic acid) (PLGA) and similar polymers, such as poly(glycolic acid) (PGA) and poly(lactic acid) (PLA), are used in FDA-approved drug delivery systems, including Lupron Depot®, Zoladex®, and Atridox®, applied to treatment of prostate cancer, endometriosis, fibroids, and periodontal disease. Additionally, these materials are extensively investigated for tissue engineering and other controlled release applications, with increasing emphasis on nanostructures (e.g., reviewed in (Burdan et al., 2009; Pattison et al., 2005; Prasad et al., 2008; Wu et al., 2001)). PLGA is biodegradable and can exhibit biocompatible properties, such as minimal inflammation at the implantation site and minimal presence of foreign body giant cells, that make it suitable for tissue engineering purposes (Kitchell et al., 1985; Shive et al., 1997). PLGA is commonly used in the form of microspheres having tunable properties by altering the

polymer molecular weight, the ratio of lactic to glycolic acid, or the end group. In recent years, microspheres have been fabricated into scaffolds having a variety of degradation and mechanical properties using sintering, solvent casting with particle leaching, or sphere-templating processes (Brown et al., 2008; Jabbarzadeh et al., 2012; Linnes et al., 2007; Lo et al., 1995; Mikos et al., 2000).

Once microspheres are fabricated, they can be made into scaffolds with specific properties by controlling the type(s) of microspheres used. Pore size, porosity and mechanical properties can be tailored using the salt leaching method, and with the addition of an incubation step the mechanical properties can be tailored as well (Chen et al., 2003). Incubation of the scaffold allows the microspheres to fuse together, wherein the polymer chains relax and entangle with neighboring chains. Additionally, the microsphere composition results in a wide range of scaffold types and properties. Depending on the scaffold composition, the degradation time can vary from weeks to months, which will also influence the release profile of drug/growth factor that may have been encapsulated. All aspects of the scaffold (size, shape, composition, incubation temperature) can be manipulated to achieve an array of design criteria.

Thus, PLGA scaffolds can be fabricated to have characteristics similar to those of the implant site by altering polymer chemistry, pore size, and overall porosity. The idea behind this approach is that, by implanting a scaffold that has the same microstructure and mechanical properties as the site of implantation, the cellular responses will be a desired, natural response (Willie et al., 2010). For example, PLGA and PGA have been used to create an external sheath for vein grafts, matching the mechanical properties necessary to sustain the mechanical loading of the physiological conditions (Liao et al., 2007). While not able to fully replace the body's functions, PLGA scaffolds have been used to replicate specific functions. Similarly, PLGA based scaffolds have been used to mimic bone matrix properties, such as cell interaction and composition, for better biocompatibility (Buschmann et al., 2012; Shen et al.).

In the present study, the fundamental mechanical properties of microsphere-based PLGA scaffolds were investigated. The scaffolds consisted of microspheres fabricated from polymers having different molecular weights that were subsequently processed at different temperatures. All of these types of scaffolds can be fabricated with little

14

variation of the fabrication methods, making it an advantageous system to achieve a wide range of mechanical properties. The compressive modulus, degradation properties, and morphology play crucial roles in determining the capabilities of the scaffold system. Once the scaffold properties have been characterized, the scaffold can then be tailored to suit the needs of varying tissue engineering applications.

3.2 Material and Methods

3.2.1 Polymers

Poly(lactic-co-glycolic acid) (PLGA; 50:50, acid-terminated; Durect Corporation, Pelham, AL) was used in this study. Two different molecular weights were used for the fabrication of the scaffolds, a lower molecular weight (LMW) of 5,500 Da and a higher molecular weight (HMW) of 30,000 Da as listed in Table 3.1.

3.2.2 Microsphere Fabrication

Two types of PLGA microspheres, designated uniform and blended, were prepared using the $W_1/O/W_2$ double emulsion technique, as seen in Figure 3.1. Uniform PLGA microspheres consisted of one molecular weight of polymer, either LMW or HMW. The blended microspheres had both polymer crystals (LMW and HMW) at a 50:50 weight ratio. The oil phase was made by dissolving PLGA at 13 wt/v% in dichloromethane. During the first emulsification, 10 v/v% PBS (W_1) and polymer were emulsified by sonication at 25W for 10 seconds. This W_1/O was added to aqueous 1% poly(vinyl alcohol) (PVA; Sigma-Aldrich, St. Louis, MO) and homogenized for 3 minutes as the second emulsion at 3500 rpm. The resulting microspheres were then allowed to stir overnight, after which they were washed with dionized water three times and then lyophilized. The microspheres were sieved, collecting only those that were <250 μm for further use.

3.2.3 Scaffold Fabrication

Uniform scaffolds contained 100% of microspheres made from one molecular weight of polymer, either LMW or HMW. Mixed scaffolds contained a 50:50 weight ratio of LMW and HMW microspheres. Blend scaffolds contained 100% blended microspheres. As shown in Figure 3.1, the microspheres were mixed with NaCl at a

15

Table 3.1. Explanation of scaffold types by composition and incubation temperature.

Scaffold Name	Scaffold Compostion (%LMW: %HMW)		Incubation Temp (°C)
Low Molecular Weight (LMW)	100	0	42
Blended	50	50	45
50:50	50	50	49
High Molecular Weight (HMW)	0	100	49

16
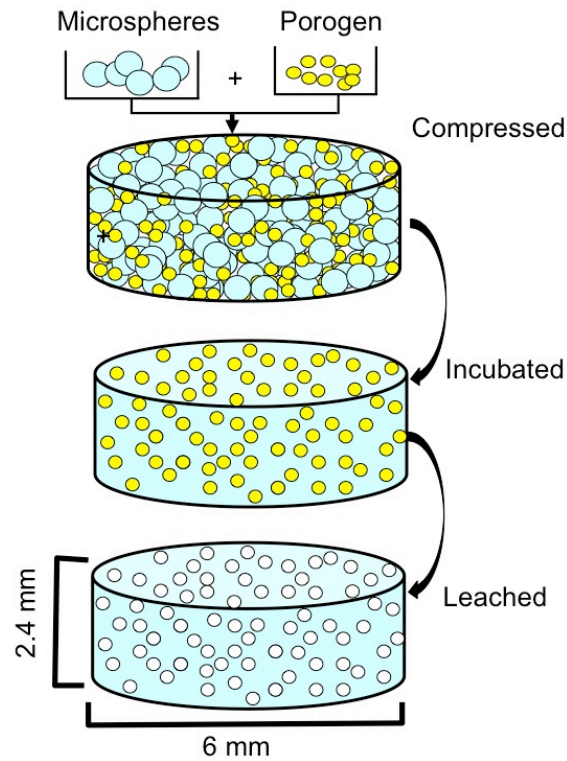
Figure 3.1. Schematic representation of scaffold fabrication. After mixing microspheres with the porogen, they were compressed and incubated at the T_g. The solid sample was then salt leached and dried to result in a porous PLGA scaffold.

17

weight ratio of 40:60 (microspheres:salt) to obtain an overall porosity of approximately 70% with interconnected pores (verified by microCT; see Morphology section) (Jabbarzadeh et al., 2012). The salt size was <150 μm, controlled through grinding and sieving. The microsphere-salt mixture was shaken by hand in a 0.6 mL microcentrifuge tube for 45 seconds and then poured into a 6 mm diameter die. A Carver press was used to compress the mixture into a disk at 1.5 ton for 2 minutes. The compacted disks were placed into an incubator to fuse for 2 days. The glass transition (T_g) temperatures, used as the fusion temperatures, were determined using differential scanning calorimetry (DSC). The T_g for the HMW, LMW and blended microspheres was found to be 49, 37, and 45 ^{o}C, respectively as listed in Table 3.1. The fusion temperature varied depending on the composition of the disk and is indicated for each test in later sections. The salt was leached from the fused scaffold into deionized water overnight on a stir plate. The final scaffolds had a mass of approximately 41 mg, disk diameter of 6.0 mm, and thickness of 2.4 mm.

3.2.4 Morphology

The morphology of the scaffolds was studied by microcomputed tomography (microCT) using a Scanco μCT40 (SCANCO Medical, Switzerland). At various time points throughout degradation, samples were imaged at 6 μm voxel resolution using scan parameters of 55 kV and 145 mA. One scaffold of each type was scanned in its dry initial state, five day degraded, 50% degraded, and 95% degraded, based on weight percentage. For the quantitative evaluation, a bone morphometry script was performed using a built-in evaluation program (version: 6.0) with the threshold manually set from 21 to 132 to most closely match the physical structure of the scaffold. This evaluation reported total scaffold volume, porosity, and average pore size. To determine the pore size distribution and interconnectivity, a simulated mercury intrusion porosimetry script was used. This script reports the accessible volume for spheres of varying diameters, where the diameter is set from 0 to the largest radius of pore size reported.

3.2.5 Degradation

To measure degradation, samples were shaken at 37 °C in 4 mL phosphate-buffered saline (PBS), pH7.4, which was changed every two to three days. At each time

18

point, three disks of each type were removed, lyophilized, and the remaining mass was measured. In addition, the volume was measured using digital calipers to monitor swelling.

3.2.6 Gel Permeation Chromatography

Molecular weight and polydispersity index (PDI) of the microspheres and degraded scaffolds were measured using gel permeation chromatography using a Shimadzu Prominence LC-20 AB HPLC system with a Waters 2410 refractive index detector and two columns (300 x 7.5 mm, 3 μm particle size, ResiPore; Agilent Technologies) in series. Polystyrene standards were used for calibration. Tetrahydrofuran (THF) was used to dissolve the samples at a concentration of 1 mg/mL, and samples were injected at a flow rate of 1.0 ml/min. A labSolutions software interface was used to calculate averaged molecular weights. The samples tested were LMW, HMW and blended microspheres. Additionally, LMW, blended, 50:50, HMW scaffolds were tested at 5 days degraded, 50% and 80% degraded. Insufficient mass remained for analysis of 95% degraded scaffolds.

3.2.7 Mechanical Testing

A Bose ELF 3300 mechanical testing system was used to determine the compressive modulus of dry samples as well as samples incubated in PBS for five days. Starting with no initial preload, samples were deformed at a rate of 0.06 mm/sec until the sample has been compressed approximately 1.5 mm. A stress-strain curve was plotted and analyzed to find the compressive modulus. Figure 3.2A shows a representative plot for a dry scaffold and where the slope was analyzed for the modulus. For the 5 day degraded scaffolds, the stress-strain curve had an initial linear region followed by a second linear region as seen in Figure 3.2B. Because of incomplete initial contact of degrading samples with the compression platen, the slope of the second linear region was used to determine the compressive modulus.

3.2.8 Statistical Analysis

Analysis was conducted using GraphPad InStat software using ANOVA followed by a Tukey–Kramer Multiple Comparisons Test. Results were considered significant if $p < 0.05$.

19
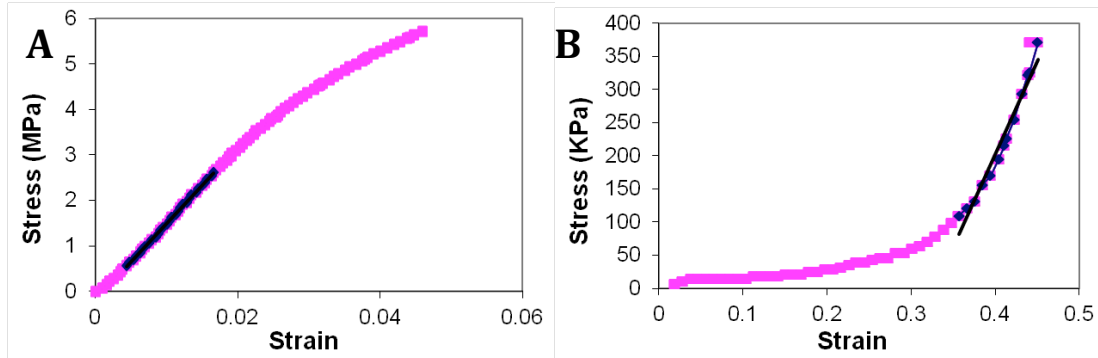
Figure 3.2. Representative stress-strain curves determined by testing (A) dry and (B) 5 day degraded scaffolds. The black line overlaying the graph represents the region used to calculate the modulus.

3.3 Results

3.3.1 Degradation

Figure 3.3 shows degradation curves for the different scaffold types fabricated. Scaffolds containing only LMW microspheres (0:100) degraded at a significantly ($p<0.001$) faster rate than the other scaffolds at 2.4% mass loss per day and were fully degraded in 40 days. The scaffolds containing only HMW microspheres (100:0) degraded at the slowest initial rate of 0.5% mass loss per day ($p<0.001$), while the blended and 50:50 scaffolds degraded at 1.0% and 1.4% per day, respectively ($p<0.05$). Once the scaffolds reached 80% of their original mass, all scaffolds containing any amount of HMW microspheres degraded at a similar rate until only 20% mass remained; they were fully degraded by 120 days. The time it took to reach 5% mass loss was 15, 11, 5, <1 day for the 100:0, blended, 50:50 and 0:100 scaffolds, respectively. By the time the scaffolds were at 50% mass loss, a more distinct difference was apparent between the scaffolds, where the 100:0, blended, 50:50 and 0:100 scaffolds took 56, 45, 39 and 16 days, respectively, to reach this level of degradation (Table 3.2).

3.3.2 Morphology

Fusion of microspheres within the scaffolds was initially assessed by SEM (Figure 3.4). Images showed that the internal structure of truly sintered scaffolds was consistent between scaffold types; dense, solid walls were apparent between the pores. Differences were apparent only when sintering did not occur, when incompletely fused microspheres were visible.

In the initial dry state, all the scaffolds had similar morphology, with average pore sizes of 46, 48, 44, and 49 μm in the LMW, 50:50, blended, and HMW scaffolds, respectively (Table 3.2). Initially, scaffolds sintered at or above the T_g looked the same (Figure 3.5A-C), regardless of the T_g values (LMW at 43°C, blended at 45°C, and HMW at 49°C). At day 5, the pore sizes began to differ as the various degradation rates took effect. The LMW scaffolds had the largest increase in pore size and porosity, while the HMW scaffolds experienced minimal change by day 5; the 50:50 and blended scaffolds were in between, as a trend of decreasing pore size can be seen in Figure 3.5D-F. At 50 and 95% degradation, the LMW scaffolds were too fragile to handle and could not be

21
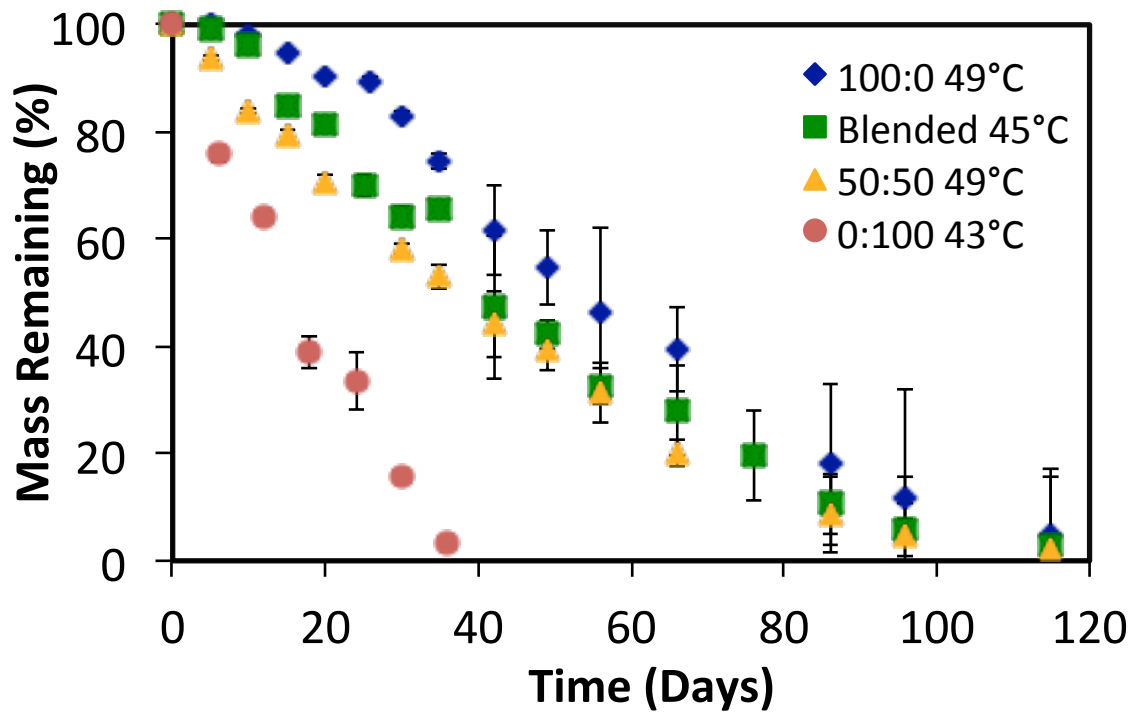
Figure 3.3. Degradation (mass loss) curves for HMW 49°C (incubation temperature), blended 45°C, 50:50 49°C, and LMW 43°C scaffolds. Data are shown as means ± standard error (n≥3).

Table 3.2. Time (days) to reach 5%, 50% and 95% mass loss for each scaffold type.

(HMW:LMW)	Time (days) to % mass loss		
	5%	50%	95%
100:0	15	56	115
blended	11	45	115
50:50	5	39	115
0:100	<1	16	36
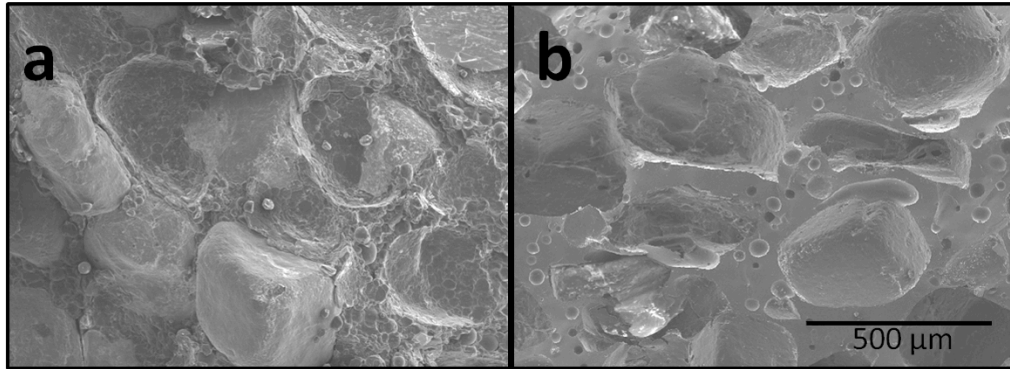
Figure 3.4. SEM images of (a) non-sintered and (b) sintered scaffolds. No difference was seen between the various scaffolds type, the one shown is a HMW scaffold. Sintering was done at 49°C ($\geq T_g$) specific to the scaffold type. The black arrow points to incompletely fused microspheres, and the white arrow points to a dense, fused portion of the scaffold.
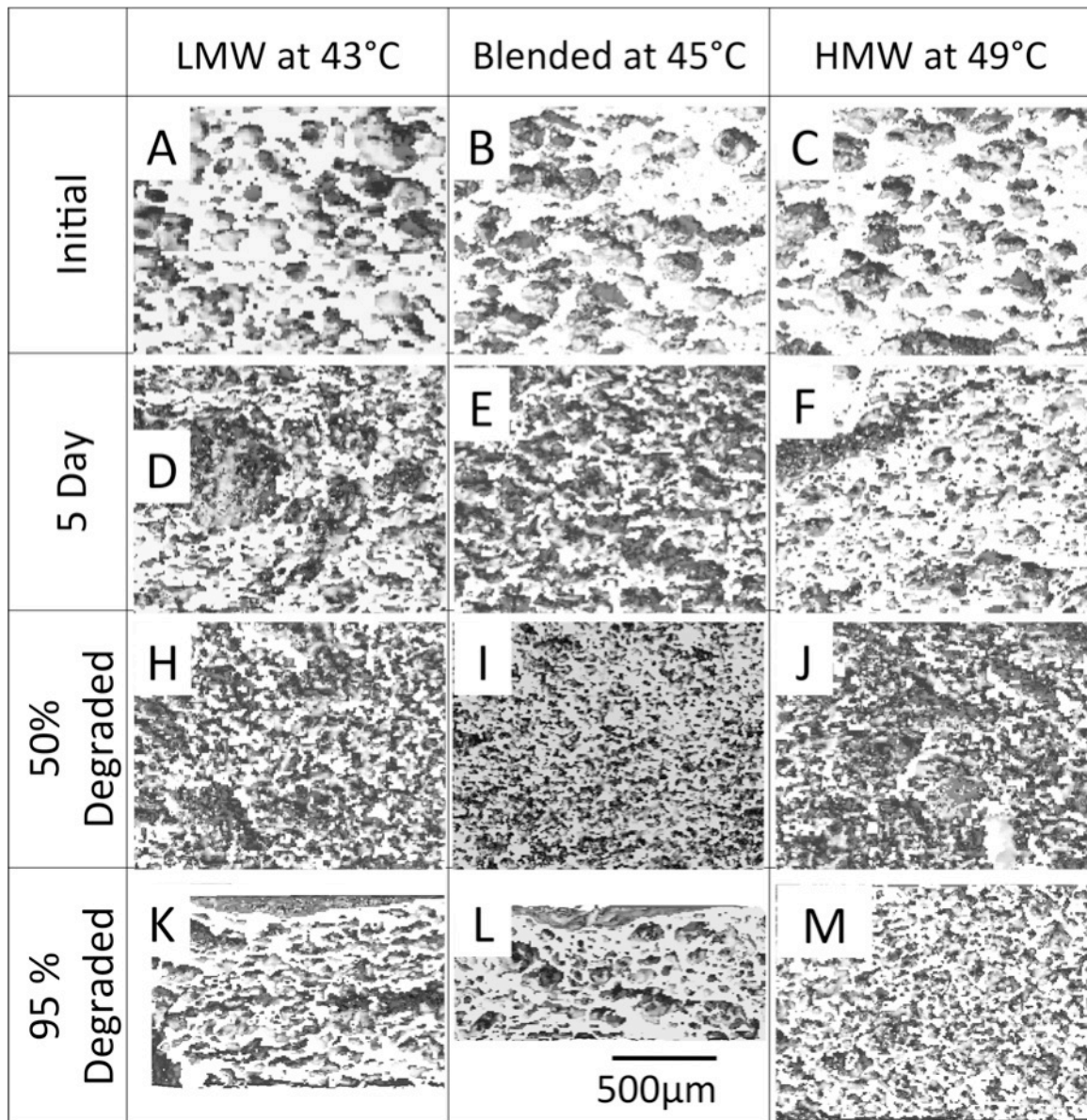
Figure 3.5. MicroCT images illustrating the microstructure of degrading scaffolds' fabricated using different compositions and fusion temperatures. To demonstrate the effect of incubation temperatures between scaffold types, structures are shown for LMW at 43°C (A), blended at 45°C (B), and HMW at 49°C (C). To show different scaffold types throughout degradation, D, E, are F are at 5 days degraded of the 50:50, blended, and HMW scaffolds, respectively, followed by H, I, and J at 50% degradation and K, L, and M at 95% degradation.

imaged. At 50% degradation, the 50:50, blended, and HMW scaffolds all showed an increase in pore size to 61, 47, and 63 μm, respectively, along with an increase in porosity to 82, 65, and 74%, respectively, from 55, 59, and 63% (Table 3.2). The same scaffolds then experienced a decrease in pore size and porosity at 95% degradation. The 50:50 and blended scaffolds behaved similarly to each other, and after reaching 50% degradation, their porosity and degradation time were comparable to those for the HMW scaffolds. The volumes reported in Table 3.3 show that the HMW scaffolds swelled the most at 50% degradation, with a 4.5-fold increase in volume from the initial dry state, while the 50:50 and blended scaffold had 3.5 and 2.9-fold increases, respectively.

The simulated MIP analysis showed that the 50:50, HMW, and blended scaffolds had an accessible volume percentage (defined as a continual interconnectivity space of ≥12 μm) of 99, 95, 99 for 5 day degradation, 99, 100, 99 for 50% degradation, and 96, 94, 90 for 95% degradation, respectively.

3.3.3 Gel Permeability Chromatography

Initially, the LMW and HMW microspheres had molecular weights of 8.5±0.25 and 40.7±2.5 kDa, respectively, both with a PDI of 1.7 (Figure 3.6). The blended microspheres had two initial molecular weights at 44.7±4.2 and 10.4±0.4 kDa.. Only one peak appeared for the blended and 50:50 scaffolds at 5 days and thereafter, having PDI values of 2.5 and 2.9, respectively. At day 5, molecular weights of polymer in all scaffolds were significantly different ($p<0.001$), with the blended and 50:50 scaffolds being relatively similar at 12.0±0.7 and 14.5±0.2 kDa, respectively, which was between the HMW and LMW scaffolds at 22.8±0.4 and 6.6±0.3 kDa, respectively. After 5 days, the LMW scaffolds were significantly lower than any of the other scaffolds ($p<0.01$).

3.3.4 Mechanical Properties

Figure 3.7 illustrates the effect of sintering temperature and scaffold composition on the compressive modulus of the scaffolds in the dry state. Increasing the sintering temperature above the Tg resulted in a statistically significant (p<0.001), nearly ten-fold increase in compressive modulus for all scaffold types. Results for the 0:100 scaffolds are shown at only 43°C since this is the Tg. In the initial dry state, there were no statistical differences between scaffolds sintered at the same temperature, even though the

26

Table 3.3. Morphology data for LMW, 50:50, blended and HMW scaffolds at the dry initial, 5 days degraded, and 50% and 95% degraded states. Data are not available for LMW scaffolds at 50 and 95% degradation because they were too fragile to handle.

Degradation Point	Scaffold Type							
	LMW				50:50			
	Time (Days)	Volume (cm^3)	Porosity (%)	Pore Size (μm)	Time (Days)	Volume (cm^3)	Porosity (%)	Pore Size (μm)
Dry Initial	0	135.7	54	45.5	0	135.7	55	48.2
5 Day Degraded	5	87.8	57	92.4	5	145.8	70	67.2
50% Degraded	16	106.2	-	-	39	472.6	82	61.4
95% Degraded	36		-	-	115	9.8	62	45.3

Degradation Point	Scaffold Type							
	Blended				HMW			
	Time (Days)	Volume (cm^3)	Porosity (%)	Pore Size (μm)	Time (Days)	Volume (cm^3)	Porosity (%)	Pore Size (μm)
Dry Initial	0	135.7	59	44	0	135.7	63	49.2
5 Day Degraded	5	154.4	57	76.4	5	116.9	55	55.4
50% Degraded	45	391.5	65	46.8	56	609.8	74	62.8
95% Degraded	115	10.6	56	70	115	31.3	59	64.2
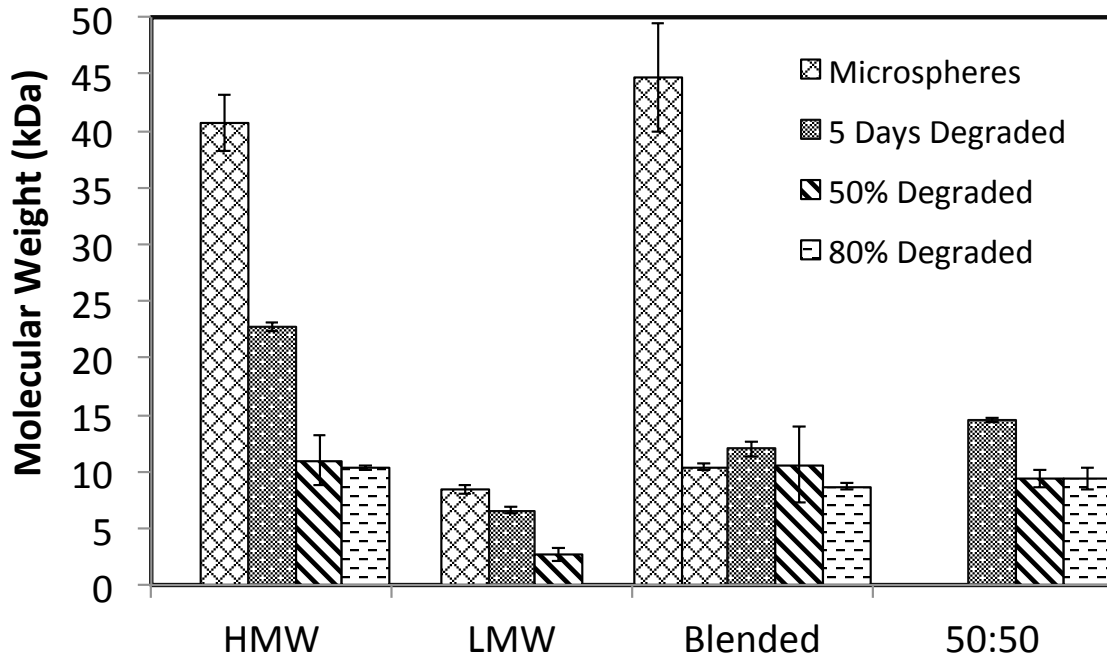
Figure 3.6. Molecular weight analysis of initial microspheres (used to form scaffolds) and throughout degradation of HMW, blended, 50:50, and LMW scaffolds. Initial results are not shown separately for the 50:50 scaffolds because they comprised 50% HMW and 50% LMW microspheres, which were tested individually. Data are shown as means ± standard deviation (n≥3).
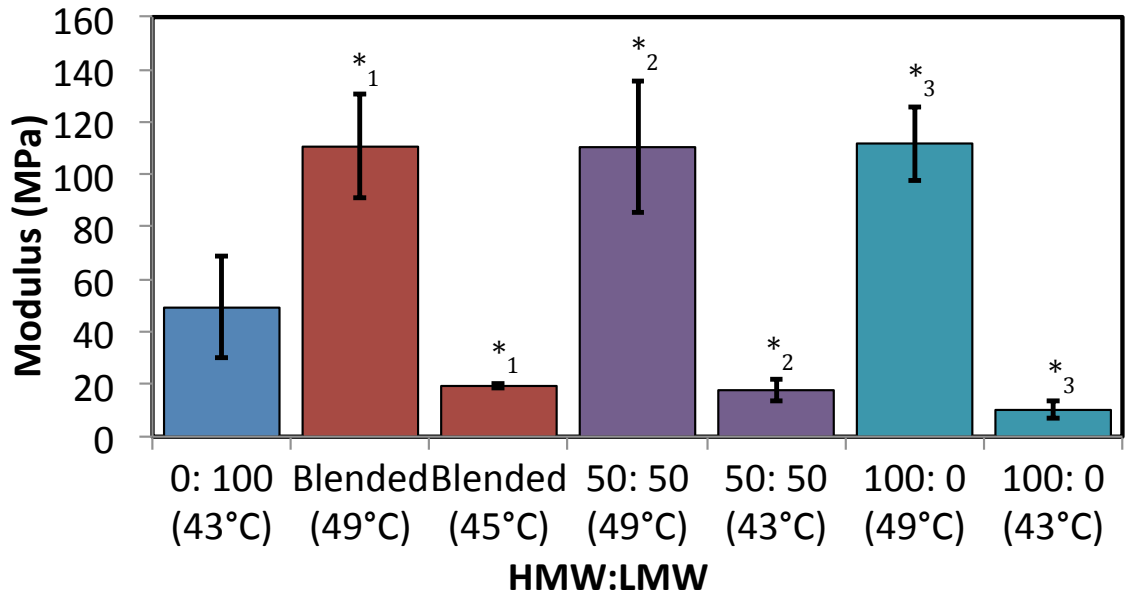
Figure 3.7. Compressive modulus of dry scaffolds made with different fusion temperatures, illustrating the significant effect temperature had on the mechanical properties. Data are shown as means ± standard error (n≥3).*[1,2,3] p<0.001.

microsphere compositions were different. After the scaffolds had been degraded for only 5 days and tested in their wet state, a statistically significant decrease in modulus was seen ($p<0.001$), and differences in the scaffold composition became apparent (Figure 3.8). Scaffolds sintered at 49°C retained approximately 2 to 5.5% of the original modulus, while the scaffolds sintered at 43°C retained only 0.2 to 1.3% and were significantly lower than the dry state modulus ($p<0.01$) than at their wet state after five day degradation.

3.4 Discussion

3.4.1 Scaffold Fabrication

The effect of PLGA molecular weight on mechanical properties was seen in the scaffolds that contained some amount of HMW microspheres, which increased the compressive modulus. Even during degradation, more structural integrity was retained in comparison to the LMW scaffolds, as quantified by the compressive modulus.

Increasing the scaffold sintering temperature up to or above the T_g during the fabrication process allowed for increased molecular mobility of the polymeric chains that led to the microspheres fully fuse together around the porogen (NaCl crystals) to become a solid polymeric mass, whereas scaffolds sintered below the T_g likely only partially fused, leaving small voids in the material that acted as stress concentrators (Borden et al., 2002). The dry compressive modulus of the LMW scaffolds, at 49 MPa, was higher than the 3.2 MPa modulus reported by Thomson et al. who tested a similarly porous PLGA (50:50) (MW 10 kDa) scaffold made from a PLGA matrix and gelatin porogen, similar to the salt leaching method, but the scaffolds were not sintered (Thomson et al., 1996). This difference illustrates the significance of the added sintering step to fuse microspheres instead of simply compressing them together. Brown et al. used a solvent-based sintering method that wets the outside of the microspheres with solvent and allows for neighboring microspheres to join together. Varying the concentration of the solvent in the solution (low, medium, and high) resulted in different amounts of microsphere fusion within the scaffolds. The results showed that the compressive modulus increased with increasing levels of "sintered" microspheres. At the highest degree of sintering, however, there was a decrease in the modulus, likely due to the fusion solution causing dissolution of the
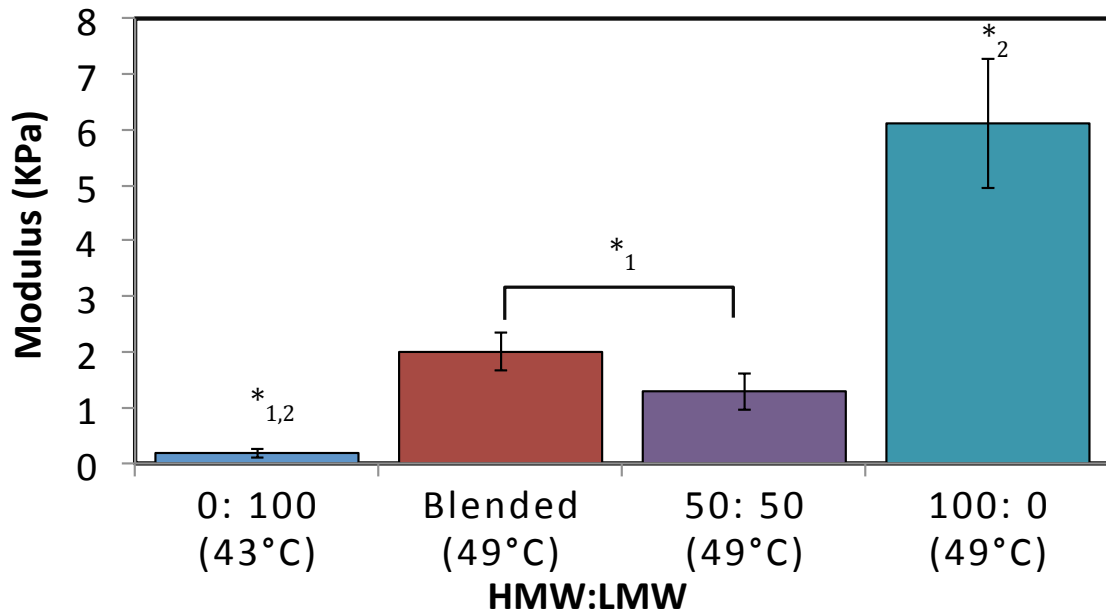
Figure 3.8. Compressive modulus of five day degraded scaffolds made using fusion temperatures at or above the T_g. Data are shown as means ± standard error (n≥3). $*_1$ $p<0.01$ $*_2$ $p<0.001$.

surface chains and leading to premature failure (Brown et al., 2008). The current method allows for full microsphere fusion of the scaffold around the porogen particles without loss of structural integrity, and it was not dependent on a solvent to sinter the microspheres equally. The proposed scaffolds can have an increased compressive modulus simply by increasing the molecular weight of the PLGA, and they also maintained a higher modulus throughout degradation by having a slower degradation rate, prolonging the time it will take to see a decrease in the modulus. Specifically, the presence of HMW microspheres in the blended and 50:50 scaffolds gave them a higher compressive modulus, and as the scaffold started degrading, the compressive modulus decreased due to LMW microsphere content. After five days of degradation, all of the scaffolds experienced a significant decrease in modulus, an important fact to consider depending on the intended site for implantation and the length of time needed for structural support. The LMW saw the highest loss of compressive modulus, followed by the blended and 50:50 scaffold, with the HMW scaffolds retaining the largest fraction of their initial modulus. Whereas muscle may take only approximately 10 days to regenerate, bone may take weeks or months (Lowry, 2006; Nettesheim, 1972).

Once the scaffolds are implanted, they will start to degrade, and cells will begin to infiltrate through the pores. The intended site for implantation will determine the compressive modulus necessary. For a trabecular bone implant, a compressive modulus of 50-78 MPa would be necessary (Lotz et al., 1990; Shea et al., 2000), whereas for articular cartilage, the compressive modulus has been reported to be approximately 0.079-2.1 MPa, depending on the location (Schinagl et al., 1997). The present study demonstrates that a wide range of compressive modulus can be obtained by varying the molecular weight of PLGA used and scaffold composition. The HMW scaffolds sintered at their T_g possessed a higher modulus and would be more suitable for higher load-bearing sites in comparison to other polymer scaffold preparation methods. LMW scaffolds sintered at their T_g or HMW scaffolds sintered below their T_g would be suitable for bone implants. The implant site, however, would have to be an area of relatively low load bearing, such as the upper extremities or cranial region. The present scaffolds have compressive moduli similar to those of other reported polymer scaffolds fabricated for such implants (Liu et al., 2010; Wu et al., 2004). The blended scaffolds could potentially

be used in an epiphyseal plate fracture since their five day degraded compressive modulus is 2.0 MPa, compared to 0.25-0.48 MPa reported for various regions of the growth plate, will lend the necessary structural support for the implant site (Sergerie et al., 2009).

3.4.2 Morphology

The morphology of the scaffolds was influenced by the molecular weight and microsphere composition, and the scaffolds could be fabricated to have different pore size and porosity even at the same degradation time points. Initially the scaffolds had comparable microstructure and porosity. The addition of pores helped create a greater surface area and reduced the amount of acid build up in the scaffold (Fu et al., 2000). The scaffolds degraded through ester linkage hydrolysis, creating lactic and glycolic acid monomers and oligomers that can diffuse out of the scaffold or be carried out as liquid circulates through the porous scaffold. The LMW scaffolds degraded the quickest because they had the lowest molecular weight chains of all the scaffolds in this study, resulting in fewer ester linkages, along with a higher number of carboxylic end groups, which slightly increased acidity of the scaffold interior, all contributing to a faster degradation (Houchin et al., 2008; Tracy et al., 1999). By day 5, the pore size of the LMW was almost doubled, whereas the HMW pore size had hardly changed, illustrating the effect of the increased molecular weight that contributed to a slower degradation time and increased swelling. The increased porosity at day 5 in the 50:50 scaffolds over the rest of the scaffolds is thought to have resulted from particles breaking off the outer surface of the scaffold as a result of mixing different types of microspheres that have different degradation rates. Certain areas of the scaffold could be primarily LMW microspheres that degraded quicker, creating voids and weaker areas in the material that caused neighboring particles, especially HMW, to break off while being shaken during sintering. This was apparent in images of the 50:50 scaffolds, which showed less homogenous porosity compared to the blended scaffolds, while the HMW scaffolds showed the smallest change in pore size. Inconsistencies in porosity can be attributed to the fabrication method that relies on hand mixing of the microspheres and NaCl particles.

A likely reason that the scaffolds containing HMW microspheres experienced significantly more swelling and maintained their swollen state longer is that they have

33

higher molecular weight polymer chains, and therefore more ester linkages, compared to the other microspheres. Furthermore, as the scaffolds containing HMW microspheres degraded, the entangled chains gradually loosened, and the accumulation of acidic monomers and oligomers entrapped in the polymer chains creating osmotic pressure and contributed to the swelling of the scaffold (Houchin et al., 2008; Kenley et al., 1987). At 95% degradation, all that remained was the HMW microsphere content of each of the scaffolds.

3.4.3 Gel Permeability Chromatography

The LMW scaffolds had a linear decrease in molecular weight throughout degradation, similar to the profile of LMW scaffold degradation. The HMW, blended, and 50:50 scaffolds (all containing HMW polymer) experienced a significant drop in molecular weight initially, likely due to the porous nature of the scaffold, and consequently increased accessible surface area, enabling accelerated bulk degradation. At 5 days, the HMW scaffolds maintained a higher molecular weight than the blended and 50:50 scaffolds, which was expected since the blended and 50:50 scaffolds contained 50% of the LMW polymer initially. After the first 3 weeks, the HMW, blended, and 50:50 scaffolds began to level off and became similar. At this point, the LMW polymer largely degraded, leaving the HMW component of each scaffold. As degradation continued, the chains became shorter and diffused out of the porous scaffolds, leaving only the longer chains that averaged approximately 10 kDa.

3.4.4 Degradation

PLGA hydrolysis takes place throughout the bulk of the material, not just at the surface (Burkersroda et al., 2002). This occurs at any place water can diffuse into, cleaving chains within the scaffold as compared to surface-eroding scaffolds that degrade one surface layer at a time. The rate at which the scaffolds degraded was dictated by the type of microspheres used for fabrication, allowing for degradation times from 40 days to 120 days. The degradation rate is known to be accelerated *in vivo* (up to two times faster than *in vitro*), which should be taken into consideration for design of porous PLGA scaffolds (Zolnik et al., 2008). The rate of degradation increased with the amount of LMW microspheres because of their shorter chain length and increased overall number of

34

carboxylic acid end groups, creating a more reactive, acidic environment. This trend can be seen by the increasing degradation rate going from 100:0 to 50:50 (HMW:LMW) or blended to 0:100 scaffolds. In the degradation study, the blended scaffolds were fabricated using a sintering temperature of 45°C, whereas the 50:50 scaffolds were sintered at 49°C but yielded similar degradation rates, a process that offers a new fabrication technique requiring a lower sintering temperature and yet still has the same overall degradation rate. There was a slight variance between the blended and 50:50 scaffolds degradation as seen in the time it took to reach 5% mass loss, 11 and 5 days respectively. Similar to the difference in porosity between blended and 50:50 scaffolds at 5% mass loss, the 50:50 scaffolds had some initial particle breakage, likely due to inconsistency of LMW and HMW microsphere mixing, that contributed to an increased initial mass loss as compared to the blended. The two scaffolds having a similar overall degradation rate could be advantageous should the scaffold be used as a drug delivery device either through the addition of a coating or encapsulating a drug/protein that is heat sensitive. Research on thermal degradation and heat shock proteins has shown that 45 to 47°C is the temperature of permanent denaturation that cannot be reversed (Kampinga et al., 1995; Westra et al., 1971). For example, amylase is used for treatment of pancreatitis but starts to become denatured around 50°C, especially with extended time, which would make it difficult to encapsulate in the 50:50 or HMW scaffolds without compromising the bioactivity (Liang-chang et al., 1992; Yadav et al., 2009). The time to reach 50% degradation increased with polymer molecular weight, as expected. By the time the scaffolds reached 95% degradation, their volume had decreased significantly, retaining only 3-5% of the volume seen at 50% degradation. What remained was the center part of the scaffold that had experienced the least amount of fluid exchange. Limited fluid flow ultimately decreased the degradation and swelling of the center most part of the scaffold, as reflected by the porosity and pore sizes that were similar to those seen initially and at 5 day degraded.

3.4.5 Mechanical Properties

In comparing current mechanical results to other porous PLGA polymer scaffolds, the compressive modulus obtained here was significantly higher than scaffolds made with a variation to or entirely without the sintering step. Wu et al. reported a dry compressive

35

modulus of 7.7 MPa following a modified room temperature compression molding method to create a porous scaffold, where PLGA (85:15) microspheres were mixed with a porogen in solvent fusing the microspheres, as opposed to the present sintering method (Wu et al., 2004). Not only are their moduli lower by over ten-fold, the use of high concentrated solvents can be damaging to any encapsulated proteins (Asakura et al., 1978; Wu et al., 2004). More similar to the methods used in this study, Lu et al. developed a PLGA (MW= 50,000 Da) scaffold out of microspheres made through W/O/W emulsion, followed by sintering at 70°C for 20 hours, to generate scaffolds having dimensions of 0.5 cm diameter and 1.0 cm in height. These materials differed from the present scaffolds by the lack of compression resistance, varying processing temperature, time and scaffold dimensions. Lu et al. reported a compressive modulus of ~26 MPa, an increase over solvent-based scaffolds, but still not as high as ~110 MPa obtained in the current study (Lu et al., 2003). Little information is published about the compressive modulus of degraded, porous, PLGA scaffolds tested in their wet state, which was used to simulate more of an *in vivo* environment. The present study shows the importance of reporting this data since only 5 days of degradation and testing the scaffolds in their wet state attributed to a significant decrease in compressive modulus.

The effect of varying temperature and length of sintering time is shown in the work of Jiang and Laurencin, where the compressive modulus increased with temperature and time (Jiang et al., 2006). Their work showed how increasing the temperature from 100 to 110 to 115°C, while maintaining a sintering time of 4 hours, will significantly increase the compressive modulus from ~232 to 341 to 429 MPa. Additionally, increasing the sintering time from 4 to 6 hours, while holding the sintering temperature at 100°C, showed an increase in compressive modulus from 340 to 412 MPa.

In order to improve the mechanical properties of biodegradable materials, some groups mix the PLGA scaffold with hyaluronic acid (HA), chitosan, poly(ethylene glycol) (PEG), ceramic fillers (Miao et al., 2007). Addition of another material adds the complexity of fabrication, biocompatibility, and potentially higher sintering temperatures that would be damaging to any drug or protein in the scaffold (Jiang et al.; Popp et al.). Other methods are also employed to make PLGA scaffolds but are unable to obtain the compressive moduli presented. Gas foaming and salt leaching scaffolds with similar

porosity can only obtain a compressive modulus 100X lower than the current method (Harris et al., 1998; Nazarov et al., 2004).

3.5 Conclusion

The present study showed the significance of the sintering temperature and how the additional step of sintering at or above T_g changed the microstructure of microsphere-based PLGA scaffolds by allowing for the microspheres to fuse together. Overall, a novel blended microsphere-based scaffold was developed that required only a 45°C sintering temperature while still maintaining a similar degradation rate to the 50:50 scaffolds, which required a 49°C sintering temperature. This could potentially be important when a heat sensitive drug or protein is encapsulated in the microspheres. Furthermore, the heat sintering step allowed for fusion of the microspheres, which played a significant role in determining the range of attainable mechanical properties. Properties similar to hard and soft tissue were obtained, expanding applicability of the scaffolds. The compressive moduli achieved here (~50-110 MPa dry and ~0.2-6 MPa for five day degraded), along with the degradation rates (40-120 days), can be tailored to fit a specific range as well, yet the fabrication method minimizes use of solvents and avoids high temperatures that would be damaging to encapsulated proteins or drugs. The only alterations needed during the fabrication process are molecular weight and sintering temperature. The present results show the versatility of a simple PLGA scaffold system that can be "tuned" to meet requirements for different tissue engineering applications.

Chapter 4 Retention of Insulin-like Growth Factor I Bioactivity during Fabrication of Sintered Polymeric Scaffolds

4.1 Introduction

Drug- or growth factor-encapsulating devices offer an alternative to localized injections or oral dosage forms and can help improve tissue repair at the site of implantation. Furthermore, fabricating a device (or scaffold) that is biodegradable and biocompatible eliminates the need for retrieval surgery or potential long-term effects, sometimes associated with metal-based implants (Black, 1984; McGee et al., 2000; Steinemann, 1996). While polymeric implants have certain advantages over metals, there are still some barriers in creating a polymeric drug delivery system. Some of the difficulties associated with encapsulating drugs or growth factors into a scaffold are controlling the drug loading and release rate while maintaining bioactivity (Ghaderi et al., 1997; Lu et al., 1995; McCall et al., 2012; Steinemann, 1996; Tabata et al., 1993). By changing the material properties and scaffold fabrication technique, a balance between each of these difficulties can be reached. Fabricating the scaffold from polymeric microspheres allows for control over the drug loading by adjusting the amount of drug added and type of polymer used. Additionally, choosing a polymer that has a tunable degradation rate will allow control over the drug release rate when the drug or protein incorporated has a degradation-controlled release (e.g., macromolecules such as proteins). Finally, using a fabrication method that does not require extreme temperatures or harsh solvents can prevent loss of drug bioactivity.

Poly(lactic-co-glycolic) acid (PLGA) is a material that possesses all the necessary properties to develop a drug delivery device. It has been used extensively to encapsulate hydrophilic and lipophilic drugs (Lee et al., 2004) and proteins (Benita, 2006) . PLGA systems are currently approved for drug delivery in the form of microspheres for the treatment of prostate cancer (Lupron Depot®) and endometriosis (Zoladex®). To alter the drug release rate and degradation time of the microspheres, the properties of PLGA can be changed. PLGA comprises polymeric chains made up of lactic and glycolic acid. Changing the ratio of lactic acid to glycolic acid, the end group terminating the

macromolecules, or the overall length of the chain (e.g., molecular weight) will affect the degradation time.

Besides the already FDA-approved drug delivery systems, a wide range of research currently exists on encapsulating growth factors into scaffolds. Growth factors can be quite effective for tissue regrowth and can promote cell proliferation and differentiation. Insulin-like growth factor I (IGF-I) is a commonly used growth factor because it has the ability to increase proliferation of various cell types, such as mesenchymal stem cells, osteoblasts, and chondroblasts, that form new tissue. Studies showed that IGF-I increased bone growth and increased aggrecan and collagen-II content *in vivo* (Damien et al., 2003; Hock et al., 1988; McCarthy et al., 1989; Morisset et al., 2007; Yun et al., 2007). Also, IGF-I soaked into cartilage disks caused an increase in matrix deposition and glycosaminoglycan (GAG) production (Guenther et al., 1982). For IGF-I to be effective, however, the bioactivity must not be comprised when the growth factor is being incorporated into an implant or scaffold. This area of research has been often overlooked, and the IGF-I bioactivity must be verified. Some scaffold fabrication methods require elevated temperatures, mechanical forces, and harsh solvents that could potentially denature proteins and compromise the bioactivity of an incorporated growth factor (Coleman et al., 2012; England et al., 2011; Yeo et al., 2001). Currently, IGF-I denaturation is mostly studied in agricultural research involving the proteins in cow milk and the effects of milk processing at temperatures exceeding 100°C, and these findings are not necessarily translatable to scaffold fabrication techniques (Collier et al., 1991; Yun et al., 2007).

The objective of the present studies was to investigate whether incorporation of IGF-I into PLGA scaffolds formed by a microsphere sintering method compromised bioactivity. Specifically, activity of IGF-I was measured after being heat-treated in solution and then again after it had been released from PLGA scaffolds. The scaffolds used in this study have been previously characterized (Clark et al., 2013), and their mechanical properties can be suitable for soft or hard tissue applications. Addition of IGF-I to the scaffolds would provide the potential to enhance tissue regrowth and reduce recovery time.

4.2 Material and Methods

4.2.1 Microsphere Fabrication

Poly(lactic-co-glycolic acid) (50:50, acid-terminated; Durect Corporation, Pelham, AL) with an inherent viscosity of 0.55–0.75 dL/g (molecular weight approximately 40 kDa) was used. PLGA microspheres were fabricated using a water/oil/water ($W_1/O/W_2$) emulsion technique. Two types of PLGA microspheres were fabricated, blank and IGF-I-loaded, which differed only in the W_1 phase. The W_1 phase was phosphate-buffered saline (PBS), pH 7.4, for blank microspheres, whereas the W_1 phase for the IGF-I loaded microspheres contained 1.1 mg/mL IGF-I (PeproTech, Rocky Hill, NJ) in PBS, targeting a release of 2-20 ng/mL. For both types of microspheres, the oil phase (O) consisted of PLGA dissolved in dichloromethane (DCM) at 13wt/v%, and the W_2 phase was made by dissolving 1% poly(vinyl alcohol) (PVA; Sigma-Aldrich, St. Louis, MO) into deionized water. W_1 was emulsified into the O phase by sonication at 25 W for 10 seconds. The W_1/O was homogenized into W_2 at 3500 rpm for 3 minutes. The resulting microspheres were stirred overnight, washed six times in deionized water, and lyophilized. Only microspheres <250 μm were used for scaffold fabrication.

4.2.2 Scaffold Preparation

Scaffolds were fabricated using a salt-leaching method at a weight ratio of 40:60 (microspheres:salt) (Clark et al., 2013). The salt size was <150 μm, controlled through grinding and sieving. Each scaffold was weighed out individually into a 0.6 mL microcentrifuge tube and mixed by hand for 45 seconds. The mixture was then compressed for 2 minutes at 1.5 ton using a 6 mm diameter die in a Carver press. The scaffolds were then incubated for two days at 49°C, the glass transition (T_g) temperature of the PLGA used, which allowed for the microspheres to fuse around the NaCl particles. Lastly, the scaffolds were stirred in deionized water overnight to leach out the NaCl particles and dried the following day. The final mass of the scaffolds was approximately 41 mg, with scaffold dimensions of 6.0 mm in diameter and a thickness of 2.4 mm, with an overall porosity of approximately 70%. Scaffolds were disinfected by washing in 70% ethanol and twice in cold PBS.

40

4.2.3 Encapsulation Efficiency and Loading

Encapsulation efficiency was measured by dissolving microspheres in DCM and then adding acetone at a volume ratio of 3:7 (DCM:acetone) followed by centrifugation at 14,000 g for 5 minutes and discarding the supernatant. The sample was washed and centrifuged three times using the DCM/acetone mixture and then left overnight for solvent evaporation. The dried samples were rehydrated in PBS, and the protein concentration was measured using MicroBCA assay (Thermo Fisher Scientific, NJ) according to the manufacturer's instructions.

4.2.4 Release Study

Scaffolds were placed in 12-well plates with 4 mL PBS and incubated at 37°C while on an orbital shaker. The supernatant was collected every 3-5 days and stored at -20°C until analyzed. Before being assayed, the supernatant was concentrated using centrifugal filters having a molecular weight cutoff of 3,000 Da (Amicon Ultra; Millipore, MA) following the manufacturer's instructions. The MicroBCA assay was then used to quantify the IGF-I concentration at each time point.

4.2.5 Bioactivity Studies

Two experiments were conducted to verify the bioactivity of IGF-I. First, the IGF-I activity was measured after incubated growth factor solutions at elevated temperatures for two days, and in the second, activity was determined as the IGF-I was released from the scaffolds during degradation. Before starting these experiments, effects of known concentrations of IGF-I (0-100 ng/mL) were examined to ensure samples were within the linear range of cell responsiveness to the growth factor. Both of the experiments used the same initial conditions, where SaOS-2 human osteosarcoma cells (ATCC HTB-85) were seeded in McCoy's 5A medium supplemented with 10% fetal bovine serum (FBS; HyClone, ThermoScientific) at a density of 2.5×10^4 cells/mL and allowed to attach overnight.

To test the bioactivity of IGF-I after being incubated at elevated temperatures for two days (which is experienced during scaffold fabrication, as described in the Scaffold Preparation section), an IGF-I solution with a concentration of 12 µg/mL in PBS was incubated at 37, 43, 45, 49, or 60°C for two days. A day after cell seeding, heat-treated

41

IGF-I solution was diluted into McCoy's 5A medium containing 0.1% charcoal and dextran-treated fetal bovine serum (CDTFBS), which has reduced serum levels of growth factors, and added to the cells. The overall IGF-I concentration in medium was adjusted to 12 ng/mL, which pilot studies demonstrated was within the range of SaOS-2 responsiveness. The positive control was an IGF-I solution with no heat treatment, and the negative control was incubated at 100°C.

To measure the bioactivity of IGF-I released from the protein-loaded scaffolds, release supernatant was diluted in McCoy's medium containing 0.1% CDTFBS to be within the linear range of the IGF-I dose response. The released supernatant made up 15% of the total well volume. The same study was performed using unprocessed IGF-I to create a standard curve of expected cell proliferation based on a given IGF-I concentration.

At the end of both experiments, cell proliferation was assessed by measuring DNA contents with a Hoechst assay adapted from Labarca et. al (Labarca et al., 1980). Briefly, each well was washed twice with PBS before salt solution (50 mM NaH_2PO_4, 2 M NaCl, 2 mM EDTA) was added and sonicated for 10 seconds at 25 W. Hoechst 33258 (Sigma-Aldrich) was added to a final concentration of 1.25 µg/mL, shaken, and left in the dark. Ten minutes later, fluorescence readings (λ_{ex}= 356 nm, λ_{em}=458 nm) were taken. Bioactivity, reflected by cell proliferation, was expressed as a percentage of the effect of control treatments.

4.2.6 Bone Marrow Stromal Cell Responses

Bone marrow stromal cells were harvested from 40-45 days old Sprague-Dawley rats shortly after euthanization. The femurs were dissected and the epiphyses removed. The diaphyses were flushed with MEM, Alpha modification medium (αMEM; HyClone, ThermoScientific) containing 10% FBS and antibiotic-antimycotic solution (100 U/mL penicillin G, 100 µg/mL streptomycin, 250 ng/mL amphotericin B; HyClone, ThermoScientific). The cells were transferred to a flask and cultured. Once confluent, the cells were seeded onto either blank or IGF-I-loaded scaffolds at a density of 150,000 cells per scaffold with 4 mL of αMEM containing 0.5% transferrin and 0.05% sodium selenite. The wells were coated with 2% agarose to prevent cell adhesion on the polystyrene, which enabled measurement of cell activity on only the porous PLGA scaffolds. The

42

medium was changed every 2-3 days. After three and six weeks of culture, the scaffolds were washed twice with PBS and transferred to a 2 mL microcentrifuge tube and incubated with 300 μL Cell Lytic-M (Sigma-Aldrich, St. Louis, MO) for 15 minutes on an orbital shaker. Afterwards, the samples were centrifuged for 15 minutes at 12,000 g. The cell lysate was assayed according to the manufacturer's instructions for DNA and GAG content using a Quant-iT$^{©}$ PicoGreen™ Assay (Thermo Scientific, NJ) and Blyscan™ Glycosaminoglycan Assay, respectively. In addition, alkaline phosphatase activity was measured to assess pre-osteoblastic response. Briefly, the substrate consisted of 10 mM *p*-nitrophenyl phosphate in 0.6 M 2-amino-2-methyl-1-propanol buffer solution (pH 10) and just before use 4 mM magnesium chloride was added. In a 96-well plate the sample was mixed with the substrate at a 1:3 ratio (sample:substrate) and read at 400 nm (Vreven et al., 1973).

4.2.7 Statistics

Analysis was carried out using GraphPad InStat software running ANOVA followed by a Tukey–Kramer Multiple Comparisons Test. Results were considered significant if $p < 0.05$.

4.3 Results

4.3.1 Encapsulation Efficiency and Loading

The encapsulation efficiency of IGF-I in PLGA microspheres was found to be 38±3% for a total loading of approximately 0.5 μg of IGF-I per mg of microspheres. Each scaffold contained 18-23 μg IGF-I. As reported previously (Clark et al., 2013), initial porosity of the scaffolds was 63% with an average pore size of 49 μm.

4.3.2 IGF-I Release

Figure 1 shows the release of IGF-I from the scaffolds over time. In the first five days, there was an initial release of 1.28 μg IGF-I per day, followed by a decreased rate of 0.24 μg/day through day 10, after which it became 0.11 μg/day throughout the rest of the release. The scaffolds degradation was done previous where full degraded was reached at 120 days (Clark et al., 2013).
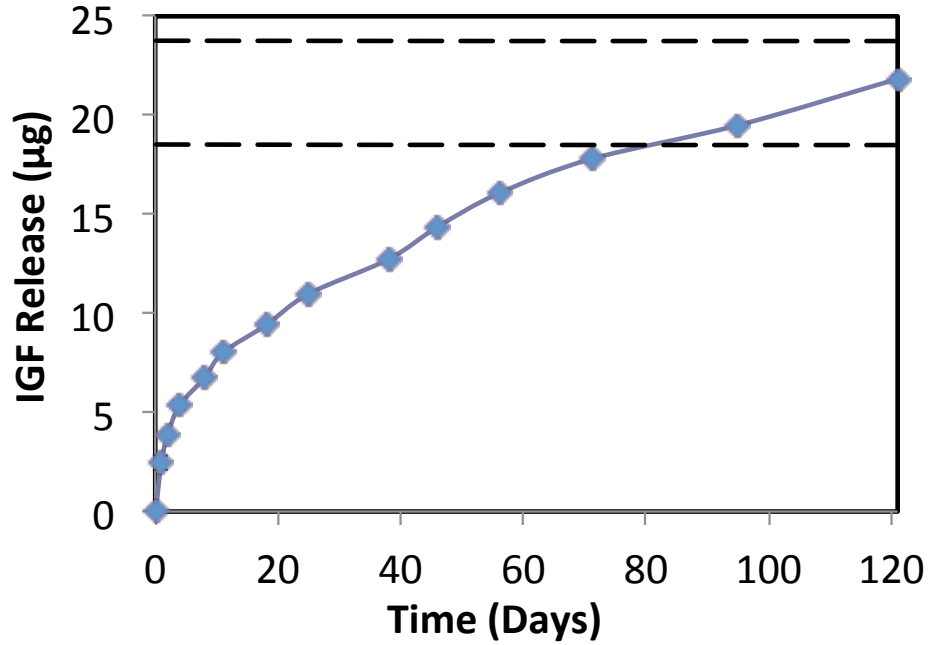
Figure 4.1. Cumulative release of IGF-I release from PLGA scaffolds. The dashed lines represent the range of expected drug release based on the loaded amount. Data are mean ± standard deviation (n=3). Standard deviation is shown, ranging from 0.06-0.12 μg.

4.3.3 IGF-I Dose-Response

To determine the concentration-dependent effect of IGF-I on cell proliferation, DNA contents were measured for SaOS-2 cells cultured with IGF-I at increasing concentrations. Figure 2 shows that IGF-I began to have an effect at 2 ng/mL and then reached the maximal effect around 20 ng/mL.

4.3.4 Bioactivity of IGF-I

The bioactivity of IGF-I solutions was tested after incubation for two days at 37, 43, 45, 49, 60 or 100°C. The solutions incubated at 37, 43, 45, and 60°C caused a statistically significant increase ($p<0.001$) of about a 140% in cell proliferation compared to cultures without growth factor (Figure 3). Proliferation in response to solutions that were not incubated (preserved at 4°C) or incubated at 37, 43, 45, 49, and 60°C was not significantly different. The negative control (100°C) was not statistically different than cells cultured without growth factor, indicating that heat treatment to 100°C eliminated IGF-I activity.

Bioactivity of the supernatants collected throughout the period of degradation of IGF-I-loaded scaffolds was measured at the time points 1, 24, 31, 43, 57 days. The actual activity was compared to the expected activity based on mitogenicity of unprocessed IGF-I at the same concentration. The results are shown in Figure 4, where 100% activity indicates no loss of bioactivity. The percentages of expected activity (±SEM) were 97±6, 110±8, 102±2, 100±8 and 91±4% at 1, 24, 31, 43 and 57 days, respectively, and were not statistically different from 100%.

4.3.5 Bone Marrow Stromal Cell Responses

Figure 5 shows that the encapsulation of IGF-I in microspheres caused an increase in DNA production at 3 and 6 weeks compared to the blank scaffolds. A statistically significant difference ($p<0.01$) was seen between the blank and IGF-I-loaded scaffolds at 3 weeks with 4.1±0.7 and 10.6±2.3 μg of DNA and at 6 weeks with 4.0±1.0 and 5.08±0.9 μg of DNA, respectively. There was an overall significant decrease in DNA between 3 and 6 weeks for the IGF-I scaffolds ($p<0.01$) but not for the blank scaffolds. The GAG content is shown in Figure 6, where no statistical difference was seen at 3 weeks between the blank and IGF-I-loaded scaffolds with 1.9±0.3 and 1.8±0.1 μg of GAG, respectively.
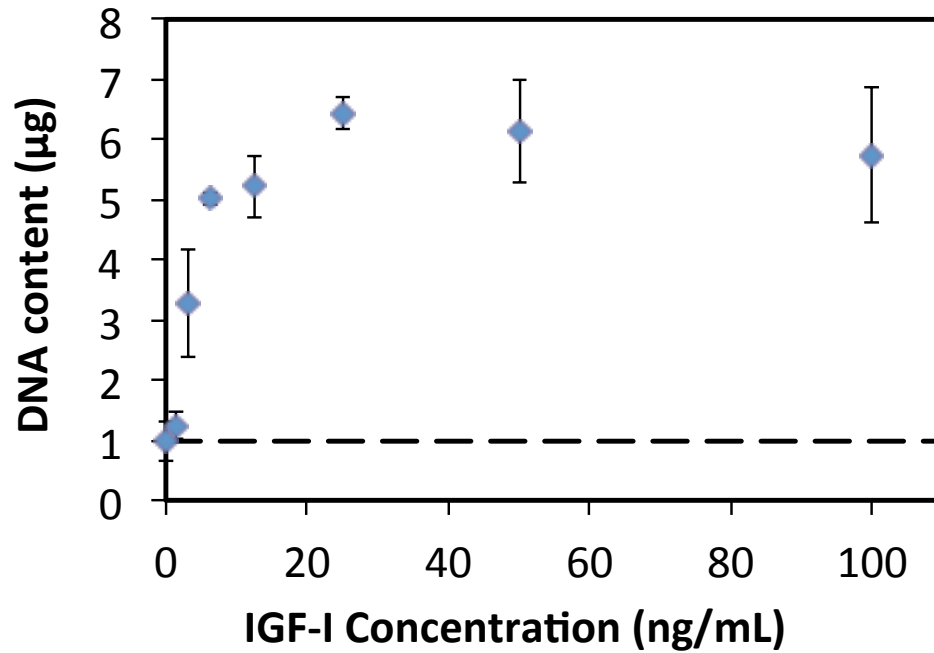
Figure 4.2. Concentration-dependent effect of IGF-I on cell proliferation measured by DNA content, showing a plateau after approximately 20 ng/mL. The dashed line represents the control where no IGF-I was added. Data are mean ± standard deviation (n=3).
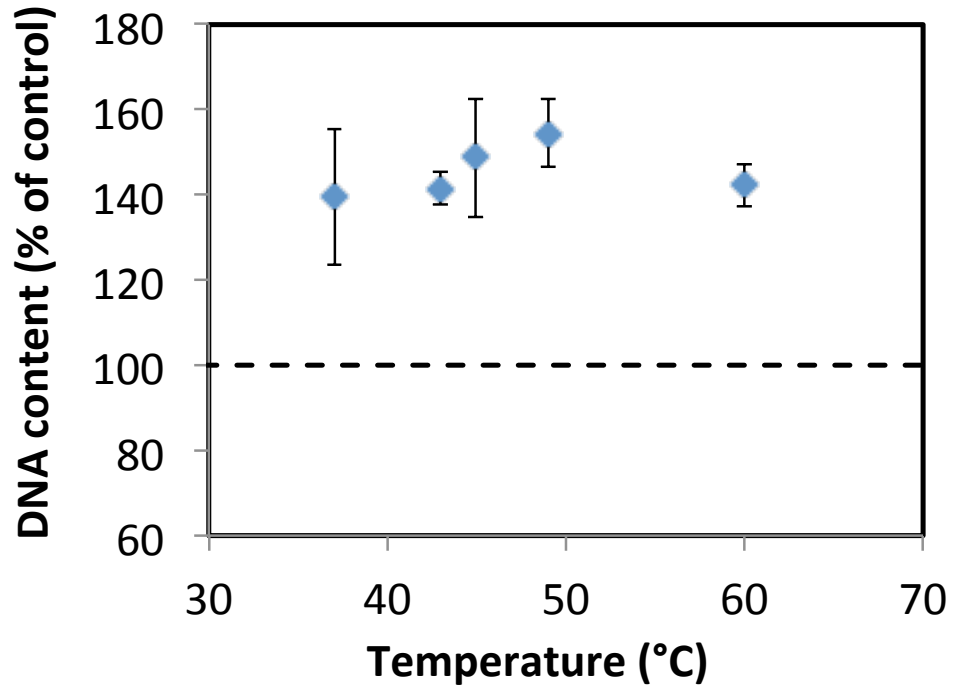
Figure 4.3. Effect of heat-treated IGF-I solution on cell proliferation as measured by DNA content. The dashed line represents the DNA content in cells cultured without growth factor. IGF-I solution that had been incubated at increasing temperatures for 2 days. Data are mean ± standard deviation (n=3).
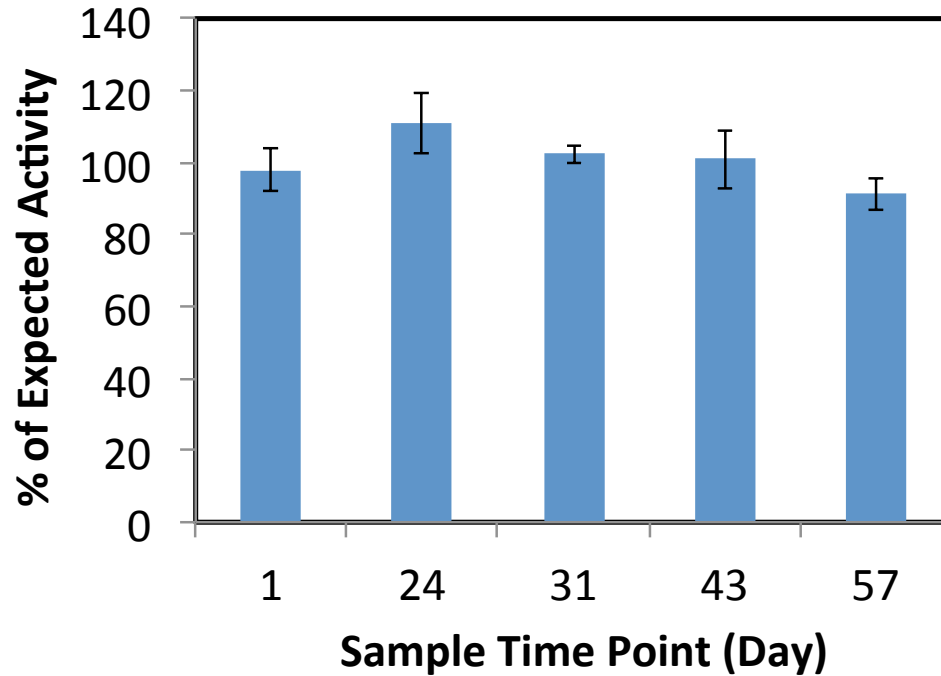
Figure 4.4. Bioactivity of IGF-I in the release supernatant at increasing times scaffold degradation. Each time point was compared to the expected level of activity for the amount of IGF-I released at the respective time point. Data are mean ± standard deviation (n=3).
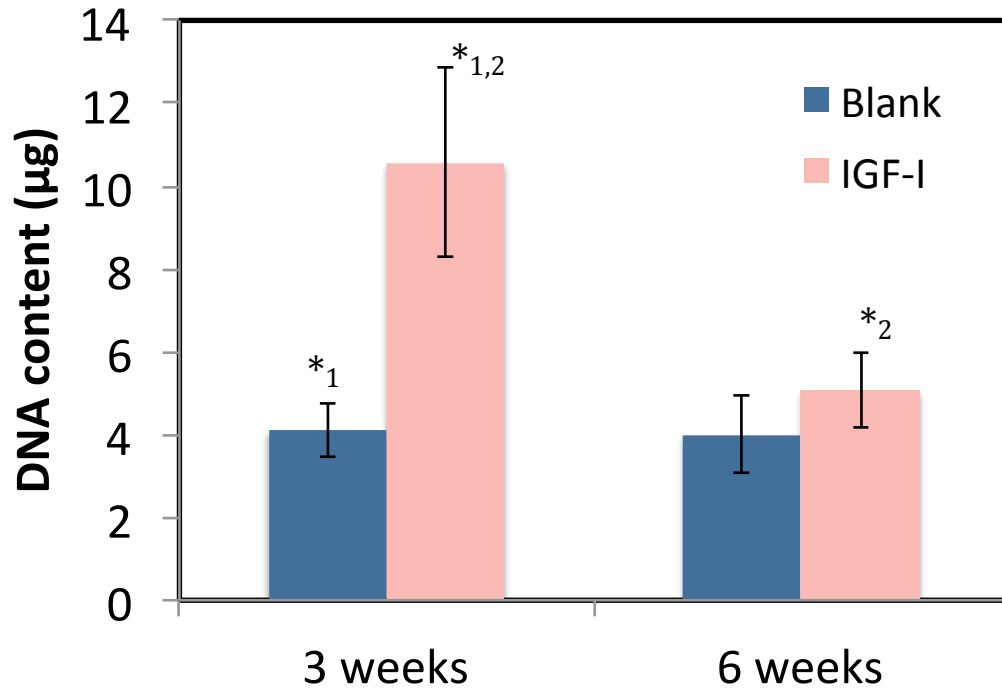
Figure 4.5. DNA content after culturing BMCs on blank and IGF-I-loaded scaffolds for 3 and 6 weeks. Data are mean ± standard deviation (n=3). $*_{1,2}$ $p<0.001$
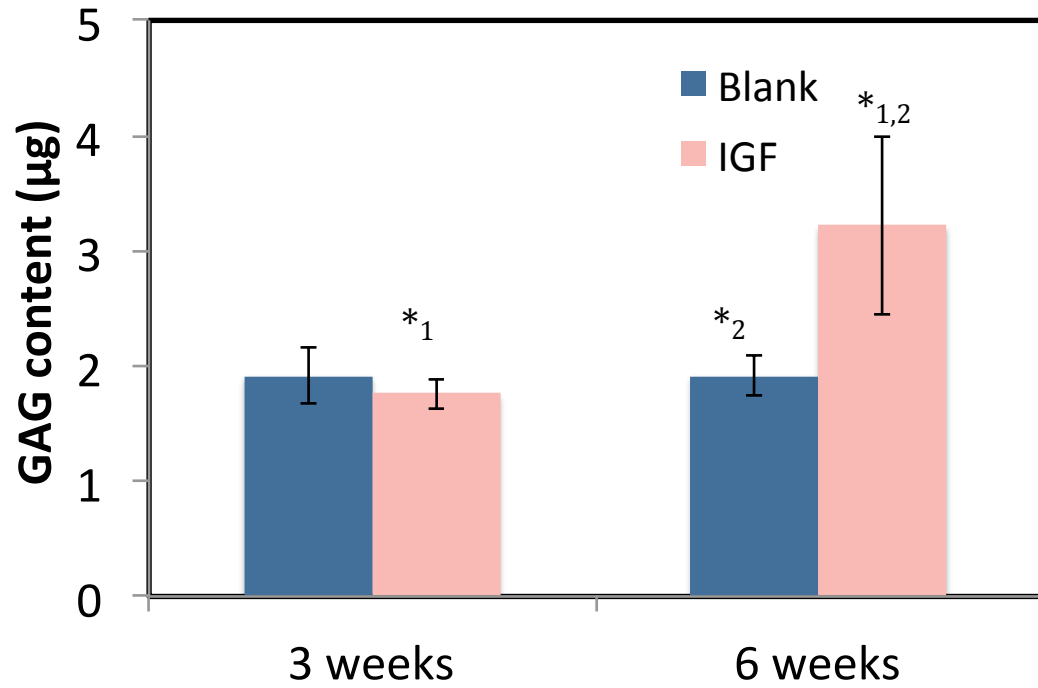
Figure 4.6. GAG content after culturing BMCs on blank and IGF-I-loaded scaffolds for 3 and 6 weeks. Data are mean ± standard deviation (n=3). *[1,2] $p < 0.001$

After 6 weeks, the blank scaffolds showed no change in GAG content at 1.9±0.2 µg, while the IGF-I-loaded scaffold saw a significant increase to 3.2±0.8 µg of GAG ($p < 0.01$).   AP activity did not increase between 3 and 6 weeks, and no significant difference was seen between scaffold types (results not shown).

4.4 Discussion

4.4.1 IGF-I Release

PLGA has been widely used for drug delivery options in the form of microspheres and scaffolds (Cohen et al., 1991; Crotts et al., 1998; Makadia et al., 2011; Schwendeman, 2002). PLGA microspheres can be advantageous for injectable delivery due to their size, but they present more of a problem for extended release due to drug diffusion and the large surface area of microspheres. The release profile of PLGA microspheres commonly starts with an initial burst followed by a second phase of sustained release and then a third phase of a slower sustained released (Garcia et al., 1999; Raghuvanshi et al., 1993). The initial burst release is caused by a combination of drug dissolution from microsphere surfaces and initial diffusion. The second phase is attributed to diffusion from deeper in the microspheres and initial matrix degradation, whereas the third phase is primarily due to matrix degradation.

The amount of IGF-I released from microspheres during the initial burst usually accounts for a large portion of the overall loaded protein and can be an excessive amount, not necessary to see an effect and can possibly cause adverse effects such as swelling and joint aches (Nehrer et al., 1997). Approximately 20% of the IGF-I loaded in PLGA microspheres, using the same type of PLGA (50:50) polymer as in the present study, was released within the first 24 hours of a 13-18 day degradation time, releasing 1.1 to 2.2 µg of IGF-1 (Elisseeff et al., 2001; Meinel et al., 2001). IGF-I burst release also occurs in other scaffold types, such as tricalcium phosphate, which released 10-78% of the protein within 24 hours when degraded in water and serum, respectively (Laffargue et al., 2000). The present results, however, showed that sintering the microspheres into a scaffold reduced the 24 hour burst, with 20% release not reached until three days. The decreased burst release can also be attributed to the microsphere wash steps to remove surfactant and the salt leaching process, both of which reduced the amount of surface protein.

51

Altering the burst release will help prevent drug loss during the initial increase in blood flow around the implant site as a result of the inflammatory response (Guo et al., 2010).

Other methods for decreasing the burst release from microspheres involve changing the polymer properties (molecular weight, end group, and lactic to glycolic ratio), polymer concentration, PVA concentration, the water phase volume, and homogenization speed during microsphere fabrication (Mao et al., 2007). Mao et al. evaluated each step of the W/O/W process and found that increasing the PVA concentration, homogenization speed, and drug loading or decreasing the water phase (W_2) volume and drug molecular weight all caused a decrease in the burst release. Another way to avoid the burst is pre-degrading/washing the microspheres, and start the drug release after the initial burst (Hickey et al., 2002). However, this could be costly to waste expensive drugs or growth factors, and it reduces the amount of drug delivered.

The present IGF-I loaded scaffolds released 50% of the IGF-I within the first 24 days, which is a crucial time frame to allow for the development of new tissue ingrowth throughout the scaffold. New bone tissue can take 4 weeks to fill a non-critical size wound (Uematsu et al., 2005), and cartilage formation can take 2 weeks before GAG and collagen I and II production become apparent based on histological staining for GAG chondrogenic markers (Veilleux et al., 2005). Capito et al. saw an effect of scaffold fabrication on DNA and GAG content at 2 weeks. Their collagen scaffold with and without crosslinking IGF-I plasmid into the scaffold resulted in no significant difference without the crosslinking. Additionally, they seeded 4 million cells onto their scaffold compared to the 150,000 cells in this study, which could be another factor in the non-significant difference of GAG content with and without IGF-I (Capito et al., 2007).

Techniques used to decrease the burst release from scaffolds include varying the internal porosity and microstructure of the scaffold. To alter the internal porosity of the microspheres, it has been shown that increasing the temperature during the second emulsion to 38-42°C resulted in a lower burst release, which may be a problem for drug bioactivity (Yang et al., 2000). For PLGA scaffolds, the burst release is also affected by the scaffold porosity, which increases surface area and allows for more drug diffusion. However, interconnected pores in a PLGA scaffold help prevent acid build up and allow for cell migration into the scaffold, improving tissue ingrowth (Fu et al., 2000). Using a

non-porous PLGA (50:50) system can have a negative effect on the implant site and inhibit new tissue formation (Rhee et al., 2007). The present scaffold fabrication method yielded an overall scaffold porosity of approximately 70%, yet eliminated the burst release (Clark et al., 2013).

4.4.2 Bioactivity of IGF-I

Some growth factors, such as vascular endothelial growth factor, transforming growth factor-beta and bone morphogenetic protein 2, have already been shown to maintain their bioactivity after heat treatment or solvent interaction (Gentry et al., 1990; Lawrence et al., 1985; Lyons et al., 1988; Schwarz et al., 2013; Winkler et al., 2006). Jabbarzadeh et al. incorporated vascular endothelial growth factor into sintered PLGA scaffolds and were able to show retained bioactivity (Jabbarzadeh et al., 2012). However, little is known about the effects that scaffold fabrication will have on IGF-I protein and the ability to maintain bioactivity. IGF-I encapsulated in PLGA retained mitogenicity. The small amount loaded, which was appropriate for achieving physiologically relevant concentrations of the growth factor, was at least partially responsible for avoiding adverse effects because of solvent exposure. Regarding the influence of temperature during scaffold sintering, most of the research surrounding heat treatment of IGF-I is in the agricultural sciences studying the protein in bovine milk during pasteurization. Collier et al. examined IGF-I denaturation after heat treatment at 121°C for 5, 15, and 30 minutes and found that, after only 5 minutes, 93% of the IGF-I was unrecognizable and therefore considered denatured (Collier et al., 1991). Even heat-treating IGF-I at 75 or 85°C for 15 minutes caused a decrease of 45 and 45.2%, respectively, in active IGF-I (Kang et al., 2006). Furthermore, the same group found that heating IGF-I to 121°C, resulted in no active IGF-I.

The present study analyzed the temperature range of 37-60°C, which was used for scaffold fabrication. The temperatures were based on glass transition temperature of different types of PLGA used to fabricate the scaffold (Clark et al., 2013). After 2 days of incubation at these elevated temperatures, IGF-I retained full bioactivity as shown by the analysis of cell proliferation compared to non-heat-treated growth factor. Additionally, there was no effect from scaffold fabrication, involving the use of solvents, sonication, homogenization, and compression, on IGF-I bioactivity. Other types of PLGA scaffolds

53

containing IGF-I have been fabricated using solvents, but no heat treatment was used. Jaklenec et al. verified the bioactivity of IGF-I as it was released from scaffolds using a MCF-7 proliferation assay similar to the present methods (Jaklenec et al., 2008). The scaffolds were fabricated using dichloromethane vapor method, whereas the current method used temperature treatment to fuse the microspheres. Heat treatment (or sintering) allows for a 10-fold increase in mechanical properties compared to non-sintered scaffolds (Clark et al., 2013). No mechanical properties were reported for scaffolds fabricated using solvent vapor (Jaklenec et al., 2008).

4.4.3 Bone Marrow Stromal Cell Responses to Growth Factor

Seeding cells on tissue engineering scaffolds allows cell infiltration and subsequent tissue responses. For example, pore sizes of 20-120 μm have been shown to be appropriate for cell infiltration in scaffolds for hard and soft tissues regeneration (Lee et al., 2004; Nehrer et al., 1997; Sundararaj et al., 2012). Although the present study focused on bioactivity measurements, we have previously demonstrated infiltration of cells into our scaffolds (Sundararaj et al., 2012). In the present studies, encapsulation of IGF-I into PLGA scaffolds increased cell proliferation. Prolonged release of IGF-I continued to have an effect on bone marrow stromal cells since there was a 2.6 fold increase at 3 weeks and a 1.3 fold increase at 6 weeks over blank scaffolds. In other studies, Longobardi et al. showed that IGF-I had an effect on chondrogenesis through increased cell proliferation, decreased apoptosis, and increased collagen II expression (Longobardi et al., 2006). Their findings on IGF-I dose-dependent cell proliferation were similar to the present data, which show that the IGF-I effect plateaued around 20 ng/mL.

The DNA production between 3 and 6 weeks did not change for the blank scaffolds but significantly decreased in the IGF-I-loaded scaffolds, which was likely due to a combined effect of scaffold degradation, cell maturation, and scaffold saturation. Between 3 and 6 weeks, the scaffolds lost approximately 30% mass, for a total of 12.6 mg, which accounts for a total of 57% of the total volume reported in previous studies (Clark et al., 2013). Normalizing the DNA content to milligrams of scaffold remaining, the IGF-I scaffolds had 0.28 ± 0.06 μg of DNA per mg of scaffold at 3 weeks, significantly ($p < 0.01$) more than the blank scaffolds had with 0.11 ± 0.02 μg. The same trend was seen at 6 weeks, though not statistically significant, where the IGF-I-loaded

www.manaraa.com

scaffolds had more DNA content per milligram of scaffold than the blank scaffolds with 0.20 ± 0.04 μg and 0.16 ± 0.04 μg, respectively. The combined effect of scaffold mass loss and scaffold saturation can account for the similarity in DNA contents seen between the IGF-I-loaded scaffolds and blank scaffolds at 6 weeks, and it may not be due to a lack of IGF-I activity but rather a lack of space or surface area for cell proliferation.

The increased cell content seen at 3 week did not cause an effect on GAG content, with no statistical difference in GAG content between the blank and IGF-I-loaded scaffolds. However, at 6 weeks the GAG content in IGF-I-loaded scaffolds was 1.7 times higher than that in the blank scaffolds. It has been reported that human marrow cells can take 2-4 weeks before showing chondrogenic markers or producing GAG, so it is possible that a difference in GAG content between the scaffold types may not be detectable at 3 weeks (Martin et al., 1998; Pittenger et al., 1999). Lastly, it is relevant to note that alkaline phosphatase, commonly used as an indicator of early osteoblastic activity (Rajamannan et al., 2003; Van der Kraan et al., 2002; Weinreb et al., 1990), was not increased during the 6 weeks of culture of bone marrow stromal cells on either the blank or IGF-I-loaded scaffolds.

4.5 Conclusion

The present study demonstrated that sintering IGF-I-loaded, PLGA microspheres into three-dimensionally porous scaffolds allowed for the release of active IGF-I. Scaffold fabrication process and temperatures up to 49°C did not compromise the bioactivity of IGF-I. Cell proliferation was initially enhanced with the addition of IGF-I to the scaffold, which lead to an eventual increase in GAG production after 6 weeks. Additionally, the sintered scaffolds eliminated the typical initial burst release seen with PGLA microspheres. Preventing the burst release helps to reduce growth factor waste, avoid adverse effects possibly caused by a large localized dose of growth factor, and instead creates a long slow release (~120 days) that can aid in tissue repair and growth.

Chapter 5 Mechanical Properties and Dual Drug Delivery Application of PLGA Scaffolds Fabricated with a Poly(β-amino ester) Porogen

5.1 Introduction

Tissue engineering with the use of polymeric materials enables fabrication of Tissue engineering with the use of polymeric materials enables fabrication of scaffolds for various applications. Some polymers, such as poly(lactic acid), poly(glycolic acid), polycaprolactone, are biodegradable and biocompatible, which minimizes adverse physiologic responses to foreign materials in the body. The use of biodegradable polymeric scaffolds allows for cell ingrowth while the scaffold degrades over time, leaving only newly regenerated tissue at the site of implantation. To further promote healthy tissue growth and reduce recovery time, drug-containing scaffolds have become a popular option (Tabata, 2000; Zhang et al., 2013). Using scaffolds loaded with two drugs offers a multitude of combinations to invoke the appropriate tissue responses. Incorporating drugs into the scaffold provides a local delivery of the drug and reduces or eliminates the need for oral administration. Only 50% of patients take prescriptions properly, and even when taken correctly, some drug will be lost due to poor absorption and first-pass elimination (Martinez et al., 2002). Absorption is dependent on many physicochemical and physiologic factors, such as age, gender, health, concomitant medication, and transporter mechanisms (Martinez et al., 2002).

Poly(lactic-co-glycolic acid) (PLGA) is a biodegradable polymer that is already being used clinically in the form of microspheres and injected into the body for extended drug release. For example, ATRIDOX® is used in the treatment of periodontal disease, and Decapeptyl® SR is being used to treat endometriosis and liver and prostate cancer. The drug release rate from these polymer systems can be tailored to achieve various dosages by altering the material properties, such as molecular weight, end groups, and side chains (Fredenberg et al., 2011). Additionally, PLGA microspheres and scaffolds are being investigated for a variety of tissue engineering applications, including growth plate regeneration, bladder tissue repair, cartilage reconstruction, and diaphyseal bone growth (Pattison et al., 2005; Shin et al., 2006; Sundararaj et al., 2012; Yoon et al., 2007). PLGA

microspheres can be fabricated into scaffolds through many techniques, such as solvent evaporation, molding, and sintering (Clark et al., 2013; Makadia et al., 2011). These methods, however, require solvents, elevated temperature, and/or mechanical force, which can be problematic for incorporating a drug or protein into the scaffold because these conditions could cause deactivation or denaturation (Coleman et al., 2012; England et al., 2011). Incorporating bioactive molecules enables localized treatment at the implant site and can be used to promote desired tissue responses.

Hydrogels are another promising family of materials for tissue engineering and drug delivery applications (Hoare et al., 2008). Poly(β-amino ester) (PBAE) hydrogels offer a wide range of properties, are biodegradable, and are cytocompatible (Hawkins et al., 2011). The degradation time can be adjusted from hours to months, while the mechanical properties can range from 4 to 350 MPa, simply by changing the type of diacrylate and amine used to synthesize the macromer (Anderson et al., 2006). Drug delivery is possible by mixing the active agent with the macromer before polymerizing the hydrogel, an approach that has been investigated for the delivery of paclitaxel (Meenach et al., 2012). Additionally, degradation and drug delivery can be altered through the use of a hydrogel porogen entrapped in a hydrogel outer matrix (Hawkins et al., 2013). PBAE microspheres and nanospheres containing plasmid DNA have been made by a double emulsion/solvent evaporation technique (Pfeifer et al., 2005). Modifying PBAE with poly(ethylene oxide) (PEO) yields a system that undergoes pH-sensitive degradation for treatment of tumors (Shenoy et al., 2005).

Salt-leached scaffolds are made porous prior to use/implantation, which reduces modulus and strength (Pan et al., 2012). Furthermore, these scaffolds typically allow delivery of a single biomolecule from the polymeric matrix (Makadia et al., 2011). Simultaneous or sequential release of two drugs can promote desired responses, whether it is reducing inflammation or promoting specific cell proliferation and differentiation. Some examples include apoptosis of tumor cells or the proliferation of chondroblast, myoblast and fibroblast in tissue regeneration (Baserga et al., 1998). Sequential release has been achieved using a layering system of films that degrade through surface erosion, one layer at a time (Sundararaj et al., 2013). Other methods have involved coating scaffolds that would yield one large burst release upon implantation or mixing different

types of microspheres together to release two drugs at the same time (Jaklenec et al., 2008; Kempen et al., 2009).

The objective of the present studies was to create a scaffold scaffold system comprising a PLGA matrix and different amounts of degradable PBAE porogen. The physical and mechanical properties were evaluated to determine the effects of different amounts of porogen on the scaffolds. Drug loading options and bioactivity were explored as well. To demonstrate the approach, ketoprofen and bone morphogenetic protein 2 (BMP-2) were used because of their roles in controlling inflammation and endochondral bone formation, respectively. By characterizing the full spectrum of mechanical properties and drug release rates, scaffold design can be readily adjusted to meet the needs for different hard and soft tissue engineering applications.

5.2 Materials and Methods

5.2.1 Microsphere Fabrication

Poly(lactic-co-glycolic acid) (50:50, IV: 0.55-0.75 dL/g, acid-terminated; Durect Corporation, Pelham, AL) microspheres were fabricated using a water/oil/water ($W_1/O/W_2$) double emulsion technique. For the first emulsion, 10% v/v phosphate-buffered saline (PBS) was sonicated in a solution of 13% wt/v PLGA dissolved in dichloromethane (DCM). For the second emulsion, the above solution was homogenized into 1% poly(vinyl alcohol) (PVA; Sigma-Aldrich, St. Louis, MO) in deionized water. The resulting microspheres were stirred overnight, washed, and lyophilized. The microspheres were sieved, collecting only those <250 μm. PLGA microspheres containing BMP-2 (GenScript, Piscataway, NJ) were made the same way, except with the addition of BMP-2 to the PBS at a concentration of 0.25 mg/mL.

5.2.2 Porogen Synthesis

Hydrogel particles comprised a biodegradable PBAE. The macromer was synthesized through a step-wise reaction between poly(ethylene glycol) 400 diacrylate (Polysciences, Inc., Warrington, PA) and isobutylamine (Sigma-Aldrich) to make H6 macromer (Anderson et al., 2006). Macromer then underwent chemically-initiated free radical polymerization with the addition of 2 wt% ammonium persulfate (Thermo Fisher Scientific, Bridgewater NJ), 50 wt% dimethyl sulfoxide (DMSO), and 2 wt%

tetramethylethylenediamine (Sigma-Aldrich). The macromer was added and vortex for 30 seconds and then pipetted between two glass plates with a 1 mm spacer. The plates were placed in a sonication bath for 30 minutes and then left at room temperature for 48 hours. The gel was then removed, washed in ethanol overnight, and then air-dried. The gel slab was ground using a mortar and pestle to obtain particles that were sieved (<500 μm) for use as the porogen. Hydrogels loaded with ketoprofen (Sigma-Aldrich) were synthesized by adding drug to the macromer mixture at 10 wt%.

5.2.3 Encapsulation Efficiency and Loading

The encapsulation efficiency of BMP-2 in PLGA microspheres was measured by dissolving a fixed amount of polymer in DCM, adding acetone to a 3:7 ratio (DCM:acetone), and then centrifuging at 14,000 g for 5 minutes. After discarding the supernatant, and the sample was washed with the same DCM/acetone mixture and centrifuged three additional times. After evaporating solvent overnight, the sample was rehydrated in PBS, and the MicroBCA assay (Thermo Fisher Scientific) was performed to determine the protein concentration.

To measure the ketoprofen loading in hydrogel particles, a fixed amount of gel was immersed in PBS for 7 days to ensure full degradation. Ketoprofen concentration was quantified by high-performance liquid chromatography (HPLC; Hitachi Primaide, Tokyo, Japan). The mobile phase consisted of acetonitrile and 0.1% trifluoroacetic acid at a ratio of 60:40, with analyte separated on a Kinetix C18 column (Phenomenex, Torrance, CA). Absorbance was read at 260 nm. The area under the peak was calculated and compared to standards to determine ketoprofen concentration.

5.2.4 Scaffold Fabrication

A fixed mass of PLGA microspheres (42 mg) was mixed with increasing amounts of hydrogel particles at weight ratios of 40:60, 50:50, and 60:40 (PBAE:PLGA) to yield samples having overall masses of 70, 84, and 105 mg, respectively. The mixture was gently ground using a mortar and pestle and then consolidated into a mold having dimensions of 2.4 mm height and 6 mm diameter. The mold was then incubated for 2 days to allow samples to sinter. The sintering temperature was selected to be 49 °C,

59

which was the glass transition temperature of the PLGA used in this study, to allow fusion of the microspheres around the hydrogel particles.

5.2.5 Microarchitecture

Scaffold microarchitecture was assessed using microcomputed tomography (microCT; Scanco μCT40 SCANCO Medical, Switzerland). To evaluate porogen degradation and development of porosity, scaffolds were incubated and shaken at 37°C in PBS, pH 7.4. At 1, 2, and 5 days, the PBS was removed, and the scaffolds were lyophilized and analyzed. Scaffolds were also evaluated in their dry state before degradation. Samples were scanned at 55 kV and 145 mA and imaged at a voxel resolution of 6 μm. In order to quantify porogen degradation, the scaffold porosity and pore size was calculated using a built-in bone morphometry evaluation program (version: 6.0).

5.2.6 Degradation

Degradation studies were conducted using 2 mL of PBS, pH 7.4, per scaffold on a plate shaker at 37°C. Mass loss from the scaffolds was measured over 120 days. For each time point, three samples of each type (40:60, 50:50, and 60:40 PBAE:PLGA) were removed, lyophilized, and weighed. The degradation was calculated by (end mass)/(initial mass) x 100%.

5.2.7 Drug Release

As for measurement of degradation, samples were incubated in 2 mL PBS, pH 7.4, on a plate shaker at 37°C. At each time point, the supernatant was collected and replaced. To measure ketoprofen release, HPLC was used as described in the Encapsulation Efficiency and Loading section. To measure BMP-2, samples were concentrated using centrifugal filters with a molecular weight cut off of 3,000 Da (Amicon Ultra; Millipore, MA) following the manufacturer's instructions, after which protein concentrations were determined using the MicroBCA assay.

5.2.8 Compressive Modulus

Compression testing was utilized to evaluate the modulus of samples in their initial dry state and after five days of degradation. Five days ensured that the hydrogel

porogen had degraded, leaving only the PLGA matrix. After incubation, samples were taken directly out of the PBS and evaluated. As reported previously (Clark et al., 2013), a Bose ELF 3300 system was used to test samples at a compression rate of 0.06 mm/sec until sample failure, approximately 1.5-2 mm of compression. A stress-strain curve was plotted and used to determine the compressive modulus of each sample type.

5.2.9 Bioactivity Assay

The bioactivity of released ketoprofen was determined using a COX Inhibitor Screening Assay Kit (Cayman Chemicals, Ann Arbor, MI). Bioactivity was expressed as the percentage of expected inhibitory activity, meaning that the inhibitory activity of release supernatants was compared to that of fresh ketoprofen at the same concentrations.

The bioactivity of released BMP-2 was assessed by measuring alkaline phosphatase activity. Briefly, mouse myoblastic C2C12 cells (ATCC CRL-1772) cultured in Dulbecco's Modified Eagle Medium (DMEM; Thermo Fisher Scientific) with 10% fetal bovine serum (FBS; Thermo Fisher Scientific) were seeded into a 48-well plate at 80,000 cells/mL and allowed to adhere overnight. The medium was then replaced with DMEM containing 1% FBS plus release supernatants that had been centrifugally concentrated (3,000 Da MWCO). Five days later, wells were washed twice with PBS and lysed with 100 μL CelLytic M solution (Sigma-Aldrich) according to the manufacturer's directions. The lysate solution was mixed at a 1:3 ratio with the substrate solution (4 mM $MgCl_2$ and 10 mM p-nitrophenyl phosphate in 0.6 M 2-amino-2-methyl-1-propanol buffer, pH 10.0), and the absorbance at 400 nm was measured as a function of time. Alkaline phosphatase activity was normalized by DNA content, which was quantified using a Quant-iT™ PicoGreen® assay kit (Thermo Scientific) following the manufacturer's instructions. As for ketoprofen, bioactivity was expressed as percentage of expected activity based on fresh BMP-2 standard solutions.

5.2.10 Statistical Analysis

ANOVA followed by a Tukey-Kramer multiple comparison test was performed using GraphPad InStat software to determine the significance of results. Results were considered significant if $P < 0.05$.

5.3 Results

5.3.1 Protein and Drug Loading

The BMP-2 microspheres had an encapsulation efficiency of 50±7% for a total loading of approximately 7.2 μg BMP-2 per scaffold. The hydrogel particles had a 43±2% loading efficiency for an overall loading of 1.13, 1.55, and 2.06 mg of ketoprofen for the 40:60, 50:50, and 60:40 PBAE:PLGA scaffolds, respectively.

5.3.2 Microarchitecture

Figure 1 shows cross-sections of the different scaffold types in the initial dry state and after 1 and 2 days of degradation. Initially, all the scaffolds were a solid mass with no differentiation between the scaffold types. The porosity of the 40:60, 50:50, and 60:40 after 1 day degradation was 66±3%, 67±3, and 74±5 (p>0.05), followed by an increase at day 2 to 79±2%, 82±4, and 87±3 (p>0.05), respectively (Figure 2). No statistically significant changes occurred between day 2 and 5, with porosities of 85±4, 81±1 and 79±3% for the 60:40, 50:50, and 40:60 scaffolds, respectively. The pore size was not significantly different between the scaffold types or time points, with an average pore size of 142 ± 20 μm.

5.3.3 Degradation

Degradation profiles for the 40:60, 50:50, and 60:40 scaffolds are shown in Figure 3. Part A shows degradation in terms of absolute mass. Because all scaffolds started with the same amount of PLGA, no statistical differences in degradation rates were observed after the porogen degraded within the first two to three days. Part B shows degradation expressed as a percentage of mass remaining, which illustrates how the 40, 50, and 60% porogen loadings caused a 40, 50, and 58% mass loss by day 3, respectively. All scaffolds experienced a plateau once the porogen had degraded. At day 8, there were no statistically significant differences in mass, with 38±2, 34±5, and 39±2 mg of mass

62
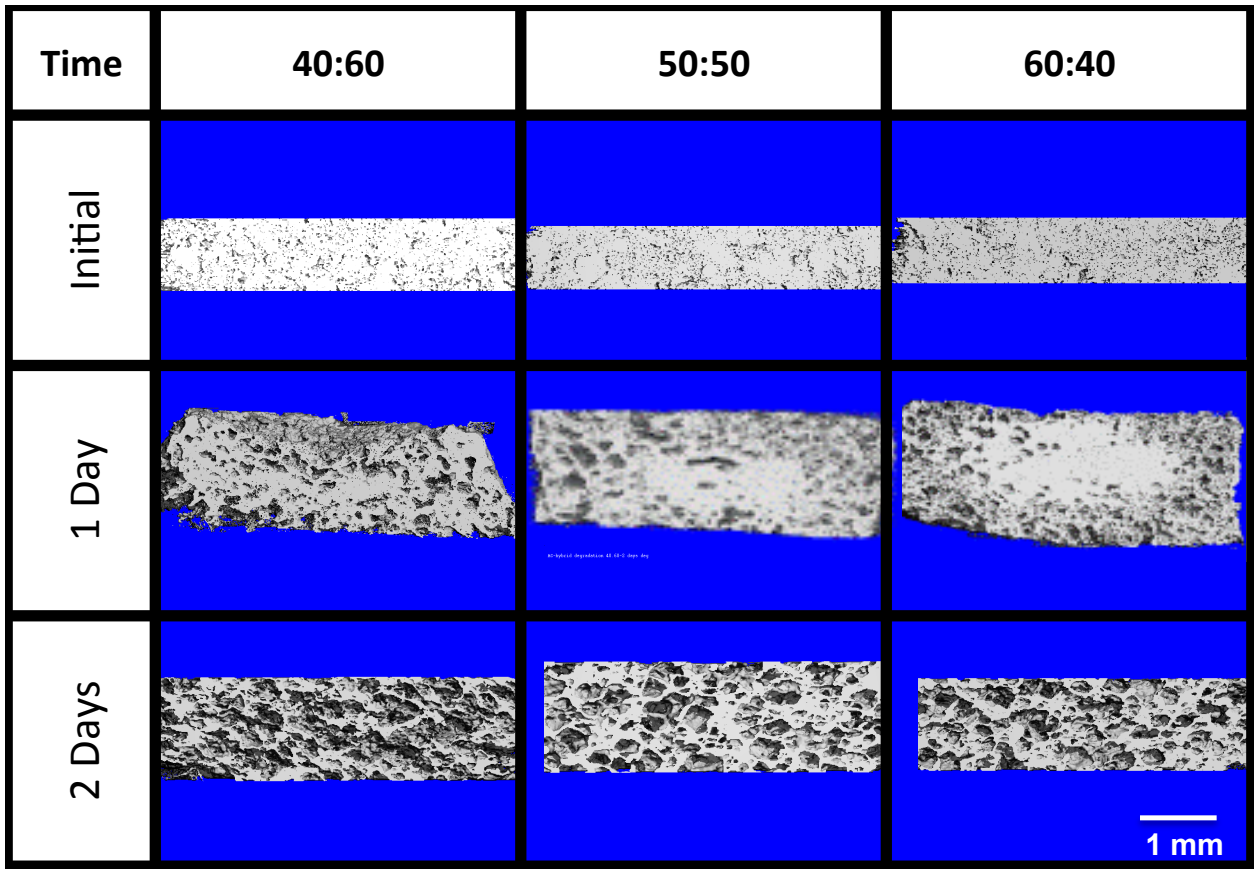
Figure 5.1.Representative microCT images of the cross-sections of 40:60, 50:50, and 60:40 (PBAE:PLGA) scaffolds in the initial dry state and degraded for 1 or 2 days.
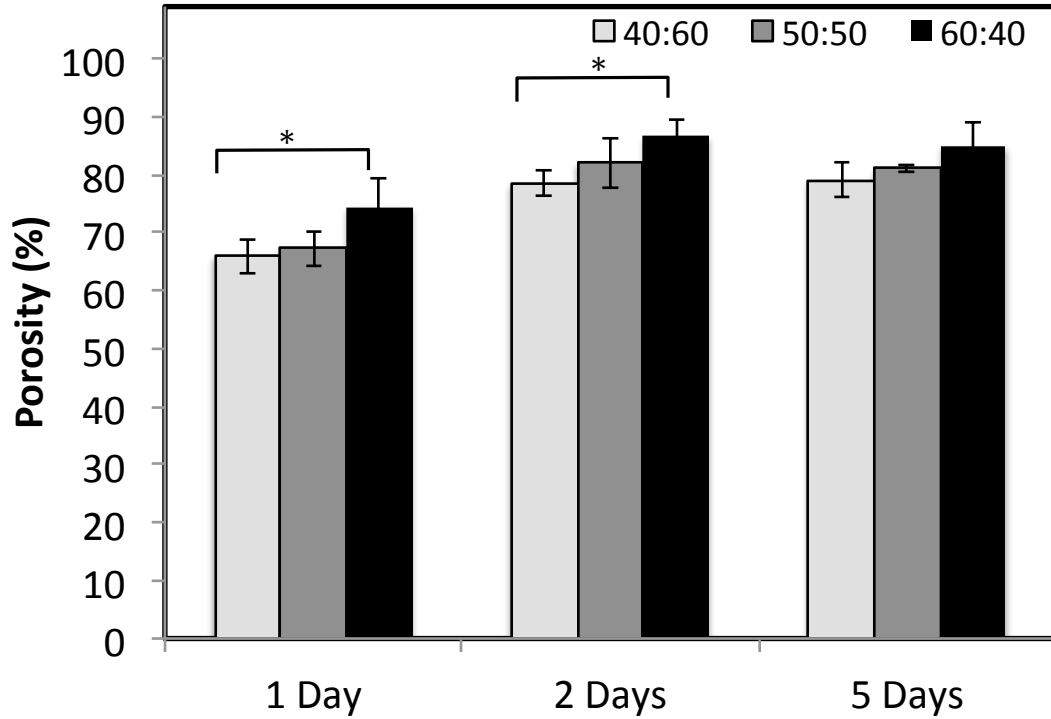
Figure 5.2. Porosity of 40:60, 50:50 and 60:40 (PBAE: PLGA) scaffolds after 1, 2, and 5 days of degradation in PBS. Data are shown as mean ± standard error (n≥3). *p<0.01
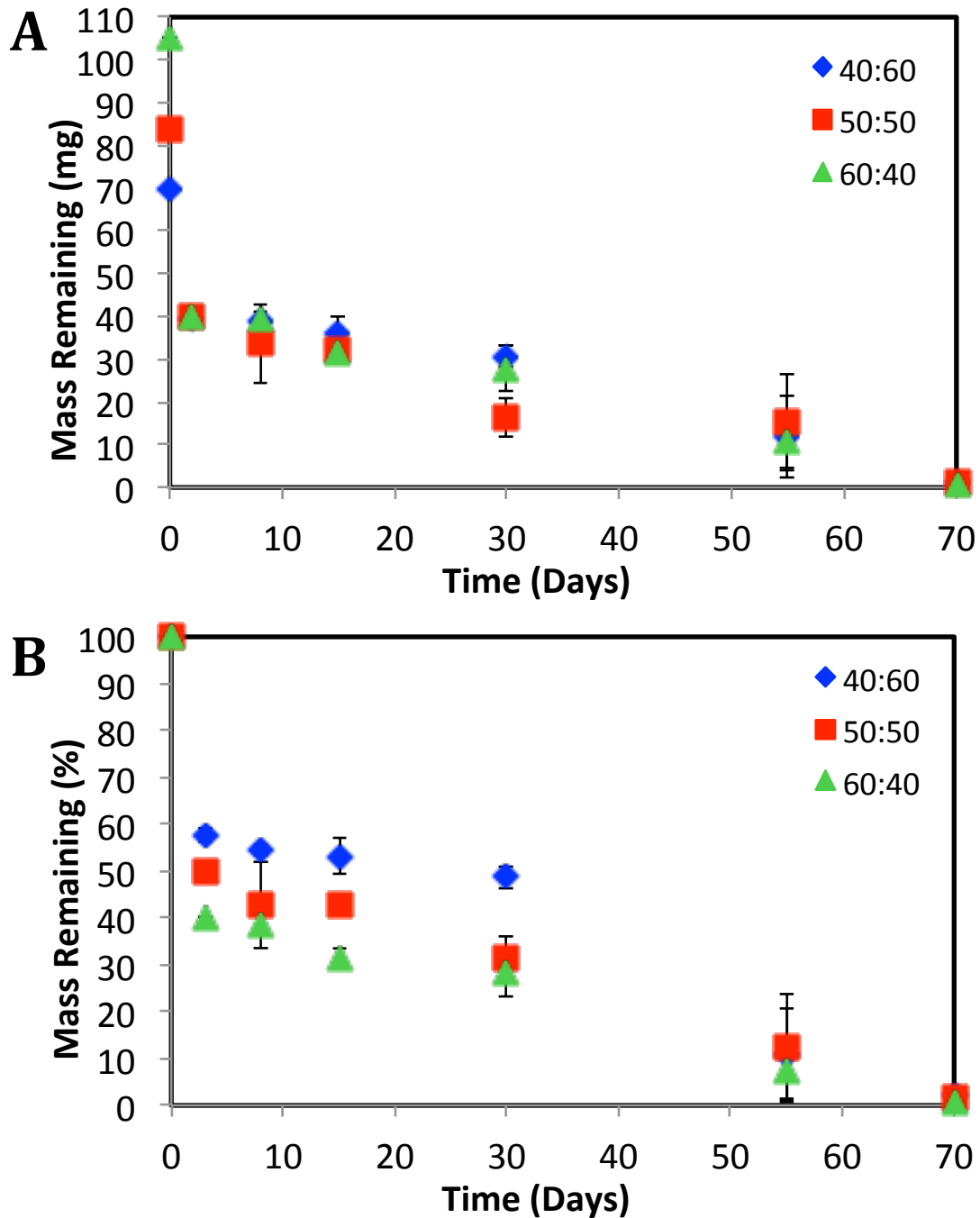
Figure 5.3. Degradation curves for 40:60, 50:50, and 60:40 (PBAE:PLGA) scaffolds shown as (A) absolute mass remaining and (B) percentage mass remaining. Data are shown as mean ± standard error (n≥3).

remaining for the 40:60, 50:50, and 60:40 scaffolds, respectively. From day 8 to 15, the degradation rate was 0.5 ± 0.1 mg per day, followed by a rate of 0.5 ± 0.1 mg per day until scaffolds reached full degradation at day 70.

5.3.4 Mechanical Properties

Under unconstrained compression, the scaffolds did not exhibit a distinct failure point, but were flattened and spread outward because of the pliable, porous nature of the materials. The compressive modulus of as-prepared scaffolds decreased significantly ($p<0.01$) from 111 ± 10 to 74 ± 12 to 50 ± 8 MPa with an increasing amount of porogen from 40 to 50 to 60%, respectively (Figure 4). After 5 days of degradation, the 40:60, 50:50, and 60:40 scaffolds had moduli of 0.6 ± 0.1, 1.1 ± 0.2, and 0.7 ± 0.2 kPa, respectively, with a statistically significant difference ($p<0.01$) between the 50:50 and other two scaffolds types.

5.3.5 Drug Release

For all scaffolds, ketoprofen was released at statistically similar rates in terms of the percentage of total drug loaded (Figure 5A). At 2, 4, 8, and 12 hours, the scaffolds had released $40\pm2\%$, $67\pm2\%$, $94\pm1\%$, and $99\pm0\%$ of the total drug loaded, respectively. In terms of absolute dose, however, the amount of ketoprofen released varied significantly ($p<0.01$) by scaffold composition. For the first 4 hours, the 40:60, 50:50, and 60:40 scaffolds had rates of 185 ± 10, 262 ± 22, and 357 ± 26 μg/hour followed by a slight decrease to 79 ± 8, 100 ± 18, and 130 ± 48 μg/hour, respectively.

All of the scaffolds released comparable amounts of BMP-2, 7.2 ± 0.6 μg, with similar triphasic profiles (Figure 5B). Significantly different release rates ($p<0.01$) were observed for each of the phases: 0.49 ± 0.05, 0.15 ± 0.02, and 0.02 ± 0.007 μg/day for the initial (0-3 days), second (3-35 days), and third phases (35 to 70 days), respectively.

5.3.6 Bioactivity

Two hours into the release, the bioactivity of ketoprofen was found to be $101\pm15\%$, $92\pm10\%$, and $104\pm8\%$ of the expected activity for the 40:60, 50:50, and 60:40 scaffolds, respectively, while at four hours, the bioactivity was $117\pm27\%$, $105\pm14\%$, and $106\pm17\%$ of the expected activity for the 40:60, 50:50 and 60:40 scaffolds, respectively

66
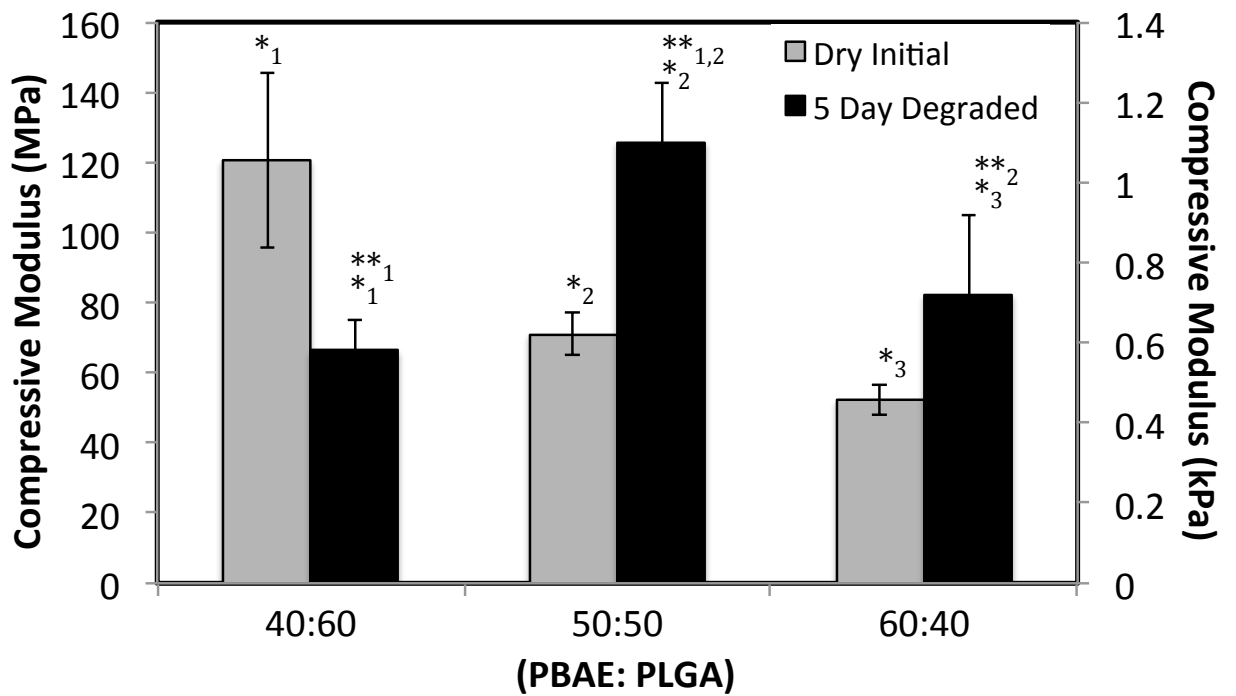
Figure 5.4. Compressive modulus of 40:60, 50:50, and 60:40 (PBAE:PLGA) scaffolds in their initial dry state and after 5 days of degradation (tested in their wet state). Data are shown as mean ± standard error (n≥3). $*_{1,2,3}$ $**_{1,2}$ $p<0.01$
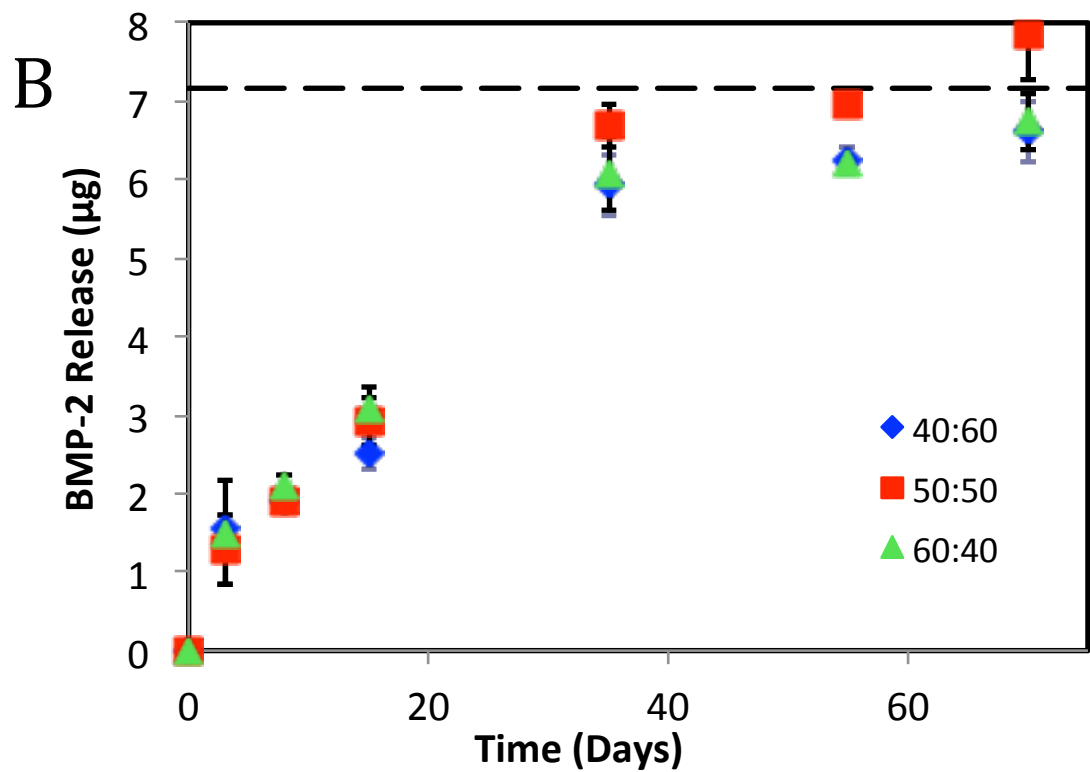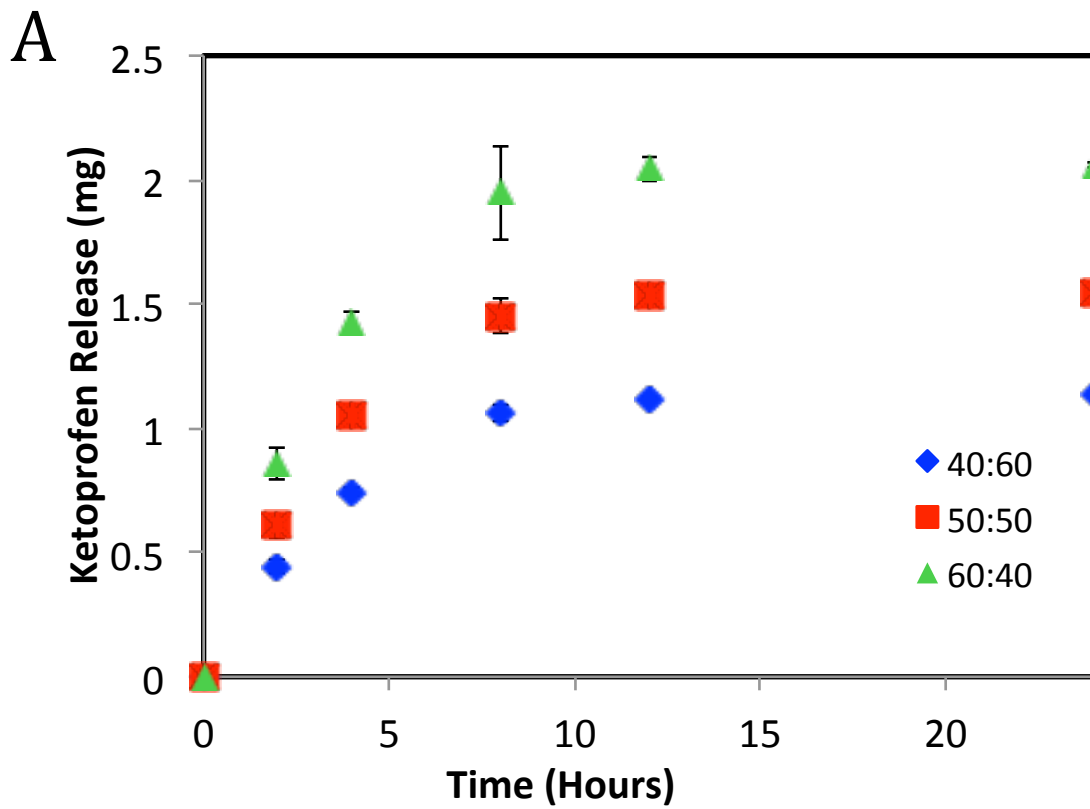
Figure 5.5. Cumulative profiles for release of (A) ketoprofen and (B) BMP-2 from 40:60, 50:50, and 60:40 (PBAE:PLGA) scaffolds. The dashed line represents the amount of expected BMP-2 release based on the loaded amount. Data are shown as mean ± standard error (n≥3).

(Figure 6A). Regardless of the scaffold type or varied concentration of ketoprofen, bioactivity was retained, and no statistical differences were found between the samples.

BMP-2 bioactivity was measured at days 30 and 70 to determine whether activity was affected during degradation of the PLGA scaffolds (Figure 6B). Based on the alkaline phosphatase activity stimulated for each scaffold type, the percentages of expected activity were comparable, with 97± 3%, 95±4%, and 96±2% for the 40:60, 50:50, and 60:40 scaffolds, respectively.

5.4 Discussion

5.4.1 Development of Porosity

The initial state of all the scaffolds was a solid mass with negligible porosity, but porosity increased as the PBAE porogen particles began to degrade. The difference in porosity between the scaffolds was due to the difference of the porogen loading. The 40:60, 50:50, and 60:40 scaffolds started with 42 mg of PLGA microspheres and 28, 42, and 63 mg of hydrogel particles, respectively. Within 1 day, the PBS infiltrated the scaffolds and hydrolysis began, causing degradation of the porogen (Hawkins et al., 2013). After 2 days of incubation in PBS, the porogen particles were gone, as indicated by the mass loss results where about 40 mg remained for all types of scaffolds. Previous research involving porous PLGA scaffolds showed similar masses at 48 hours (Clark et al., 2013). The remaining mass was the PLGA matrix that degraded at a much slower rate, which was why none of the scaffolds experienced a significant change in porosity between day 2 and 5. At 1 and 2 days, however, the 60:40 scaffolds were more porous, likely due to the increased porogen loading that resulted in more PBAE particle surface area for the PLGA microspheres to surround. Without enough PLGA to fully surrounding the particles, areas within the scaffold had more neighboring PBAE particles that led to increased porosity. Initially, from day 2 to 15, the mass loss was slower as hydrolysis of the ester linkages occurred, but the chains were likely too long still to diffuse out. Later in the degradation process, from day 15 to 70, hydrolysis continued, and the matrix began to lose mass more quickly as the lactic and glycolic acid oligomers more easily diffused out.

Utilizing the combined effect of a quick-degrading porogen and a porosity that allows for rapid aqueous infiltration is advantageous because it will not impede cell
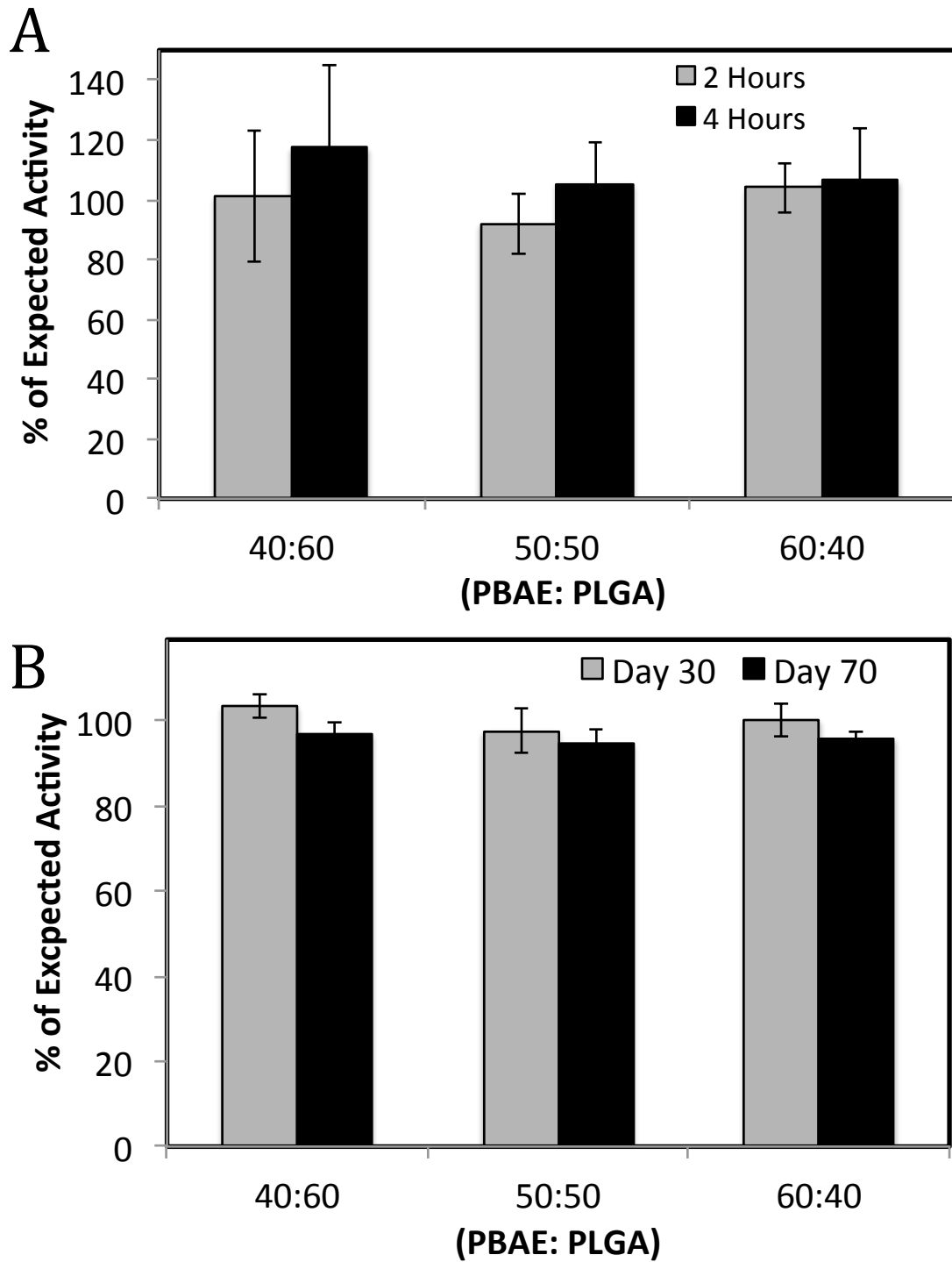
Figure 5.6. Bioactivity of (A) ketoprofen and (B) BMP-2 released from the 40:60, 50:50, and 60:40 (PBAE:PLGA) scaffolds. Data are shown as mean ± standard error (n≥3).

migration into the scaffold. Once cells have entered the scaffold, tissue regrowth can begin. The measured average pore size of approximately 140 µm was smaller than the size of the PBAE particles used (<500µm), mostly likely due to the particles breaking up during the gentle grinding with PLGA microspheres during scaffold fabrication. Microspheres were likely embedded at the periphery of the particles, thereby decreasing the resulting pore size. Pore sizes above 100 µm have been shown to be appropriate for bone infiltration (Klawitter et al., 1976) and for growth of other tissues, such as skin and cartilage (Griffon et al., 2006; Yannas, 1992).

5.4.2 Mechanical Properties

For the as-prepared scaffolds, the increasing amount of porogen reduced the compressive modulus. This was to be expected because the hydrogel particles had a lower modulus than did the PLGA microspheres (Brey et al., 2008). Further proving this point, once the porogen had degraded, all scaffolds had similar compressive moduli, because they all contained the same amount of PLGA microspheres. The achievable range of modulus, 50-120 MPa, is comparable to properties of trabecular bone (50-78 MPa) and would initially exceed the compressive modulus of articular cartilage (0.079-2.1 MPa) until degradation occurred (Lotz et al., 1990; Schinagl et al., 1997). The larger decrease in modulus of the 60:40 scaffolds at 5 days could be attributed to the lack of microsphere fusion, and beyond 60% porogen loading, the modulus would be expected to continue to decrease as integrity of the scaffold is compromised. All of the scaffolds exhibited a decrease in modulus after 5 days of degradation, and although there was a statistical difference between the 50:50 scaffolds and the other two types, the difference represented <1% of the original modulus. In previous research using NaCl as the porogen that was leached prior to testing, the compressive modulus after 5 days was about 6 kPa, which was significantly higher than for the current scaffolds following degradation of PBAE porogen from PLGA matrix (Clark et al., 2013). A likely explanation is due to the natural swelling properties of the hydrogel that put added stress on the fused microspheres. The same PBAE hydrogel system (H6) has been shown to swell from 150-400% within hours when unconstrained (Hawkins et al., 2011), but because the hydrogel particles are embedded as porogens, the PLGA matrix confines the particles and impairs their swelling. Thus, the internal walls of the PLGA matrix that support the scaffold will

71

experience stress as the hydrogel particles try to expand in aqueous solutions. This preexisting stress may cause the modulus to decrease since it would take less force to break the PLGA matrix. Additionally, the effect of "wetting" the scaffold (being immersed in PBS at 25 or 37 °C) has been shown to cause a decrease in compressive modulus. Wu et al. fabricated 88% porous PLGA scaffolds using a lower molecular weight (estimated at about 10 kDa; exact number not reported) than in the current study and found that wetting the scaffolds for only a few minutes in a vacuum system reduced the compressive modulus by almost 50% (Wu et al., 2006).

5.4.3 Drug Release

The encapsulation efficiencies obtained for ketoprofen in PBAE and BMP-2 in PLGA demonstrated that almost half of the drug remained in the material. The percentage for BMP-2, however, was slightly lower than other reported values, ranging from 58-70% (Cleland et al., 1997; Yang et al., 2000; Yang et al., 2001). The numerous wash steps to remove unreacted monomer from PBAE to avoid cytotoxicity and to remove surfactant from PLGA to enable fusion of microspheres allowed some of the drug and protein to diffuse from the scaffolds.

Release of ketoprofen lasted approximately 12 hours. The release time and rate could be varied, however, by altering the degradation rate of the PBAE particles. By changing the diacrylate and amine, the degradation time can range from 7 hours to 4 months (Hawkins et al., 2011). The H6 PBAE used for the present studies was selected for providing fast release of ketoprofen because it undergoes rapid swelling and hydrolysis. The drug was completely released prior to full development of porosity, which indicates a prominent role of diffusive release. This behavior reflects bulk degradation, which has been modeled by many groups, as reviewed by Lin and Metters (Lin et al., 2006).

After a scaffold has been implanted, the inflammatory response begins and neutrophils, monocytes, and macrophages become apparent in a matter of hours, making the initial early release of ketoprofen relevant (Ebara et al., 2002; Ricci et al., 2005). The purpose of the drug release from the porogen particles was to show a model for a small molecule drug (ketoprofen, 254 Da) that could also be applicable for the treatment of local inflammation without interfering with the cell ingrowth. Ketoprofen is FDA-

72

approved for oral delivery by the brand names of Orudis® or Orvuail® at a much higher dose than seen in this study. The ideal amount of NSAID release for a localized treatment remains unknown, and more investigation would be needed to definitively answer the question. However, ketoprofen has been shown to reduce inflammation at concentrations as low as 100-130 μg/mL (Ricci et al., 2005). Inflammation will likely occur upon implantation of the present scaffolds as well as any others, and reducing, not eliminating, the magnitude of this response to prevent fibrous encapsulation could be beneficial. Using a localized treatment would eliminate the side effects seen with high oral doses of ketoprofen, such as gastrointestinal bleeding (Cabre et al., 1998). To tailor ketoprofen release for tissue-specific needs, the hydrogel particle drug loading, size, and amount can be altered, and even the hydrogel properties, such as composition and crosslink density, can be modified.

The BMP-2 profile showed a much longer, slower release, lasting 70 days. The triphasic release profile observed is characteristic of PLGA scaffolds (Garcia et al., 1999; Raghuvanshi et al., 1993). During this process, BMP-2 was initially released by diffusion, then a combination of diffusion and matrix degradation, and lastly by degradation alone. Release of macromolecules from PLGA has been extensively studied, and models proposed by Batycky et al. predict similar behavior to the release profiles measured in the present study (Batycky et al., 1997). The higher initial release of 490 ng BMP-2 per day should help the differentiation of surrounding mesenchymal cells into bone or cartilage cells, followed by a second phase of release of approximately 150 ng BMP-2 per day that will continue to affect cells recruited to the area (Inai et al., 2008; Pan et al., 2008). BMP-2 stimulates cartilage growth at concentrations from 10-200 ng/mL (Li et al., 2004). Even at low concentration (10 ng/mL), BMP-2 created a 1.5 fold increase of glycosaminoglycans (GAG; used as a chondrogenic marker) content over 21 days. For a higher concentration of 200 ng/mL, a 4-fold increase in GAG content was seen (Li et al., 2004). Similar findings were reported by Seykia et al., with a dose-dependent increase in cartilage production from 10-500 ng/mL (Pond et al., 1984). The overall amount of drug released and the release rate could be altered by adjusting the drug loading and the PLGA properties, such as molecular weight or latic:glycolic ratio.

During the last phase of release from 35-70 d, only about 20 ng/day of BMP-2 was measured, which will have less of an effect on the surrounding tissue. Even in small doses, however, BMP-2 can continue aiding bone growth (Kuhn et al., 2013). Also, scaffolds are likely to degrade more quickly *in vivo* (Tracy et al., 1999), so a 70 d release may not be the case once inside the body. As for ketoprofen delivery, the dose of BMP-2 could be increased by loading more protein into the microspheres used to fabricate the scaffolds.

Achieving a dual drug release is favorable either to create a synergistic effect of two drugs or growth factors or to allow for two separate actions to occur (Nishiyama et al., 2006; Richardson et al., 2001). In the present study, two separate actions were targeted, reducing inflammation and enhancing tissue regrowth. In a different approach from the present polymer-polymer composites, a PLGA/β-tricalcium phosphate scaffold used two different types of drug-loaded microspheres for the treatment of bone regeneration, releasing dexamethasone and a model protein (bovine serum albumin) (Yang et al., 2011). The release rate for both drugs was similar over a 28-day period, in contrast to the initial rapid release followed by a second sustained release in the current work. Sequential release can be achieved using a layering method, varying microsphere fabrication methods to release encapsulated drug at different rates, and coatings (Jaklenec et al., 2008; Kim et al., 2008; Sundararaj et al., 2013). A three-layer system using poly(ether-ester) was used to model dual release, however the polymer, along with several other proposed systems, degraded in less than 35 days, which may not be long enough to complete bone or cartilage formation (Dahlin et al., 1988; Holland et al., 2007; Mason et al., 2000; Uematsu et al., 2005).

Jaklenec et al. used fused PLGA microspheres encapsulated with insulin-like growth factor I and transforming growth factor-β$_1$ to demonstrate combined release of both proteins starting at day 0, 7 or 10, and lasting 56 days. While their release time was longer, sequential release was not shown (Jaklenec et al., 2008). Kempen et al. showed sequential release from poly(propylene fumarate) scaffolds containing BMP-2-loaded PLGA microspheres and coated with gelatin hydrogel loaded with vascular endothelial growth factor (VEGF) (Kempen et al., 2009). The burst release of VEGF lasted 3 days, while the BMP-2 release was sustained for 56 days. Their results showed the benefit of

74

dual drug release comprised of an initial burst and a sustained release and the increased effect it had on bone formation. However, the scaffold fabrication methods were more complex and the scaffold was non-porous, which has been shown to improve cell ingrowth (Kempen et al., 2009; Van Tienen et al., 2002). To obtain a longer degradation time and give the scaffold mechanical integrity to make it suitable for soft tissue applications (Hawkins et al., 2011; Slaughter et al., 2009), the present scaffolds were compressed and sintered for two days, allowing for the microspheres to fuse together around the hydrogel particles. Because the scaffold is made from microspheres and particles, the overall design of the scaffold can be easily adjusted, which expands the options for scaffold uses.

5.4.4 Bioactivity

Importantly, there was no loss in the bioactivity of ketoprofen after experiencing scaffold fabrication, indicating that the use of solvents, elevated temperatures, and compression had no effect on the drug. Even though the recommended storage temperature for ketoprofen is 20-25°C, studies have shown thermal stability above 200°C (Tiţa et al., 2011). For this reason, it was to be expected that ketoprofen would remain bioactive after processing, and measurement of COX-2 inhibition confirmed this hypothesis. Additionally, ketoprofen is stable in solvents used to solubilize the drug and for emulsions used to fabrication microspheres (Barichello et al., 1999; Chi et al., 1991).

BMP-2 showed similar results, with no loss of activity. Winkler et al. demonstrated that BMP-2 can be heat-treated up to 100°C without losing activity, which is much higher than the 49°C used to sinter the BMP-2-loaded microspheres in the present study (Winkler et al., 2006). Other groups have shown BMP-2 bioactivity after being encapsulated into PLGA microspheres (Kempen et al., 2008). The effect of solvent interaction and mechanical compression have also been studied, showing no loss of bioactivity (Schwarz et al., 2013). With the development of this novel scaffold, it was important to verify that the BMP-2 activity was not lost with the introduction of the new PBAE porogen material.

5.5 Conclusion

The present study showed how porogen loading at different amounts affected the microstructure and modulus of PLGA scaffolds. Incorporating 40, 50, or 60 wt% of ketoprofen-loaded PBAE hydrogel particles adjusted the drug release concentration over a 12-hour period. Regardless of the loading amount, the long-term delivery of BMP-2 encapsulated within the PLGA matrix was unchanged. Moreover, the results demonstrated that both the drug and protein released were still bioactive, unaffected by the scaffold fabrication technique. Localized delivery of ketoprofen and BMP-2 could help reduce inflammation and help regenerate tissue, respectively, potentially accelerating recovery. Degradable hybrid PLGA scaffolds enable the release of two drugs while maintaining the mechanical properties appropriate for different soft or hard tissue applications.

76

Chapter 6 Treatment to Regenerate the Proximal Tibia Growth Plate after Injury Using a Poly(lactic-co-glycolic acid) Based Scaffold

6.1 Introduction

The growth plate is a cartilaginous region of long bones that is responsible for bone growth, which continues until puberty when the influence of hormones causes it to close (Ballock et al., 2003; Burdan et al., 2009; Iannotti, 1990). In children 5-18 years old, 50% of them will experience a fracture, usually caused from trauma or playing sports. Of those fractures, an estimated 18% of the them will involve the growth plate, which can lead to angular deformation or stunted growth (Mizuta et al., 1987). A reported 30-65% of growth plate fractures lead to some level of growth disturbance, depending on the type and location of the facture (Basener et al., 2009).

The reason growth plate injuries are so detrimental is because the cartilage is unable to regenerate (Temenoff et al., 2000), which leads to the formation of bone at the place of fracture, referred to as a bony bar (or bridge) (Jaramillo et al., 1990). The bony bar act as a tether, where certain areas of the physeal line are unable to expand (Khoshhal et al., 2005). To prevent impaired growth, current treatment options involve removal of the bony bar and replacement with fat, muscle, polymeric silicone, bone wax, or bone cement as interpositional materials (Hasler et al., 2002; Tobita et al., 2002). The Langenskiöld method, first established in 1967, involves removing the bony bridge and replacing it with a free fat transplant and was shown to be a better alternative to osteotomy and limb lengthening (Langenskiöld, 1981). However, about 60% of patients who receive this treatment have fair to poor results, and approximately 30% of patients experience a reoccurrence of bony bar formation (Hasler et al., 2002).

Current research for other treatment options largely surrounds the use of mesenchymal stem cells (MSCs). Li et al. reported an example using a chitin scaffold cultured with MSCs for 7 days and implanted in the medial half of the proximal growth plate of the tibia in 6-week-old rabbits after excision of the bony bar. The results showed a significant decrease in angular deformation and longitudinal discrepancy compared to the unoperated tibia (Li et al., 2004). Similar results are seen in other work involving sodium hyaluronate/collagen or agarose scaffolds where limp length is improved, however, the drawbacks of this approach are that the MSC must first be harvested

77

requiring an additional surgery (Chen et al., 2003; Lee et al., 1998; Planka et al., 2008). The objective of this study was to regenerate the growth plate without using previously harvested MSCs but instead using BMCs taken out of the tibia during the same surgery of implanting the scaffold. The scaffolds used in this study were selected based on previous work that used the same polymer but with a lower molecular weight. Increasing the molecular weight would not only give more structural support but allow more time for the tissue to develop into a denser columnar structure capable of withstand the physiologic conditions. Additionally, the scaffolds were loaded with IGF-I, which has been shown to increase cell proliferation and increase glycosaminoglycan, a cartilage component, production over time (Clark et al., 2013).

6.2 Materials and Methods

6.2.1 Preparation of Microspheres

Poly(lactic-co-glycolic acid) (PLGA; 50:50, IV: 0.55-0.75 dL/g, acid-terminated; Durect Corporation, Pelham, AL) microspheres were fabricated using a water/oil/water ($W_1/O/W_2$) double emulsion technique. For the first emulsion, 10% v/v phosphate-buffered saline (PBS), pH 7.4, was used for the W_1 phase, which was sonicated into the O phase at 25 W for 10 seconds. The O phase consisted of 13% wt/v PLGA in dichloromethane (DCM). After sonication the solution was homogenized into the W_2 phase, a solution containing 1% poly(vinyl alcohol) (PVA; Sigma-Aldrich, St. Louis, MO) in deionized water. IGF-I-loaded microspheres were made using the same method, expect with the addition of 1.1 mg/mL IGF-I (PeproTech, Rocky Hill, NJ) to PBS in the first emulsion (W_1).

6.2.2 Hydrogel Fabrication

Poly(β-amino ester) (PBAE) hydrogels were made using a chemically-initiated free radical polymerization method. A step-wise reaction was used to synthesize H6 macromer from poly(ethylene glycol) diacrylate (PEGDA; MW: 400 g mol^{-1}; Polyscience, Warrington, PA) and isobutylamine (Sigma-Aldrich) (Anderson et al., 2006). Based on the macromer weight, 2 wt% ammonium persulfate (Thermo Fisher Scientific, NJ) in 50 wt/vol% dimethyl sulfoxide (DMSO) with 2wt/vol% tetramethylethylenediamine (Sigma-Aldrich) was used to initiate polymerization. After

78

vortexing for 30 seconds, the polymer solution was pipetted between two glass plates with a 1 mm spacer and placed in a sonication bath for 30 minutes. After 48 hours at room temperature, the gel was washed in ethanol and dried. To make particles, the gel was ground using a mortar and pestle and sieved, collecting particles <500 μm.

6.2.3 Scaffold Fabrication

Three types of scaffolds were used in this study: 1) blank, 2) IGF-I-loaded, and 3) hybrid. To fabricate the blank and IGF-I scaffolds, 120 mg of PLGA microspheres (<250 μm) were mixed with 180 mg of NaCl particles (<150 μm) and compressed in a 13 mm diameter die at 7 tons for 2 minutes using a Carver press. The scaffolds were sintered for 48 hours at 49°C (the glass transition temperature, T_g) and then leached in deionized water overnight and dried. To fabricate the hybrid scaffolds, 120 mg of PLGA microspheres (<250 μm) were mixed with 120 mg of hydrogel particles and compressed in a 13 mm diameter mold while being sintered for 48 hours at 49°C. The final dimensions of all the scaffolds were 13 mm diameter and 1.2 mm height.

For disinfection, each scaffold was placed in a 50 mL centrifuge tube and centrifuged at 200 g for 5 min in 5 mL of 70% ethanol followed by two wash steps with sterile PBS. The scaffolds were then dried in a laminar flow hood overnight.

6.2.4 Animal Surgery

Following an IGACUC-approved protocol fifteen New Zealand white female rabbits, 6 to 8 weeks old, were used in this study (Li et al., 2004). To simulate a growth plate injury, the medial one third of the proximal tibial growth plate was removed unilaterally using a 1.0 mm bur (Stryker Medical, Malvern, PA), as seen in Figures 6.1A and 6.1B. The wound was thoroughly irrigated with saline and closed using sutures. Radiographic images were taken of the first two animals to verify location of the growth plate defect and surgical technique. After three weeks, radiographs were taken of the lower limbs to confirm formation of the bony bar across the defect. The bony bar was then resected using the same procedure described previously, and an implant trimmed to fit the defect was placed in the site (Figure 6.1C). Animals were assigned to one of five treatment groups: 1) fat, removed from the infrapatellar fat pad, 2) blank (without IGF-I) scaffold, 3) IGF-I-loaded scaffold, 4) IGF-I-loaded scaffold with cells, and 5) hybrid
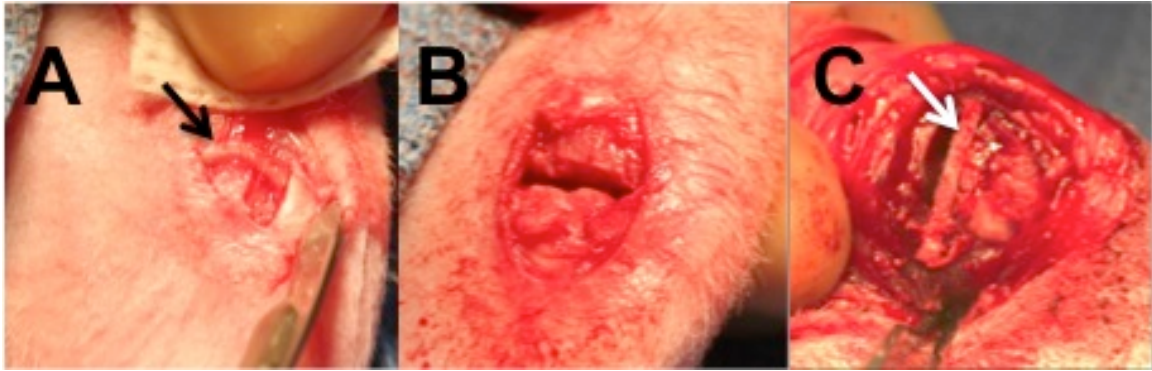
Figure 6.1. The site of implantation before (A) and after (B) growth plate removal. The black arrow indicates intact growth plate. (C) Trimmed and implanted scaffold (white arrow) following resection of the bony bar.

scaffold. For the fourth group, IGF-I-loaded scaffolds were seeded with bone marrow cells at the time of surgery (Figure 6.2). After removal of the bony bar, a syringe was used to collect bone marrow from the implant site and the diaphysis of the tibia, seeded onto the scaffold, and given 20 minutes for absorption. The animals were returned to their cages and allowed to move freely with no immobilization. After 8 weeks, the animals were euthanized and another radiograph was taken.

6.2.5 Microcomputed Tomography

At the end of the study, a 3-D reconstruction was created by microcomputed tomography (microCT) using a Scanco μCT40 (SCANCO Medical, Switzerland). Samples were imaged at 6 μm voxel resolution using scan parameters of 55 kV and 145 mA. The reconstructions were used to qualitatively evaluate the ability of the scaffolds to prevent bone formation in and around the defect area.

6.2.6 Anatomical Measurements

The lengths of the medial and lateral tibiae and the widths of fibulae were measured for each lower hind limb. Also, using the radiographic images obtained at the time if implantation and euthanasia, the medial proximal tibial angle (MPTA) and lateral distal femoral angle (LDFA) were measured (Figure 6.3). All measurements were calculated using ImageJ software.

6.2.7 Histological Analysis

After removal of the fibulae, the proximal tibiae were fixed in 10% buffered formalin for 2 weeks. Flagship Biosciences (Aurora, CO) processed the samples by bisecting them using the fibular insertion point to the opposite side as the reference point and then decalcified them in 10% formic acid. Coronal sections were cut at 4 μm thickness using a microtome and stained using hematoxylin and eosin. Stained sections were visualized and photographed using a Nikon Eclipse E600 microscope (Nikon) attached to a Nikon DN 100 digital camera (Nikon).
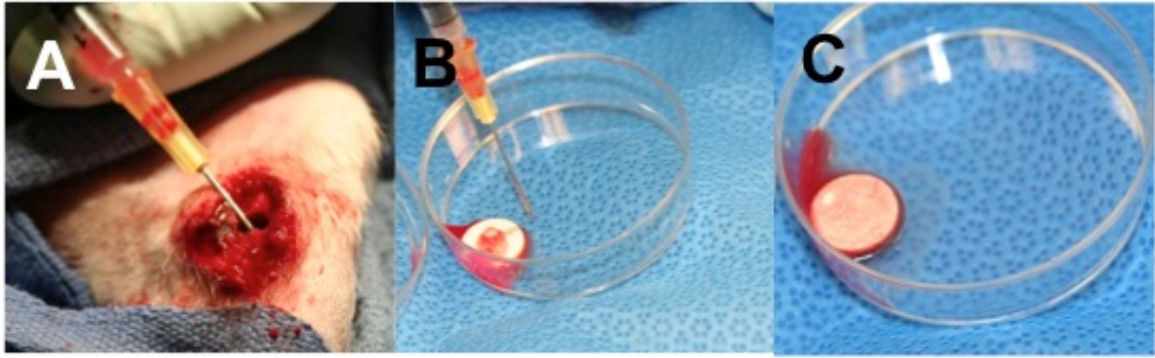
Figure 6.2. Bone marrow was harvested from the diaphysis (A), seeded on scaffolds (B), and absorbed into the scaffolds for 20 minutes.
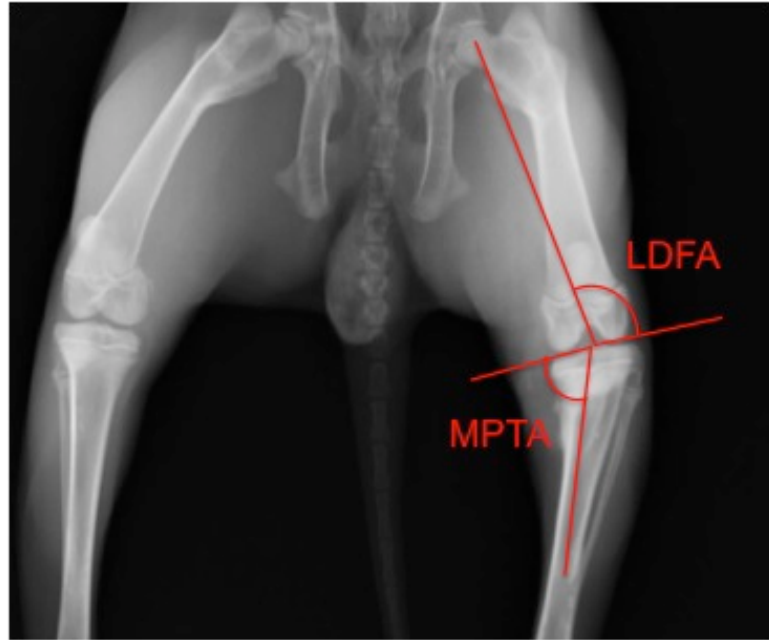
Figure 6.3. Medial proximal tibial angle (MPTA) and lateral distal femoral angle (LDFA) shown on radiograph.

6.2.8 Statistical Analysis

Analysis was carried out using GraphPad InStat software running an ANOVA followed by a Tukey–Kramer Multiple Comparisons Test. Results were considered significant if $p < 0.05$.

6.3 Results

6.3.1 Post-Operative Observations

Two of the rabbits became infected after scaffold implantation, both in the IGF-loaded scaffold group. An additional third rabbit in the cell-seeded, IGF-I loaded scaffold group showed signs of a possible infection but was treated with antibiotics.

6.3.2 Microcomputed Tomography

A bisected reconstruction of each upper tibia is shown in Figure 6.4. Varying amounts of bone growth occurred in all of the non-infected limbs. Full closure was seen for all the hybrid scaffolds, indicating bone growth with no defined growth plate line visible on implant side (left side). There appeared to be some bone forming around the implant site in the other samples, especially in the blank and IGF-I-loaded scaffold groups. The small gap on the medial side, where the defect site was created, may indicate a presence of cartilaginous tissue.

6.3.3 Anatomical Measurements

The MPTA data are shown in Figure 6.5A. All treatments resulted in an angle decrease 8 weeks after the implantation surgery. The lowest MPTA angle at 8 weeks was in the IGF-I-loaded scaffold group, which included the two infected animals. The next lowest was the fat implant group, followed by hybrid scaffold, cell-seeded IGF-loaded scaffold, and the blank scaffold. No statistical difference was seen between 3 and 11 weeks or scaffold types.

Figure 6.5B shows the LDFA results, ranging from 89.7 to 95.7°, where the fat implant group had the lowest angle, and the cell-seeded, IGF-loaded group had the highest angle 8 weeks after implantation. The blank scaffold group, IGF-I-loaded scaffold group, and hybrid scaffold group fell in between, with no statistical difference between any group.
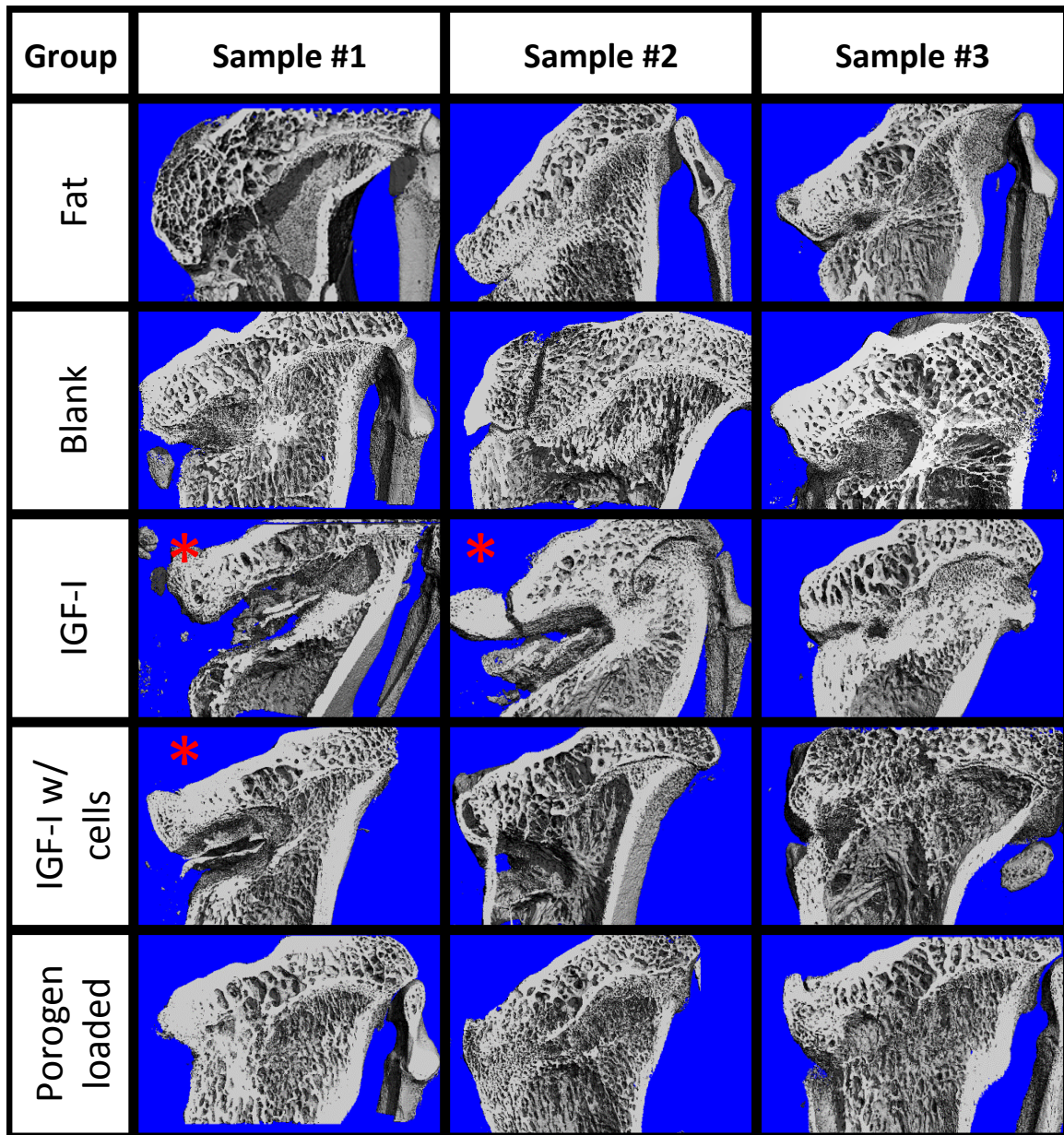
Figure 6.4. Cut-plane microCT images of each tibia for the five treatment groups: 1) fat implant, 2) blank scaffold, 3) IGF-I-loaded scaffold, 4) cell seeded, IGF-I loaded scaffold, and 5) hybrid scaffold. The defects were on the medial (left) side and the native growth plate is on the lateral (right) side. The red asterisk indicates infected animals.
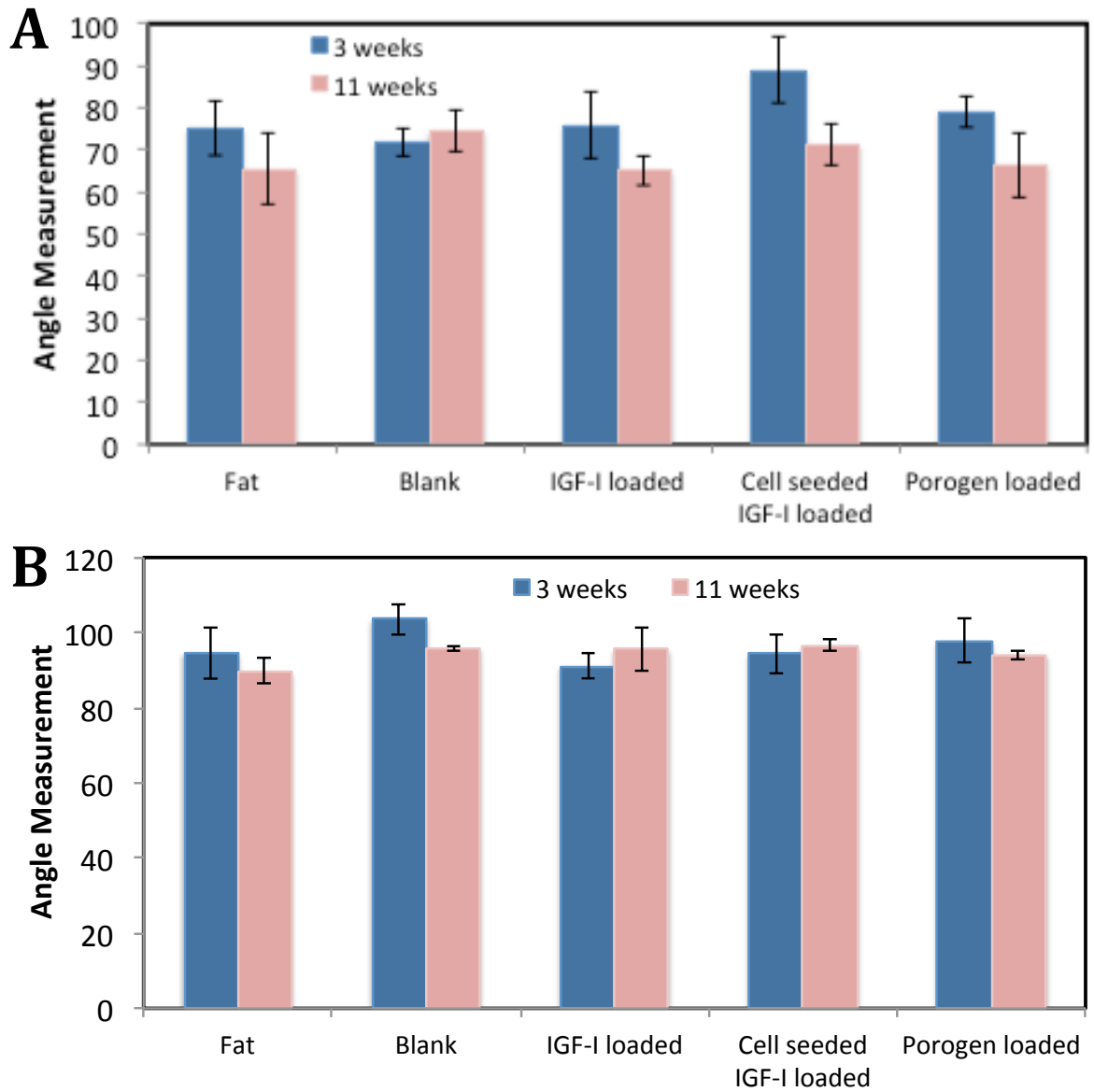
Figure 6.5. Medial proximal tibial angles (A) and lateral distal femoral angles (B) at 3 weeks after growth plate injury (before resection of the bony bar) and 8 weeks after implantation of scaffold. Data are shown as means ± standard error (n≥3).

6.3.4 Histology

Figure 6.6 shows rabbit tibiae cut in the coronal plane 8 weeks after implantation. The remnant of the native growth plate can be seen on the right side of all the images (the lateral side; L), while the implant site can be seen on the left side (or medial side; M). Figure 6.6A shows a section from one of the right legs, which served as a control. A distinct growth plate can be readily seen across the width of the tibia. Defects treated with fat grafts showed a dense region of bone tissue (stained pink and marked with an arrow) on the medial side where tissue had regrown (Figure 6.6B). A defect treated with a blank scaffold (Figure 6.6C) had a wider growth plate across the whole tibia than the fat graft. Treatment with IGF-I-loaded scaffolds with and without cells seeded resulted in a well-structured growth plate on the lateral side (Figure 6.6D) and an increase in chondrocytes on the medial side. The addition of seeding cells resulted and a large, dense area of cartilage on the upper medial side containing mostly hypertrophic chondrocytes, seen in Figure 6.6E The porogen loaded scaffold (Figure 6.6F) caused similar results to those for the IGF-I loaded scaffold, with scattered pockets of chondrocytes.

Magnified views of selected samples are shown in Figures 6.7-6.10, where the specific zones of the chondrocytes (reserve, proliferative, hypertrophic, or calcification zones) could be identified. The reserve chondrocytes were recognized by their smaller size, uniformly spherical appearance. Proliferative chondrocytes were observed more frequently in longitudinal columns with increasing volume of cytoplasm. Hypertrophic chondrocytes zone were identified based on their larger, spherical shape that eventually gave way to nuclear fragmentation as they entered the calcification zone. Figure 6.7 shows the results of the fat implant with a thin, but continual, connection of cartilage (stained purple) that goes across the width of the tibia, where the presence of chondrocytes in the reserve (R), proliferative (P), hypertrophic (H) and calcification zones (C) were seen. A defect treated with a blank scaffold had a thicker continual connection of chondrocytes (labeled in Figure 6.8B) with striations of cartilage below the growth plate area was observed, while the center of the tibia had thin patches of mostly hypertrophic chondrocytes. Treatment with IGF-I-loaded scaffolds had pockets of chondrocytes throughout the medial half of the tibia (Figure 6.9). The effect of a cell-seeded, IGF-loaded scaffold is shown in Figure 6.10, with a large pocket of chondrocytes

87
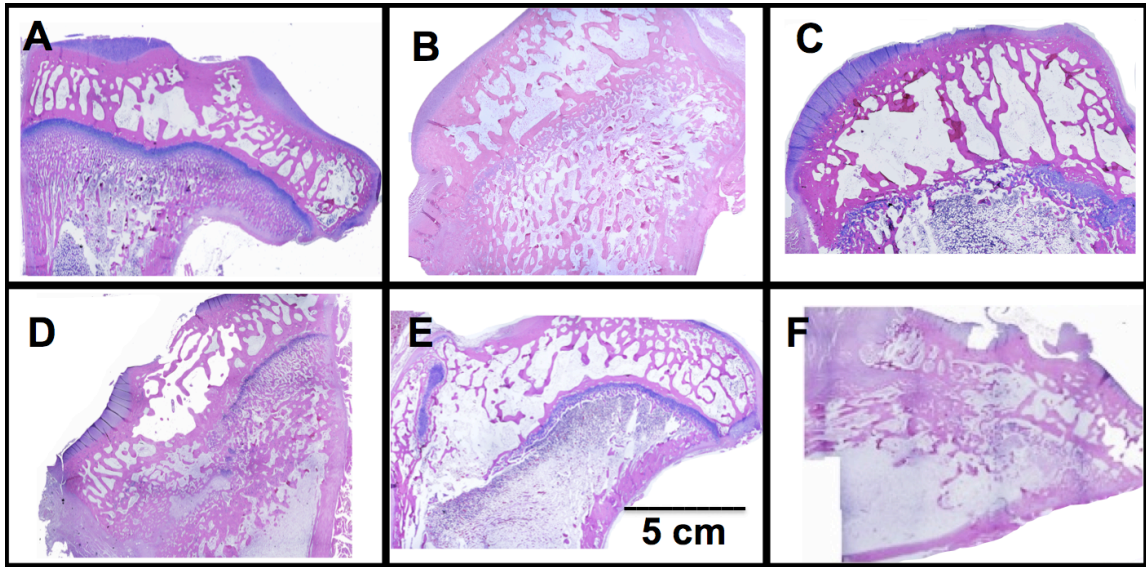
Figure 6.6. Representative histological images of proximal tibiae with A) no implant, B) fat implant, C) blank scaffold, D) IGF-loaded scaffold, E) cell seeded IGF-I loaded scaffold, and F) hybrid scaffold. For images B-F the defects were on the medial (left) side and the native growth plate is on the lateral (right) side.
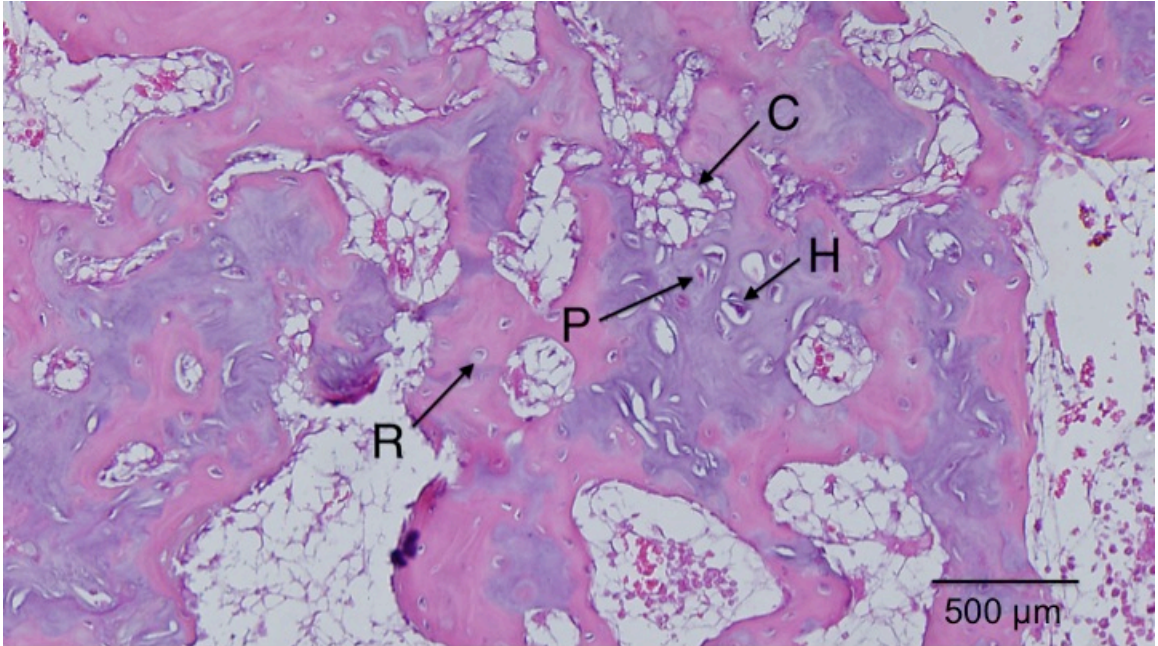
Figure 6.7. Fat implant showed thin, continual line of cells across medial side that contained reserve (R), proliferative (P), hypertrophic (H) cartilage cells and calcification zones (C).
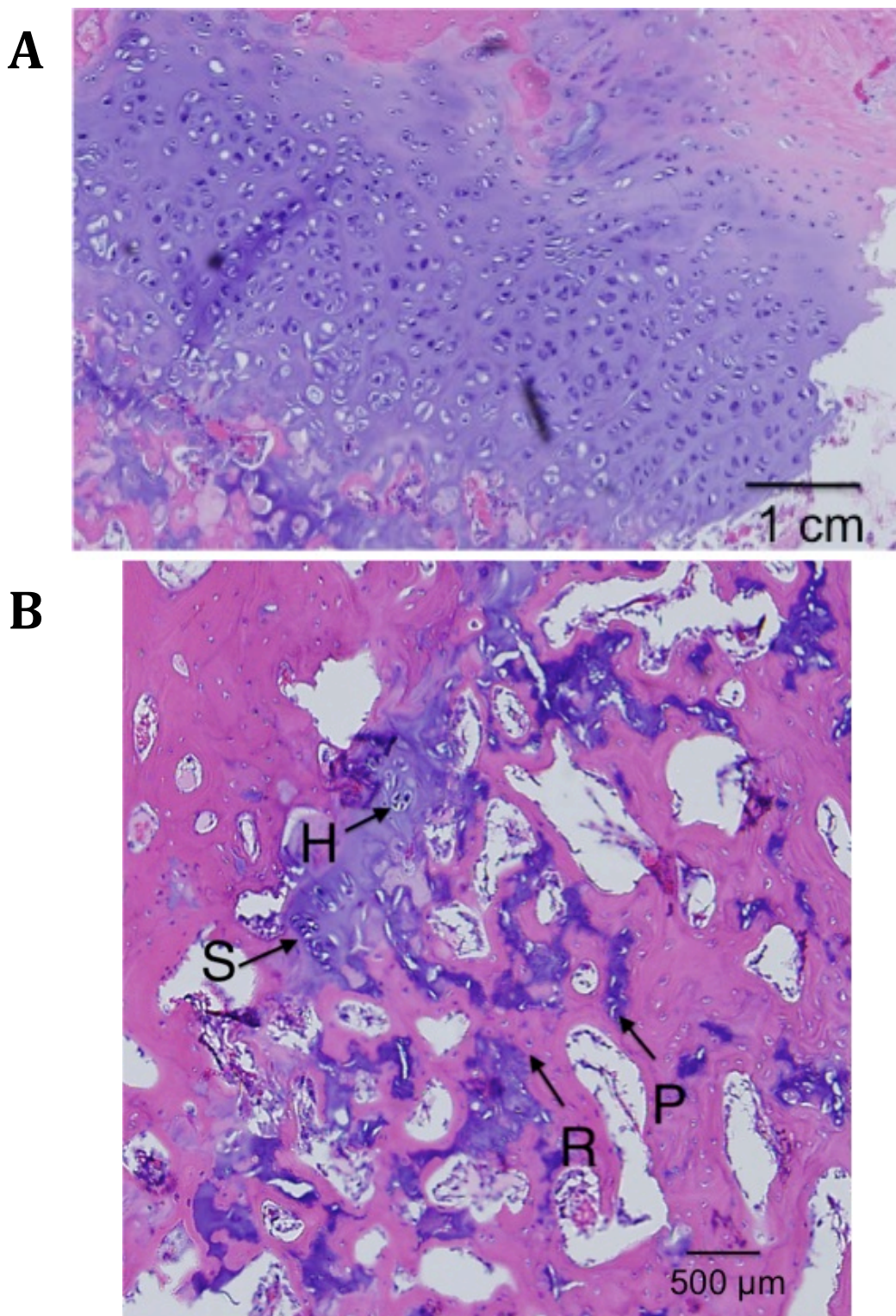
Figure 6.8. Blank scaffold on (A) the lateral side with columnar structure and (B) the medial side with the appearance of stacked (S), reserve (R), proliferative (P), and hypertrophic (H) cartilage cells.
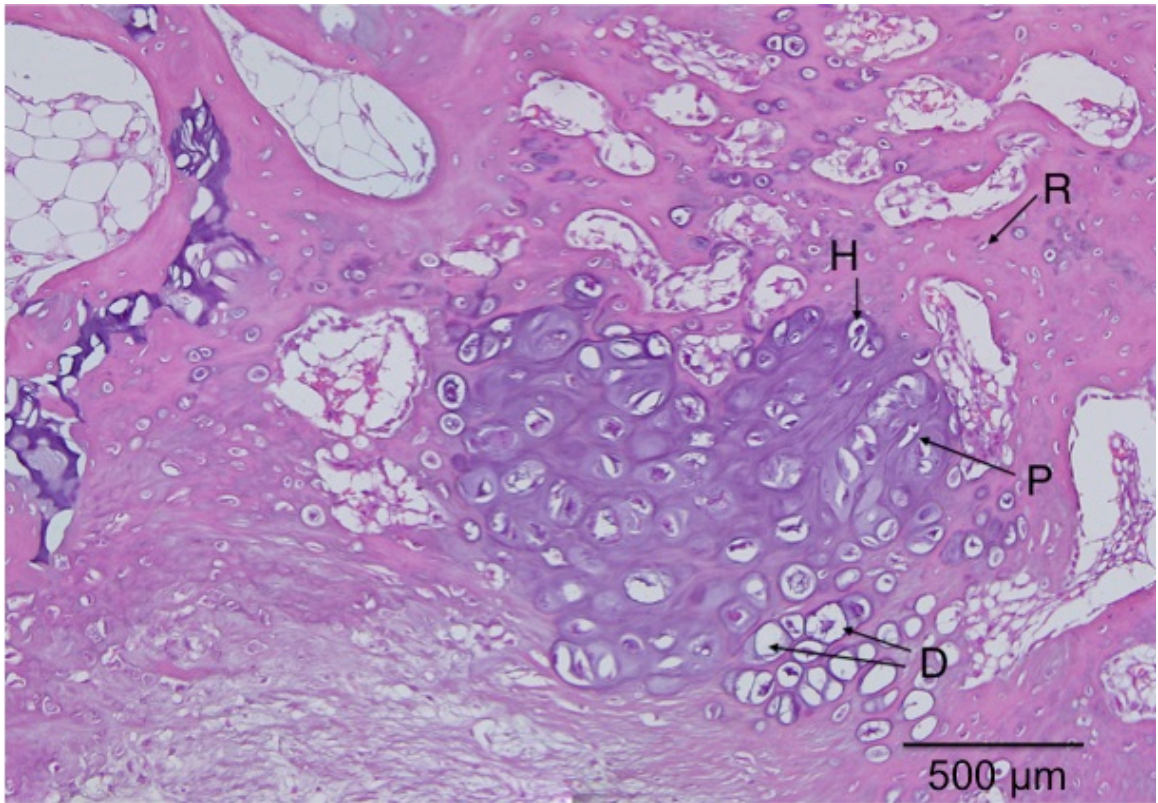
Figure 6.9. IGF-I loaded scaffold showed dispersed pockets of cartilage cells throughout the medial side with the appearance of reserve (R), proliferative (P), hypertrophic (H), and degenerative zones (D).
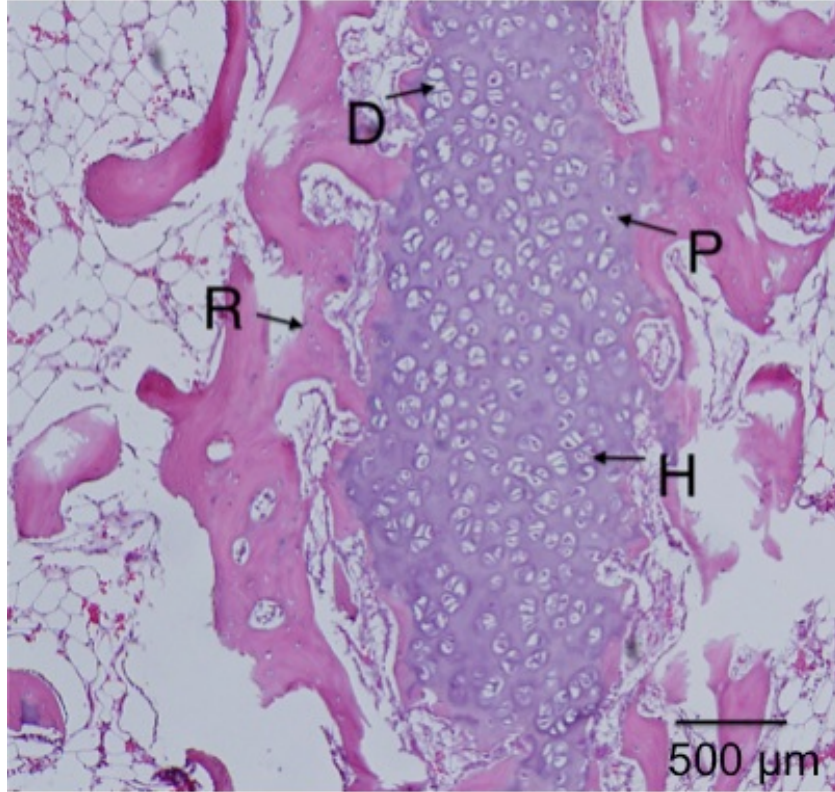
Figure 6.10. IGF-I loaded scaffolds with cells showed a large dense population of chondrocytes on the medial side with the appearance of reserve (R), proliferative (P), hypertrophic (H), and degenerative zones (D).

on the upper medial side containing mostly hypertrophic chondrocytes with reserve cells surrounding the pocket (Figure 6.10).

6.4 Discussion

6.4.1 Post-Operative Observations

The infection seen in three of the animals may be due to several possible sources for the infection, such as scaffold contamination, surgical technique or equipment, or animal tampering with the wound site.

6.4.2 Polymer and Implant Selection

In this study the molecular weight of the PLGA was ~30 kDa, which was an increase compared to previous work (Sundararaj et al., 2012). Previously, a molecular weight of ~6 kDa molecular weight was used and it was thought that the scaffold degraded too quickly and that using a higher molecular weight would increase the structural support to the implant site and allow for more tissue regrowth to occur before the scaffold degraded away. Implantation of lower molecular weight PLGA scaffolds successfully resulted in the presence of chondrocytes after 2 weeks with an increase in chondrocytes population in rabbits treated with IGF-I loaded scaffolds.

PLGA-based scaffolds were chosen because PLGA has been shown to be biocompatible and biodegradable (Kitchell et al., 1985; Shive et al., 1997). Drug delivery devices using PLGA microspheres are already FDA approved, such as, Lupron Depot[®], Zoladex[®], and Atridox[®], for the treatment of prostate cancer, endometriosis, and fibroids. The mechanical properties of PLGA scaffolds were shown to be suitable for hard and soft tissue implants with a compressive modulus of about 100 MPa (Clark et al., 2013).

To evaluate the success of a polymeric scaffold for growth plate regeneration, a fat implant was chosen to represent current clinical practice by using the Langenskiöld method where the bony bar is excised and replaced with transplanted fat (Langenskiöld, 1981; Langenskiöld et al., 1987; Tobita et al., 2002). Free fat transplants act as a space-filler that slowly undergoes ossification in an attempt to prevent total growth plate closure, but results are fair to poor in ~60% of patients (Foster et al., 2000; Hasler et al., 2002).

93

Growth factors have been theorized to enhance cartilage regeneration by increasing cell proliferation and decreasing cell apoptosis. Increasing cell proliferation using insulin-like growth factor I (IGF-I) can enhance bone and cartilage production *in vivo* (Damien et al., 2003; Hock et al., 1988; Lennox et al., 1983; McCarthy et al., 1989; Morisset et al., 2007; Yun et al., 2007). For this reason, IGF-I was loaded into the PLGA microspheres used to fabricate the scaffolds for this study. A recent study demonstrated retention of IGF-I bioactivity during scaffold fabrication (Clark et al., 2013). Seeding cells onto the scaffold was performed in an effort to add MSCs to the implant site directly instead of waiting for cell recruitment and proliferation during recovery. Hybrid scaffolds offer future possibilities for dual drug release and can be fabricated with little variation from the porous PLGA scaffold methods. Also, the hybrid scaffolds are able to maintain a similar compressive modulus to that of soft tissue.

6.4.3 Anatomical Measurements

Growth plate injury causes a decrease in both the MPTA and LDFA post operative, and therefore the higher the angle, the better the recovery. The MPTA and LDFA were both lowest in the fat implant group (excluding the infected animals), and although results were not significant, this may indicate that the fat graft does not correct angular deformation as well as a polymeric scaffold. Surprisingly, the highest MPTA and second highest LDFA were seen in the blank scaffold treatment groups. A similar trend was seen in previous work during an 8 week study, where the blank scaffold group had a higher angle than the other treatment types, although results were not significant (Ravi, 2009). It should be noted that all measurements were calculated by hand, which contributes to high standard deviations. Other groups have found a statistical difference, but their study lasted 4 months, twice as long as the current study. Planka et al. used MSCs seeded onto sodium hyaluronate/collagen scaffolds in a distal femur model and found a 0.50 ± 0.04 cm increase in bone length and a LDFA lowered by 3.6-4.5° over the control (Planka et al., 2008). Their control was no implant as compared to the clinically relevant fat implant used in the present study. In previous work, a control group, which received no implant resulted in bone formation at the implant site 8 weeks post operation and showed the lowest amount of angular correction (Ravi, 2009).

Eight weeks after implantation, defects treated with MSCs showed a greater presence of chondrocytes, yet no culturing time or additional surgery was required to harvest the cells. Li et al. have shown that chitin-based scaffolds with and without MSCs corrected angular deformation significantly after 16 weeks, yet other studies showed an improvement with the use of MSCs compared to the scaffold alone (Li et al., 2004). Chen et al. used MSCs seeded on agarose, which resulted in increased angle recovery and tibial length, while the agarose alone gave poor results (Chen et al., 2003; Lee et al., 1998). The major difference between the mentioned scaffolds is the mechanical properties. Agarose, collagen, and hyaluronan are commonly used in tissue engineering but have a low compressive modulus in the 1-150 kPa range, whereas chitosan and PLGA scaffolds have a compressive modulus of 750 kPa to 100 MPa (Awad et al., 2004; Clark et al., 2013; Lee et al., 2001; Masters et al., 2005; Nazarov et al., 2004; Zhang et al., 2001).

Within tissue engineering research, PLGA scaffolds with and without growth factors have been shown to create a microenvironment necessary for prolfieration and chondrogenic differentiation of MSCs (Foster et al., 2000; Hasler et al., 2002; Langenskiöld et al., 1987; Wattenbarger et al., 2002). Also, the PLGA scaffolds used in this study have a pore size of 50-100 μm, shown to be applicable for cell ingrowth (Griffon et al., 2006). Therefore, as long as some of the neighboring native growth plate cells remain or MSCs are around the defect site, the scaffold may be adequate to prevent bony bridge formation and allow for growth plate regeneration. Incorporating IGF-I or another type of growth factor into the scaffold may give the cellular signals necessary to initiate tissue regrowth as seen in the cells present at the implant site (discussed later).

Although the angle measurements did not show complete correction of the limb deformation, microCT images showed that bone had not completely filled the implant site, indicating that bony bar reformation was inhibited. Bony bar formation is one of the major complications associated with growth plate injures (Wattenbarger et al., 2002; Xian et al., 2004). Limb length discrepancy and angular deformation occurred in 58% of distal femur factures involving the growth plate (Basener et al., 2009). Even with the current clinical treatment of fat grafts, bony bridge reformation has been shown to occur nearly 30% of the time (Hasler et al., 2002). Johnstone et al. used a type I collagen paste

containing osteogenic protein-1 and found promising limb growth until bony bridge formation prevented further growth (Johnstone et al., 2002).

6.4.4 Histology

In this study, the attempt to regenerate the growth plate did not result in columnar structure to the degree that the native growth plate has, regardless of the treatment type. It appeared that the fat implant allowed for some cartilage regeneration, but it was only a cell wide at most points and most of the chondrocytes were in the calcification zone. The tissue surrounding the cartilage areas was woven bone, which has been known to appear after fractures (Hernandez et al., 2004; Shefelbine et al., 2005). The blank scaffold treatment resulted in tissue having a similar structure to that for the fat implants with a couple exceptions. First, there were a few areas where blank scaffolds had been placed with some cellular stacking, and secondly, the lateral side retained more structure, resembling that of the native growth plate, compared to defects treated with fat graft. The blank scaffolds gave the epiphyseal region more structural support, preventing further collapse of the lateral growth plate, while the fat graft implant had a thinner growth plate region across the whole tibia.

The defects treated with IGF-I-loaded scaffolds, both with or without seeded cells, showed a similar appearance on the lateral side as that of the blank scaffold group, however the medial sides were quite different. Without cells, the IGF-I-loaded scaffold resulted in pockets of chondrocytes throughout the medial side along the epiphyseal line that contained cells in all zones of cartilage development. The addition of cells created a large vertical pocket (~3 mm long) of chondrocytes located in the upper epiphyseal region. Interpretation of the IGF-I loaded samples was limited because only one sample could be used for observation so it is difficult to say if this cellular organization would occur again. The cells were mostly in the hypertrophic state and had no columnar organization. Both types of IGF-I loaded scaffolds (with and without cells seeding) increased the density of hypertrophic chondrocytes compared to the fat, blank, and hybrid scaffolds. Cells seeded on scaffolds containing IGF-I created the largest population of chondrocytes, which was to be expected based on the extensive literature surrounding IGF-I (Anderson et al., 2006; Clark et al., 2013; Hernandez et al., 2004; Kitchell et al., 1985; Lennox et al., 1983; Sundararaj et al., 2012). One such example is Masters et al.,

96

who showed that IGF-I can mediate bone marrow cells in chondrogenesis through increased cell proliferation and chondrocyte markers (Masters et al., 2005).

Compared to the study of Chen et al., which that lasted for 16 weeks, the histological results for this 8 week study are encouraging, having similarity in the types of cells present, albeit without columnar structure (Chen et al., 2003). Without MSCs, the hyaluronate/collagen, agarose, and chitin scaffolds had either similar hypertrophic pockets of chondrocytes or minimal presence of chondrocytes at all (Chen et al., 2003; Lee et al., 1998; Li et al., 2004; Planka et al., 2008). However, the use of MSCs seeded on the chitin or agarose scaffolds gave more of a columnar structure but had twice as much time to develop compared to samples in this study (Li et al., 2004).

6.5 Conclusion

The goal of this study was to develop a biodegradable scaffold to regenerate the growth plate without the use of previously harvested MSC. Using cells harvested from the tibia during surgery showed improvement over treatment with the scaffold implant alone, and avoided the invasive, costly procedure of harvesting MSCs from the iliac crest. All the PLGA scaffolds led to better retention of the lateral native growth plate compared to the current clinical treatment of using fat grafts. Incorporating IGF-I into the scaffolds increased the presence of chondrocytes at the defect site. Further enhancement of cartilage formation was observed with the addition of bone marrow cells collected at the time of the surgery to IGF-I-loaded scaffolds. Although the angular deformation did not recover significantly after 8 weeks regardless of the treatment type, the histological results indicated the necessary cells were present and perhaps more time was necessary to see an effect in overall growth plate regeneration. This study showed that adding mechanical support to the implant site helped retain more native growth plate. Additionally, chondrocyte population could be increase using a growth factor and tibia BMCs, offering a better alternative to current clinical treatment and a different perceptive than current research.

Chapter 7 Summary and Conclusion

In this dissertation, a variety of PLGA scaffolds were developed and characterized. Porous PLGA scaffolds were made to be suitable for soft or hard tissue applications by tailoring the salt leaching method and adding a microsphere fusion step during the scaffold fabrication process. Significant mechanical properties were maintained longer and increased degradation times were possible with scaffolds that had been fused. Additionally, a novel blended microsphere was created by mixing two molecular weights during microsphere fabrication. This scaffold required a lower fusion temperature than a scaffold made from a 50:50 mix of HMW and LMW microspheres, advantageous for drug encapsulation.

To characterize the drug delivery and in vitro properties, the HMW scaffold was loaded with a growth factor. To show the applicability the scaffold has for soft tissue applications, IGF-I was used, which also lead to significant findings on the thermal stability of IGF-I. The bioactivity of IGF-I was retained through heating, compression and solvent interaction, which had not previously been published to our knowledge. The tri-phasic release of IGF-I was able to create an increase in bone marrow cell proliferation after 3 weeks, and a GAG content increase after 6 weeks. To further expand the drug delivery capabilities, a hybrid scaffold was developed, fabricated from PBAE and PLGA. Using a quick degrading PBAE created a 12-hour drug release and a 48-hour porogen degradation period, leaving a porous PLGA matrix. Adding PBAE particles at varying amounts resulted in the same drug release rate from both the PBAE particles and the PLGA matrix.

To investigate the potential clinical application of the PLGA scaffold, an *in vivo* study was performed. Treatment of growth plate injuries is an area of pediatric orthopedics that could use improvement. The blank PLGA proved to be just as effective as the current clinical treatment and with the addition of IGF-I and cell seeding, collected at the time of surgery, there was an increase in growth plate cells (chondrocytes). This method is preferable over other research options, which require harvesting and culturing cells weeks before the growth plate surgery. Though the results did not show total growth

plate regeneration, the necessary cell types were present and there is potential to improve upon these methods.

Potential options in future work may be to prolong the degradation and growth factor delivery time. Prolonging the degradation will give the BMCs more time to migrate into the scaffold and proliferate into growth plate type cells and structure. Increasing the degradation time would also increase the release time of IGF-I that would help the BMCs proliferate. Also, the cells collected during the time of surgery offered promising results and could be further investigated. Doing further *in vitro* studies on varying cell densities of BMCs on drug loaded scaffolds would be beneficial to knowing how many cells should be collected during the time of surgery.

Overall, the work presented here shows that porous, microsphere-based PLGA scaffolds can be fabricated to have a diverse rage of degradation and mechanical properties using varying fusion temperatures. A single or dual drug delivery can be accomplished by introducing a porogen without affecting the bioactivity of the drug or protein. *In vitro* and *in vivo* studies demonstrated the scaffold's use for cartilage regeneration and clinical relevance.

99

References

Agrawal CM, Ray RB. Biodegradable polymeric scaffolds for musculoskeletal tissue engineering. J Biomed Mater Res. 55(2):141-50. 2001.

Anderson DG, Tweedie CA, Hossain N, Navarro SM, Brey DM, Van Vliet KJ, Langer R, Burdick JA. A Combinatorial Library of Photocrosslinkable and Degradable Materials. Adv Mater. 18(19):2614-8. 2006.

Anderson JM, Shive MS. Biodegradation and biocompatibility of PLA and PLGA microspheres. Adv Drug Delivery Rev. 28(1):5-24. 1997.

Andres D. Tyrosine Kinase Receptors. In: Course CS, editor. Lexington: University of Kentucky; 2010.

Arakawa T, Kita Y, Carpenter JF. Protein–solvent interactions in pharmaceutical formulations. Pharm Res. 8(3):285-91. 1991.

Asakura T, Adachi K, Schwartz E. Stabilizing Effect of Various Organic Solvents on Protein. J Biol Chem. 253(18):6423-5. 1978.

Attawia MA, Uhrich KE, Botchwey E, Fan M, Langer R, Laurencin CT. Cytotoxicity testing of poly (anhydride‐co‐imides) for orthopedic applications. J Biomed Mater Res. 29(10):1233-40. 1995.

Awad HA, Quinn Wickham M, Leddy HA, Gimble JM, Guilak F. Chondrogenic differentiation of adipose-derived adult stem cells in agarose, alginate, and gelatin scaffolds. Biomaterials. 25(16):3211-22. 2004.

Ballock RT, O'Keefe RJ. The Biology of the Growth Plate. J Bone Joint Surg. 85(4):715-26. 2003.

Barichello JM, Morishita M, Takayama K, Nagai T. Encapsulation of Hydrophilic and Lipophilic Drugs in PLGA Nanoparticles by the Nanoprecipitation Method. Drug Dev Ind Pharm. 25(4):471-6. 1999.

Basener CJ, Mehlman CT, DiPasquale TG. Growth disturbance after distal femoral growth plate fractures in children: a meta-analysis. J Orthop Trauma. 23(9):663-7. 2009.

Baserga R, Morrione A, Prisco M. Growth factors, cell proliferation, and apoptosis. Heart Fail Rev. 3(1):5-14. 1998.

Batycky RP, Hanes J, Langer R, Edwards DA. A theoretical model of erosion and macromolecular drug release from biodegrading microspheres. J Pharm Sci. 86(12):1464-77. 1997.

Baxter RC. Insulin-like growth factor binding proteins in the human circulation: a review. Horm Res Paediatr. 42(4-5):140-4. 1994.

Behrens F, Shepard N, Mitchell N. Alterations of rabbit articular cartilage by intra-articular injections of glucocorticoids. J Bone Joint Surg Am. 57(1):70-6. 1975.

Benita S. Microencapsulation: Methods and Industrial Applications: CRC Press; 2006.

Black J. Systemic effects of biomaterials. Biomaterials. 5(1):11-8. 1984.

Borden M, Attawia M, Khan Y, Laurencin CT. Tissue engineered microsphere-based matrices for bone repair:: design and evaluation. Biomaterials. 23(2):551-9. 2002.

100

Bredt J, Sach E, Brancazio D, Cima M, Curodeau A, Fan T. Three dimensional printing system. In: Patent U, editor.1998.

Brey DM, Erickson I, Burdick JA. Influence of macromer molecular weight and chemistry on poly (β‑amino ester) network properties and initial cell interactions. J Biomed Mater Res A. 85(3):731-41. 2008.

Brey DM, Ifkovits JL, Mozia RI, Katz JS, Burdick JA. Controlling poly(beta-amino ester) network properties through macromer branching. Acta Biomater. 4(2):207-17. 2008.

Brown JL, Nair LS, Laurencin CT. Solvent/non-solvent sintering: a novel route to create porous microsphere scaffolds for tissue regeneration. J Biomed Mater Res B Appl Biomater. 86(2):396-406. 2008.

Burdan F, Szumiło J, Korobowicz A, Farooquee R, Patel S, Patel A, Dave A, Szumiło M, Solecki M, Klepacz R. Morphology and physiology of the epiphyseal growth plate. Folia Histochem Cytobiol. 47(1):5-16. 2009.

Burg KJL, Porter S, Kellam JF. Biomaterial developments for bone tissue engineering. Biomaterials. 21(23):2347-59. 2000.

Burkersroda Fv, Schedl L, Göpferich A. Why degradable polymers undergo surface erosion or bulk erosion. Biomaterials. 23(21):4221-31. 2002.

Buschmann J, Harter L, Gao S, Hemmi S, Welti M, Hild N, Schneider OD, Stark WJ, Lindenblatt N, Werner CM, et al. Tissue engineered bone grafts based on biomimetic nanocomposite PLGA/amorphous calcium phosphate scaffold and human adipose-derived stem cells. Injury. 43(10):1689-97. 2012.

Cabre F, Fernandez MF, Calvo L, Ferrer X, Garcia ML, Mauleon D. Analgesic, antiinflammatory, and antipyretic effects of S(+)-ketoprofen in vivo. J Clin Pharmacol. 38(12 Suppl):3S-10S. 1998.

Capito R, Spector M. Collagen scaffolds for nonviral IGF-1 gene delivery in articular cartilage tissue engineering. Gene Ther. 14(9):721-32. 2007.

Chang SH, Oh CD, Yang MS, Kang SS, Lee YS, Sonn JK, Chun JS. Protein kinase C regulates chondrogenesis of mesenchymes via mitogen-activated protein kinase signaling. J Biol Chem. 273(30):19213-9. 1998.

Chen D, Zhao M, Mundy GR. Bone morphogenetic proteins. Growth Factors. 22(4):233-41. 2004.

Chen F, Hui JH, Chan WK, Lee EH. Cultured mesenchymal stem cell transfers in the treatment of partial growth arrest. J Pediatr Orthop. 23(4):425-9. 2003.

Chen G, Sato T, Ushida T, Ochiai N, Tateishi T. Tissue engineering of cartilage using a hybrid scaffold of synthetic polymer and collagen. Tissue Eng. 10(3-4):323-30. 2004.

Chi SC, Jun HW. Release rates of ketoprofen from poloxamer gels in a membraneless diffusion cell. J Pharm Sci. 80(3):280-3. 1991.

Choi YS, Cho HY, Hoyt KR, Naegele JR, Obrietan K. IGF‑1 receptor‑mediated ERK/MAPK signaling couples status epilepticus to progenitor cell proliferation in the subgranular layer of the dentate gyrus. Glia. 56(7):791-800. 2008.

Clark A, Milbrandt TA, Hilt JZ, Puleo DA. Retention of Insulin-like Growth Factor I Bioactivity during Fabrication of Sintered Polymeric Scaffolds. Biomedical Materials. Submitted. 2013.

Clark A, Milbrandt TA, Hilt JZ, Puleo DA. Tailoring properties of microsphere-based poly(lactic-co-glycolic acid) scaffolds. J Biomed Mater Res A. 2013.

Cleland JL, Mac A, Boyd B, Yang J, Duenas ET, Yeung D, Brooks D, Hsu C, Chu H, Mukku V. The stability of recombinant human growth hormone in poly (lactic-co-glycolic acid)(PLGA) microspheres. Pharm Res. 14(4):420-5. 1997.

Cohen S, Yoshioka T, Lucarelli M, Hwang L, Langer R. Controlled Delivery Systems for Proteins Based on Poly(Lactic/Glycolic Acid) Microspheres. Pharm Res. 8(6):713-20. 1991.

Coleman J, Lowman A. Biodegradable nanoparticles for protein delivery: analysis of preparation conditions on particle morphology and protein loading, activity and sustained release properties. J Biomater Sci Polym Ed. 23(9):1129-51. 2012.

Collier RJ, Miller MA, Hildebrandt JR, Torkelson AR, White TC, Madsen KS, Vicini JL, Eppard PJ, Lanza GM. Factors Affecting Insulin-Like Growth Factor-I Concentration in Bovine Milk. J Dairy Sci. 74(9):2905-11. 1991.

Cornell CN, Lane JM, Chapman M, Merkow R, Seligson D, Henry S, Gustilo R, Vincent K. Multicenter trial of Collagraft as bone graft substitute. J Orthop Trauma. 5(1):1-8. 1991.

Crotts G, Park TG. Protein delivery from poly (lactic-co-glycolic acid) biodegradable microspheres: release kinetics and stability issues. J Microencapsul. 15(6):699-713. 1998.

Dahlin C, Linde A, Gottlow J, Nyman S. Healing of Bone Defects by Guided Tissue Regeneration. Plast Reconstr Surg. 81(5):672-6. 1988.

Damien E, Hing K, Saeed S, Revell PA. A preliminary study on the enhancement of the osteointegration of a novel synthetic hydroxyapatite scaffold in vivo. J Biomed Mater Res A. 66A(2):241-6. 2003.

Dennler S, Goumans M-J, ten Dijke P. Transforming growth factor β signal transduction. J Leukoc Biol. 71(5):731-40. 2002.

Derfoul A, Perkins GL, Hall DJ, Tuan RS. Glucocorticoids promote chondrogenic differentiation of adult human mesenchymal stem cells by enhancing expression of cartilage extracellular matrix genes. Stem Cells. 24(6):1487-95. 2006.

Dhandayuthapani B, Yoshida Y, Maekawa T, Kumar DS. Polymeric scaffolds in tissue engineering application: a review. Inter J of Polym Sci. 2011.

DiCarlo B, Hu J, Gross T, Vago R, Athanasiou K. Biomaterial effects in articular cartilage tissue engineering using polyglycolic acid, a novel marine origin biomaterial, IGF-I, and TGF-β1. Proc Inst Mech Eng H J Eng Med. 223(1):63-73. 2009.

Dorati R, Colonna C, Genta I, Modena T, Conti B. Effect of porogen on the physico-chemical properties and degradation performance of PLGA scaffolds. Polym Degrad Stabil. 95(4):694-701. 2010.

Ebara S, Nakayama K. Mechanism for the action of bone morphogenetic proteins and regulation of their activity. Spine (Phila Pa 1976). 27(16 Suppl 1):S10-5. 2002.

Elisseeff J, McIntosh W, Fu K, Blunk BT, Langer R. Controlled-release of IGF-I and TGF-beta1 in a photopolymerizing hydrogel for cartilage tissue engineering. J Orthop Res. 19(6):1098-104. 2001.

England JL, Haran G. Role of solvation effects in protein denaturation: from thermodynamics to single molecules and back. Annu Rev Phys Chem. 62257-77. 2011.

Ferguson CM, Schwarz EM, Reynolds PR, Puzas JE, Rosier RN, O'Keefe RJ. Smad2 and 3 mediate transforming growth factor-beta1-induced inhibition of chondrocyte maturation. Endocrinology. 141(12):4728-35. 2000.

Fernández‐Martín F, Otero L, Solas M, Sanz P. Protein Denaturation and Structural Damage During High‐Pressure‐Shift Freezing of Porcine and Bovine Muscle. J Food Sci. 65(6):1002-8. 2000.

Flier JS, Underhill LH, Le Roith D. Insulin-like growth factors. N Engl J Med. 336(9):633-40. 1997.

Forcino RG, Philadelphia UotSi. Characterization of Blended PLGA:PEG Scaffolds for Bone Regeneration Applications: University of the Sciences in Philadelphia; 2007.

Fortier LA, Lust G, Mohammed HO, Nixon AJ. Coordinate upregulation of cartilage matrix synthesis in fibrin cultures supplemented with exogenous insulin‐like growth factor‐I. J Orthop Res. 17(4):467-74. 1999.

Foster BK, John B, Hasler C. Free fat interpositional graft in acute physeal injuries: the anticipatory Langenskiöld procedure. J Pediatr Orthoped. 20(3):282-5. 2000.

Fredenberg S, Wahlgren M, Reslow M, Axelsson A. The mechanisms of drug release in poly (lactic-co-glycolic acid)-based drug delivery systems—a review. Int J Pharm. 415(1):34-52. 2011.

Freed L, Grande D, Lingbin Z, Emmanual J, Marquis J, Langer R. Joint resurfacing using allograft chondrocytes and synthetic biodegradable polymer scaffolds. J Biomed Mater Res. 28(8):891-9. 1994.

Fu K, Pack DW, Klibanov AM, Langer R. Visual evidence of acidic environment within degrading poly (lactic-co-glycolic acid)(PLGA) microspheres. Pharm Res. 17(1):100-6. 2000.

Fujihara K, Kotaki M, Ramakrishna S. Guided bone regeneration membrane made of polycaprolactone/calcium carbonate composite nano-fibers. Biomaterials. 26(19):4139-47. 2005.

Fukumoto T, Sperling JW, Sanyal A, Fitzsimmons JS, Reinholz GG, Conover CA, O'Driscoll SW. Combined effects of insulin-like growth factor-1 and transforming growth factor-beta1 on periosteal mesenchymal cells during chondrogenesis in vitro. Osteoarthr Cartil. 11(1):55-64. 2003.

Garcia JT, Farina JB, Munguia O, Llabres M. Comparative degradation study of biodegradable microspheres of poly(DL-lactide-co-glycolide) with poly(ethyleneglycol) derivates. J Microencapsul. 16(1):83-94. 1999.

103

Gentry LE, Nash BW. The pro domain of pre-pro-transforming growth factor .beta.1 when independently expressed is a functional binding protein for the mature growth factor. Biochemistry. 29(29):6851-7. 1990.

Ghaderi R, Carlfors J. Biological activity of lysozyme after entrapment in poly(d,l-lactide-co-glycolide)-microspheres. Pharm Res. 14(11):1556-62. 1997.

Govender S, Csimma C, Genant HK, Valentin-Opran A, Amit Y, Arbel R, Aro H, Atar D, Bishay M, Börner MG. Recombinant human bone morphogenetic protein-2 for treatment of open tibial fractures a prospective, controlled, randomized study of four hundred and fifty patients. J Bone Joint Surg. 84(12):2123-34. 2002.

Griffon DJ, Sedighi MR, Schaeffer DV, Eurell JA, Johnson AL. Chitosan scaffolds: interconnective pore size and cartilage engineering. Acta Biomater. 2(3):313-20. 2006.

Guenther HL, Guenther HE, Froesch ER, Fleisch H. Effect of insulin-like growth factor on collagen and glycosaminoglycan synthesis by rabbit articular chondrocytes in culture. Cell Mol Life Sci. 38(8):979-81. 1982.

Gunatillake PA, Adhikari R. Biodegradable synthetic polymers for tissue engineering. Eur Cell Mater. 5(1):1-16. 2003.

Guo S, Dipietro LA. Factors affecting wound healing. J Dent Res. 89(3):219-29. 2010.

Hallab NJ, Jacobs JJ. Biologic effects of implant debris. Bulletin of the NYU hospital for joint diseases. 67(2):182. 2009.

Hanada K, Solchaga LA, Caplan AI, Hering TM, Goldberg VM, Yoo JU, Johnstone B. BMP‐2 induction and TGF‐β1 modulation of rat periosteal cell chondrogenesis. J Cell Biochem. 81(2):284-94. 2001.

Harris LD, Kim BS, Mooney DJ. Open pore biodegradable matrices formed with gas foaming. J Biomed Mater Res. 42(3):396-402. 1998.

Hasler CC, Foster BK. Secondary tethers after physeal bar resection: a common source of failure? Clin Orthop. 405242-9. 2002.

Hassan MQ, Tare RS, Lee SH, Mandeville M, Morasso MI, Javed A, Van Wijnen AJ, Stein JL, Stein GS, Lian JB. BMP2 commitment to the osteogenic lineage involves activation of Runx2 by DLX3 and a homeodomain transcriptional network. J Biol Chem. 281(52):40515-26. 2006.

Hawkins AM, Milbrandt TA, Puleo DA, Hilt JZ. Synthesis and analysis of degradation, mechanical and toxicity properties of poly(β-amino ester) degradable hydrogels. Acta Biomater. 7(5):1956-64. 2011.

Hawkins AM, Milbrandt TA, Puleo DA, Zach Hilt J. Composite hydrogel scaffolds with controlled pore opening via biodegradable hydrogel porogen degradation. J Biomed Mater Res A. 2013.

Hawkins AM, Puleo DA, Hilt JZ. Effect of macromer synthesis time on the properties of the resulting poly(β‐amino ester) degradable hydrogel. Journal of Applied Polymer Science. 122(2):1420-6. 2011.

Heller J, Barr J, Ng SY, Abdellauoi KS, Gurny R. Poly (ortho esters): synthesis, characterization, properties and uses. Adv Drug Deliv Rev. 54(7):1015-39. 2002.

Heng BC, Cao T, Lee EH. Directing stem cell differentiation into the chondrogenic lineage in vitro. Stem Cells. 22(7):1152-67. 2004.

Hernandez CJ, Majeska RJ, Schaffler MB. Osteocyte density in woven bone. Bone. 35(5):1095-9. 2004.

Hickey T, Kreutzer D, Burgess DJ, Moussy F. Dexamethasone/PLGA microspheres for continuous delivery of an anti-inflammatory drug for implantable medical devices. Biomaterials. 23(7):1649-56. 2002.

Hoare TR, Kohane DS. Hydrogels in drug delivery: Progress and challenges. Polymer. 49(8):1993-2007. 2008.

Hock JM, Centrella M, Canalis E. Insulin-like growth factor I has independent effects on bone matrix formation and cell replication. Endocrinology. 122(1):254-60. 1988.

Hofmann G, Somero G. Evidence for protein damage at environmental temperatures: seasonal changes in levels of ubiquitin conjugates and hsp70 in the intertidal mussel Mytilus trossulus. J Exp Biol. 198(7):1509-18. 1995.

Holland TA, Bodde EW, Cuijpers VM, Baggett LS, Tabata Y, Mikos AG, Jansen JA. Degradable hydrogel scaffolds for in vivo delivery of single and dual growth factors in cartilage repair. Osteoarthr Cartil. 15(2):187-97. 2007.

Hollinger JO, Schmitz JP. Restoration of bone discontinuities in dogs using a biodegradable implant. J Oral Maxillofac Surg. 45(7):594-600. 1987.

Hou Q, Grijpma DW, Feijen J. Porous polymeric structures for tissue engineering prepared by a coagulation, compression moulding and salt leaching technique. Biomaterials. 24(11):1937-47. 2003.

Houchin ML, Topp EM. Chemical degradation of peptides and proteins in PLGA: a review of reactions and mechanisms. J Pharm Sci. 97(7):2395-404. 2008.

Hull C. Method for production of three-dimen- sional objects by stereolithography. In: Patent U, editor.1990.

Hutmacher DW. Scaffolds in tissue engineering bone and cartilage. Biomaterials. 21(24):2529-43. 2000.

Iannotti J. Growth plate physiology and pathology. Orthop Clin North Am. 21(1):1. 1990.

Ibim SE, Uhrich KE, Attawia M, Shastri VR, El‐Amin SF, Bronson R, Langer R, Laurencin CT. Preliminary in vivo report on the osteocompatibility of poly (anhydride‐co‐imides) evaluated in a tibial model. J Biomed Mater Res. 43(4):374-9. 1998.

Ikeda R, Fujioka H, Nagura I, Kokubu T, Toyokawa N, Inui A, Makino T, Kaneko H, Doita M, Kurosaka M. The effect of porosity and mechanical property of a synthetic polymer scaffold on repair of osteochondral defects. Int Orthop. 33(3):821-8. 2009.

Inai K, Norris RA, Hoffman S, Markwald RR, Sugi Y. BMP-2 induces cell migration and periostin expression during atrioventricular valvulogenesis. Dev Biol. 315(2):383-96. 2008.

Jabbarzadeh E, Deng M, Lv Q, Jiang T, Khan YM, Nair LS, Laurencin CT. VEGF-incorporated biomimetic poly(lactide-co-glycolide) sintered microsphere

scaffolds for bone tissue engineering. J Biomed Mater Res B. 100(8):2187-96. 2012.

Jaklenec A, Hinckfuss A, Bilgen B, Ciombor DM, Aaron R, Mathiowitz E. Sequential release of bioactive IGF-I and TGF-β1 from PLGA microsphere-based scaffolds. Biomaterials. 29(10):1518-25. 2008.

Jaramillo D, Shapiro F, Hoffer FA, Winalski CS, Koskinen MF, Frasso R, Johnson A. Posttraumatic growth-plate abnormalities: MR imaging of bony-bridge formation in rabbits. Radiology. 175(3):767-73. 1990.

Jiang T, Abdel-Fattah WI, Laurencin CT. In vitro evaluation of chitosan/poly(lactic acid-glycolic acid) sintered microsphere scaffolds for bone tissue engineering. Biomaterials. 27(28):4894-903. 2006.

Jiang T, Khan Y, Nair LS, Abdel-Fattah WI, Laurencin CT. Functionalization of chitosan/poly(lactic acid-glycolic acid) sintered microsphere scaffolds via surface heparinization for bone tissue engineering. J Biomed Mater Res. 93A(3):1193-208.

Johnstone EW, McArthur M, Solly PB, Higginson K, Byers S, Foster BK. The effect of osteogenic protein-1 in an in vivo physeal injury model. Clin Orthop Relat Res. 395234-40. 2002.

Kampinga HH, Brunsting JF, Stege GJJ, Burgman PWJJ, Konings AWT. Thermal Protein Denaturation and Protein Aggregation in Cells Made Thermotolerant by Various Chemicals: Role of Heat Shock Proteins. Exp Cell Res. 219(2):536-46. 1995.

Kang SH, Kim JU, Imm JY, Oh S, Kim SH. The effects of dairy processes and storage on insulin-like growth factor-I (IGF-I) content in milk and in model IGF-I-fortified dairy products. J Dairy Sci. 89(2):402-9. 2006.

Kang SW, Sun‐Mi S, Jae‐Sun L, Eung‐Seok L, Kwon‐Yong L, Sang‐Guk P, Jung‐Ho P, Byung‐Soo K. Regeneration of whole meniscus using meniscal cells and polymer scaffolds in a rabbit total meniscectomy model. J Biomed Mater Res A. 77(4):659-71. 2006.

Kempen DH, Lu L, Heijink A, Hefferan TE, Creemers LB, Maran A, Yaszemski MJ, Dhert WJ. Effect of local sequential VEGF and BMP-2 delivery on ectopic and orthotopic bone regeneration. Biomaterials. 30(14):2816-25. 2009.

Kempen DHR, Lu L, Hefferan TE, Creemers LB, Maran A, Classic KL, Dhert WJA, Yaszemski MJ. Retention of in vitro and in vivo BMP-2 bioactivities in sustained delivery vehicles for bone tissue engineering. Biomaterials. 29(22):3245-52. 2008.

Kenley RA, Lee MO, Mahoney TR, Sanders LM. Poly(lactide-co-glycolide) decomposition kinetics in vivo and in vitro. Macromolecules. 20(10):2398-403. 1987.

Khoshhal KI, Kiefer GN. Physeal Bridge Resection. J Am Acad Orthop Surg. 13(1):47-58. 2005.

Kim B-S, Park SW, Hammond PT. Hydrogen-bonding layer-by-layer-assembled biodegradable polymeric micelles as drug delivery vehicles from surfaces. Acs Nano. 2(2):386-92. 2008.

Kim J, Yaszemski MJ, Lu L. Three-dimensional porous biodegradable polymeric scaffolds fabricated with biodegradable hydrogel porogens. Tissue Eng Pt C-Meth. 15(4):583-94. 2009.

Kim SS, Gwak SJ, Choi CY, Kim BS. Skin regeneration using keratinocytes and dermal fibroblasts cultured on biodegradable microspherical polymer scaffolds. J Biomed Mater Res B. 75(2):369-77. 2005.

Kitchell JP, Wise DL. Poly(lactic/glycolic acid) biodegradable drug-polymer matrix systems. Methods Enzymol. 112436-48. 1985.

Klawitter J, Bagwell J, Weinstein A, Sauer B, Pruitt J. An evaluation of bone growth into porous high density polyethylene. J Biomed Mater Res. 10(2):311-23. 1976.

Klompmaker J, Jansen H, Veth R, De Groot J, Nijenhuis A, Pennings A. Porous polymer implant for repair of meniscal lesions: a preliminary study in dogs. Biomaterials. 12(9):810-6. 1991.

Kuhn LT, Ou G, Charles L, Hurley MM, Rodner CM, Gronowicz G. Fibroblast Growth Factor-2 and Bone Morphogenetic Protein-2 Have a Synergistic Stimulatory Effect on Bone Formation in Cell Cultures From Elderly Mouse and Human Bone. J Gerontol A Biol Sci Med Sci. 2013.

Labarca C, Paigen K. A simple, rapid, and sensitive DNA assay procedure. Anal Biochem. 102(2):344-52. 1980.

Laffargue P, Fialdes P, Frayssinet P, Rtaimate M, Hildebrand HF, Marchandise X. Adsorption and release of insulin-like growth factor-I on porous tricalcium phosphate implant. Journal of biomedical materials research. 49(3):415-21. 2000.

Landers R, Mülhaupt R. Desktop manufacturing of complex objects, prototypes and biomedical scaffolds by means of computer‐assisted design combined with computer‐guided 3D plotting of polymers and reactive oligomers. Macromol Mater Eng. 282(1):17-21. 2000.

Langenskiöld A. Surgical Treatment of Partial Closure of the Growth Plate. J Pediatr Orthoped. 1(1):3-11. 1981.

Langenskiöld A, Österman K, Valle M. Growth of fat grafts after operation for partial bone growth arrest: demonstration by computed tomography scanning. J Pediatr Orthoped. 7(4):389-94. 1987.

Laurencin C, Attawia M, Lu L, Borden M, Lu H, Gorum W, Lieberman J. Poly (lactide-co-glycolide)/hydroxyapatite delivery of BMP-2-producing cells: a regional gene therapy approach to bone regeneration. Biomaterials. 22(11):1271-7. 2001.

Laurencin CT, Attawia MA, Elgendy HE, Herbert KM. Tissue engineered bone-regeneration using degradable polymers: the formation of mineralized matrices. Bone. 19(1):S93-S9. 1996.

Lawrence DA, Pircher R, Jullien P. Conversion of a high molecular weight latent beta-TGF from chicken embryo fibroblasts into a low molecular weight active beta-TGF under acidic conditions. Biochem Biophys Res Commun. 133(3):1026-34. 1985.

Lee CR, Grodzinsky AJ, Spector M. The effects of cross-linking of collagen-glycosaminoglycan scaffolds on compressive stiffness, chondrocyte-mediated contraction, proliferation and biosynthesis. Biomaterials. 22(23):3145-54. 2001.

Lee E, Gao G, Bose K. Management of partial growth arrest: physis, fat, or silastic? J Pediatr Orthoped. 13(3):368-72. 1993.

Lee EH, Chen F, Chan J, Bose K. Treatment of Growth Arrest by Transfer of Cultured Chondrocytes into Physeal Defects. J Pediatr Orthoped. 18(2):155-60. 1998.

Lee SJ, Lee IW, Lee YM, Lee HB, Khang G. Macroporous biodegradable natural/synthetic hybrid scaffolds as small intestine submucosa impregnated poly (D, L-lactide-co-glycolide) for tissue-engineered bone. J Biomater Sci Polym Ed. 15(8):1003-17. 2004.

Lennox DW, Goldner RD, Sussman MD. Cartilage as an Interposition Material to Prevent Transphyseal Bone Bridge Formation: An Experimental Model. J Pediatr Orthoped. 3(2):207-10. 1983.

Li J, Yoon ST, Hutton WC. Effect of bone morphogenetic protein-2 (BMP-2) on matrix production, other BMPs, and BMP receptors in rat intervertebral disc cells. J Spinal Disord Tech. 17(5):423-8. 2004.

Li L, Hui JH, Goh JC, Chen F, Lee EH. Chitin as a scaffold for mesenchymal stem cells transfers in the treatment of partial growth arrest. J Pediatr Orthop. 24(2):205-10. 2004.

Li X, An HS, Ellman M, Phillips F, Thonar EJ, Park DK, Udayakumar RK, Im H-J. The action of fibroblast growth factor-2 on the intervertebral disc. Arthritis Res Ther. 10(2):R48. 2008.

Liang-chang D, Qi Y, Hoffman AS. Controlled release of amylase from a thermal and pH-sensitive, macroporous hydrogel. J Controlled Release. 19(1–3):171-7. 1992.

Liao CJ, Chen CF, Chen JH, Chiang SF, Lin YJ, Chang KY. Fabrication of porous biodegradable polymer scaffolds using a solvent merging/particulate leaching method. J Biomed Mater Res. 59(4):676-81. 2002.

Liao SW, Lu X, Putnam AJ, Kassab GS. A novel time-varying poly lactic-co glycolic acid external sheath for vein grafts designed under physiological loading. Tissue Eng. 13(12):2855-62. 2007.

Lin C-C, Metters AT. Hydrogels in controlled release formulations: network design and mathematical modeling. Adv Drug Delivery Rev. 58(12):1379-408. 2006.

Linnes MP, Ratner BD, Giachelli CM. A fibrinogen-based precision microporous scaffold for tissue engineering. Biomaterials. 28(35):5298-306. 2007.

Liu H, Webster TJ. Mechanical properties of dispersed ceramic nanoparticles in polymer composites for orthopedic applications. Int J of Nanomedicine. 5299-313. 2010.

Liu X, Ma PX. Polymeric scaffolds for bone tissue engineering. Ann Biomed Eng. 32(3):477-86. 2004.

Lo H, Ponticiello MS, Leong KW. Fabrication of controlled release biodegradable foams by phase separation. Tissue Eng. 1(1):15-28. 1995.

Longobardi L, O'Rear L, Aakula S, Johnstone B, Shimer K, Chytil A, Horton WA, Moses HL, Spagnoli A. Effect of IGF-I in the chondrogenesis of bone marrow

mesenchymal stem cells in the presence or absence of TGF-beta signaling. J Bone Miner Res. 21(4):626-36. 2006.

Lotz JC, Gerhart TN, Hayes WC. Mechanical properties of trabecular bone from the proximal femur: a quantitative CT study. J Comput Assist Tomogr. 14(1):107-14. 1990.

Lowry J. Bone Regeneration and Repair: Biology and Clinical Applications. Ann R Coll Surg Engl. 88(3):334. 2006.

Lu HH, El-Amin SF, Scott KD, Laurencin CT. Three-dimensional, Bioactive, Biodegradable, Polymer–Bioactive Glass Composite Scaffolds with Improved Mechanical Properties Support Collagen Synthesis and Mineralization of Human Osteoblast-like Cells in vitro. J Biomed Mater Res. 64A(3):465-74. 2003.

Lu L, Garcia CA, Mikos AG. In vitro degradation of thin poly (DL‑lactic‑co‑glycolic acid) films. J Biomed Mater Res. 46(2):236-44. 1999.

Lu W, Park TG. Protein release from poly(lactic-co-glycolic acid) microspheres: protein stability problems. PDA J Pharm Sci Technol. 49(1):13-9. 1995.

Lyons RM, Keski-Oja J, Moses HL. Proteolytic activation of latent transforming growth factor-beta from fibroblast-conditioned medium. J Cell Biol. 106(5):1659-65. 1988.

Madry H, Kaul G, Cucchiarini M, Stein U, Zurakowski D, Remberger K, Menger M, Kohn D, Trippel S. Enhanced repair of articular cartilage defects in vivo by transplanted chondrocytes overexpressing insulin-like growth factor I (IGF-I). Gene Ther. 12(15):1171-9. 2005.

Makadia HK, Siegel SJ. Poly Lactic-co-Glycolic Acid (PLGA) as biodegradable controlled drug delivery carrier. Polymers. 3(3):1377-97. 2011.

Mao S, Xu J, Cai C, Germershaus O, Schaper A, Kissel T. Effect of WOW process parameters on morphology and burst release of FITC-dextran loaded PLGA microspheres. Int J Pharm. 334(1–2):137-48. 2007.

Martin I, Padera RF, Vunjak-Novakovic G, Freed LE. In vitro differentiation of chick embryo bone marrow stromal cells into cartilaginous and bone-like tissues. J Orthop Res. 16(2):181-9. 1998.

Martina M, Hutmacher DW. Biodegradable polymers applied in tissue engineering research: a review. Polym Int. 56(2):145-57. 2007.

Martinez MN, Amidon GL. A Mechanistic Approach to Understanding the Factors Affecting Drug Absorption: A Review of Fundamentals. J Clin Pharmacol. 42(6):620-43. 2002.

Mason JM, Breitbart AS, Barcia M, Porti D, Pergolizzi RG, Grande DA. Cartilage and Bone Regeneration Using Gene-Enhanced Tissue Engineering. Clin Orthop. 379S171-S8. 2000.

Masters KS, Shah DN, Leinwand LA, Anseth KS. Crosslinked hyaluronan scaffolds as a biologically active carrier for valvular interstitial cells. Biomaterials. 26(15):2517-25. 2005.

McCall JD, Anseth KS. Thiol-ene photopolymerizations provide a facile method to encapsulate proteins and maintain their bioactivity. Biomacromolecules. 13(8):2410-7. 2012.

McCarthy TL, Centrella M, Canalis E. Regulatory effects of insulin-like growth factors I and II on bone collagen synthesis in rat calvarial cultures. Endocrinology. 124(1):301-9. 1989.

McGee MA, Howie DW, Costi K, Haynes DR, Wildenauer CI, Pearcy MJ, McLean JD. Implant retrieval studies of the wear and loosening of prosthetic joints: a review. Wear. 241(2):158-65. 2000.

Meenach SA, Otu CG, Anderson KW, Hilt JZ. Controlled synergistic delivery of paclitaxel and heat from poly(β-amino ester)/iron oxide-based hydrogel nanocomposites. Int J Pharm. 427(2):177-84. 2012.

Meinel L, Illi OE, Zapf J, Malfanti M, Peter Merkle H, Gander B. Stabilizing insulin-like growth factor-I in poly(D,L-lactide-co-glycolide) microspheres. J Control Release. 70(1-2):193-202. 2001.

Meyer F, Wardale J, Best S, Cameron R, Rushton N, Brooks R. Effects of lactic acid and glycolic acid on human osteoblasts: A way to understand PLGA involvement in PLGA/calcium phosphate composite failure. J Orthop Res. 30(6):864-71. 2012.

Miao X, Tan LP, Tan LS, Huang X. Porous calcium phosphate ceramics modified with PLGA, bioactive glass. Mater Sci Eng C. 27(2):274-9. 2007.

Mikos AG, Sarakinos G, Leite SM, Vacant JP, Langer R. Laminated three-dimensional biodegradable foams for use in tissue engineering. Biomaterials. 14(5):323-30. 1993.

Mikos AG, Temenoff JS. Formation of highly porous biodegradable scaffolds for tissue engineering. Electron J Biotechn. 3(2):23-4. 2000.

Mikos AG, Thorsen AJ, Czerwonka LA, Bao Y, Langer R, Winslow DN, Vacanti JP. Preparation and characterization of poly (L-lactic acid) foams. Polymer. 35(5):1068-77. 1994.

Mizuta T, Benson W, Foster B, Morris L. Statistical analysis of the incidence of physeal injuries. J Pediatr Orthoped. 7(5):518-23. 1987.

Mooney DJ, Baldwin DF, Suh NP, Vacanti JP, Langer R. Novel approach to fabricate porous sponges of poly (D, L-lactic-co-glycolic acid) without the use of organic solvents. Biomaterials. 17(14):1417-22. 1996.

Morisset S, Frisbie DD, Robbins PD, Nixon AJ, McIlwraith CW. IL-1ra/IGF-1 gene therapy modulates repair of microfractured chondral defects. Clin Orthop Relat Res. 462221-8. 2007.

Muggli DS, Burkoth AK, Keyser SA, Lee HR, Anseth KS. Reaction behavior of biodegradable, photo-cross-linkable polyanhydrides. Macromolecules. 31(13):4120-5. 1998.

Nazarov R, Jin H-J, Kaplan DL. Porous 3-D Scaffolds from Regenerated Silk Fibroin. Biomacromolecules. 5(3):718-26. 2004.

Nehrer S, Breinan HA, Ramappa A, Young G, Shortkroff S, Louie LK, Sledge CB, Yannas IV, Spector M. Matrix collagen type and pore size influence behaviour of seeded canine chondrocytes. Biomaterials. 18(11):769-76. 1997.

Nettesheim P. Organ and Tissue Regeneration in Mammals. New York: MSS Information Corp.; 1972.

Nielsen HM, Andreassen TT, Ledet T, Oxlund H. Local injection of TGF-beta increases the strength of tibial fractures in the rat. Acta Orthop Scand. 65(1):37-41. 1994.

Nishida T, Kubota S, Kojima S, Kuboki T, Nakao K, Kushibiki T, Tabata Y, Takigawa M. Regeneration of defects in articular cartilage in rat knee joints by CCN2 (connective tissue growth factor). J Bone Miner Res. 19(8):1308-19. 2004.

Nishiyama N, Kataoka K. Current state, achievements, and future prospects of polymeric micelles as nanocarriers for drug and gene delivery. Pharmacol Ther. 112(3):630-48. 2006.

Nof M, Shea LD. Drug‐releasing scaffolds fabricated from drug‐loaded microspheres. J Biomed Mater Res. 59(2):349-56. 2002.

Nohe A, Hassel S, Ehrlich M, Neubauer F, Sebald W, Henis YI, Knaus P. The Mode of Bone Morphogenetic Protein (BMP) Receptor Oligomerization Determines Different BMP-2 Signaling Pathways. J Biol Chem. 277(7):5330-8. 2002.

Pan Q, Yu Y, Chen Q, Li C, Wu H, Wan Y, Ma J, Sun F. Sox9, a key transcription factor of bone morphogenetic protein-2-induced chondrogenesis, is activated through BMP pathway and a CCAAT box in the proximal promoter. J Cell Physiol. 217(1):228-41. 2008.

Pan Z, Ding J. Poly (lactide-co-glycolide) porous scaffolds for tissue engineering and regenerative medicine. Interface focus. 2(3):366-77. 2012.

Park A, Wu B, Griffith LG. Integration of surface modification and 3D fabrication techniques to prepare patterned poly (L-lactide) substrates allowing regionally selective cell adhesion. J Biomater Sci Polym Ed. 9(2):89-110. 1998.

Pateder DB, Ferguson CM, Ionescu AM, Schwarz EM, Rosier RN, Puzas JE, O'Keefe RJ. PTHrP expression in chick sternal chondrocytes is regulated by TGF-beta through Smad-mediated signaling. J Cell Physiol. 188(3):343-51. 2001.

Patel ZS, Young S, Tabata Y, Jansen JA, Wong MEK, Mikos AG. Dual delivery of an angiogenic and an osteogenic growth factor for bone regeneration in a critical size defect model. Bone. 43(5):931-40. 2008.

Pattison MA, Wurster S, Webster TJ, Haberstroh KM. Three-dimensional, nano-structured PLGA scaffolds for bladder tissue replacement applications. Biomaterials. 26(15):2491-500. 2005.

Pfeifer BA, Burdick JA, Little SR, Langer R. Poly (ester-anhydride): poly (β-amino ester) micro-and nanospheres: DNA encapsulation and cellular transfection. Int J Pharm. 304(1):210-9. 2005.

Pittenger MF, Mackay AM, Beck SC, Jaiswal RK, Douglas R, Mosca JD, Moorman MA, Simonetti DW, Craig S, Marshak DR. Multilineage potential of adult human mesenchymal stem cells. Science. 284(5411):143-7. 1999.

Planka L, Gal P, Kecova H, Klima J, Hlucilova J, Filova E, Amler E, Krupa P, Kren L, Srnec R, et al. Allogeneic and autogenous transplantations of MSCs in treatment of the physeal bone bridge in rabbits. BMC Biotechnol. 870. 2008.

Pond SM, Tozer TN. First-pass elimination. Basic concepts and clinical consequences. Clin Pharmacokinet. 9(1):1-25. 1984.

Popp JR, Laflin KE, Love BJ, Goldstein AS. Fabrication and characterization of poly(lactic-co-glycolic acid) microsphere/amorphous calcium phosphate scaffolds. J Tissue Eng Regen Med. 6(1):12-20.

Prasad S, Cody V, Hanlon D, Edelson RL, Saltzman M, Sasaki CT, Birchall MA. Biopolymer nanoparticles as antigen delivery vehicles for immunotherapy of head and neck squamous cell carcinoma (HNSCC). Clin Otolaryngol. (3):304-. 2008.

Raghuvanshi RS, Singh M, Talwar GP. Biodegradable delivery system for single step immunization with tetanus toxoid. Int J Pharm. 93(1–3):R1-R5. 1993.

Rajamannan NM, Subramaniam M, Rickard D, Stock SR, Donovan J, Springett M, Orszulak T, Fullerton DA, Tajik A, Bonow RO. Human aortic valve calcification is associated with an osteoblast phenotype. Circulation. 107(17):2181-4. 2003.

Ratner BD, Hoffman AS, Schoen FJ, Lemons JE. An introduction to materials in medicine. Biomaterials Science. 484. 1996.

Ravi N. Regeneration of Damaged Grwoth Plate Using IGF-I Plasmid-Releasing Porous PLGA Scaffolds University of Kentucky; 2009.

Rhee SH, Lee SJ. Effect of acidic degradation products of poly(lactic-co-glycolic)acid on the apatite-forming ability of poly(lactic-co-glycolic)acid-siloxane nanohybrid material. J Biomed Mater Res A. 83(3):799-805. 2007.

Ricci M, Blasi P, Giovagnoli S, Rossi C, Macchiarulo G, Luca G, Basta G, Calafiore R. Ketoprofen controlled release from composite microcapsules for cell encapsulation: Effect on post-transplant acute inflammation. J Controlled Release. 107(3):395-407. 2005.

Richardson TP, Peters MC, Ennett AB, Mooney DJ. Polymeric system for dual growth factor delivery. Nat Biotechnol. 19(11):1029-34. 2001.

Riew K, Wright N, Cheng S-L, Avioli L, Lou J. Induction of bone formation using a recombinant adenoviral vector carrying the human BMP-2 gene in a rabbit spinal fusion model. Calcif Tissue Int. 63(4):357-60. 1998.

Rosen HB, Chang J, Wnek G, Linhardt R, Langer R. Bioerodible polyanhydrides for controlled drug delivery. Biomaterials. 4(2):131-3. 1983.

Rotello RJ, Lieberman RC, Purchio AF, Gerschenson LE. Coordinated regulation of apoptosis and cell proliferation by transforming growth factor beta 1 in cultured uterine epithelial cells. Proc Natl Acad Sci. 88(8):3412-5. 1991.

Sachlos E, Czernuszka J. Making tissue engineering scaffolds work. Review: the application of solid freeform fabrication technology to the production of tissue engineering scaffolds. Eur Cell Mater. 5(29):39-40. 2003.

Sakimura K, Matsumoto T, Miyamoto C, Osaki M, Shindo H. Effects of insulin-like growth factor I on transforming growth factor β1 induced chondrogenesis of synovium-derived mesenchymal stem cells cultured in a polyglycolic acid scaffold. Cells Tissues Organs. 183(2):55-61. 2006.

Satterwhite JH, Boudinot FD. Pharmacokinetics of ketoprofen in rats: Effect of age and dose. Biopharm Drug Dispos. 13(3):197-212. 1992.

Schinagl RM, Gurskis D, Chen AC, Sah RL. Depth-dependent confined compression modulus of full-thickness bovine articular cartilage. J Orthop Res. 15(4):499-506. 1997.

112

Schmid C. Insulin-like growth factors. Cell Biol Int. 19445-58. 1995.

Schmitt EE, Polistina RA. Surgical Sutures. In: Company AC, editor.1967.

Schoenle E, Zapf J, Hauri C, Steiner T, Froesch E. Comparison of in vivo effects of insulin-like growth factors I and II and of growth hormone in hypophysectomized rats. Acta Endocrinol (Copenh). 108(2):167-74. 1985.

Schugens C, Maquet V, Grandfils C, Jérôme R, Teyssie P. Polylactide macroporous biodegradable implants for cell transplantation. II. Preparation of polylactide foams by liquid‐liquid phase separation. J Biomed Mater Res. 30(4):449-61. 1996.

Schwarz C, Wulsten D, Ellinghaus A, Lienau J, Willie BM, Duda GN. Mechanical load modulates the stimulatory effect of BMP2 in a rat nonunion model. Tissue Eng Part A. 19(1-2):247-54. 2013.

Schwendeman SP. Recent advances in the stabilization of proteins encapsulated in injectable PLGA delivery systems. Crit Rev Ther Drug Carrier Syst. 19(1):73-98. 2002.

Scott C. Apparatus and method for creating three-dimensional objects. In: Patent U, editor.1991.

Sekiya I, Larson BL, Vuoristo JT, Reger RL, Prockop DJ. Comparison of effect of BMP-2,-4, and-6 on in vitro cartilage formation of human adult stem cells from bone marrow stroma. Cell Tissue Res. 320(2):269-76. 2005.

Sergerie K, Lacoursiere MO, Levesque M, Villemure I. Mechanical properties of the porcine growth plate and its three zones from unconfined compression tests. J Biomech. 42(4):510-6. 2009.

Shea LD, Wang D, Franceschi RT, Mooney DJ. Engineered bone development from a pre-osteoblast cell line on three-dimensional scaffolds. Tissue Eng. 6(6):605-17. 2000.

Shefelbine SJ, Augat P, Claes L, Simon U. Trabecular bone fracture healing simulation with finite element analysis and fuzzy logic. J Biomech. 38(12):2440-50. 2005.

Shen B, Wei A, Whittaker S, Williams LA, Tao H, Ma DD, Diwan AD. The role of BMP-7 in chondrogenic and osteogenic differentiation of human bone marrow multipotent mesenchymal stromal cells in vitro. J Cell Biochem. 109(2):406-16.

Shenoy D, Little S, Langer R, Amiji M. Poly (ethylene oxide)-modified poly (β-amino ester) nanoparticles as a pH-sensitive system for tumor-targeted delivery of hydrophobic drugs: part 2. In vivo distribution and tumor localization studies. Pharm Res. 22(12):2107-14. 2005.

Sherwood JK, Riley SL, Palazzolo R, Brown SC, Monkhouse DC, Coates M, Griffith LG, Landeen LK, Ratcliffe A. A three-dimensional osteochondral composite scaffold for articular cartilage repair. Biomaterials. 23(24):4739-51. 2002.

Shin HJ, Lee CH, Cho IH, Kim YJ, Lee YJ, Kim IA, Park KD, Yui N, Shin JW. Electrospun PLGA nanofiber scaffolds for articular cartilage reconstruction: mechanical stability, degradation and cellular responses under mechanical stimulation in vitro. J Biomater Sci Polym Ed. 17(1-2):103-19. 2006.

Shive MS, Anderson JM. Biodegradation and biocompatibility of PLA and PLGA microspheres. Adv Drug Deliv Rev. 28(1):5-24. 1997.

Slaughter BV, Khurshid SS, Fisher OZ, Khademhosseini A, Peppas NA. Hydrogels in regenerative medicine. Adv Mater. 21(32-33):3307-29. 2009.

Solheim E, Pinholt EM, Bang G, Sudmann E. Regeneration of calvarial defects by a composite of bioerodible polyorthoester and demineralized bone in rats. J Neurosurg. 76(2):275-9. 1992.

Stein D, Lee Y, Schmid MJ, Killpack B, Genrich MA, Narayana N, Marx DB, Cullen DM, Reinhardt RA. Local simvastatin effects on mandibular bone growth and inflammation. J Periodontol. 76(11):1861-70. 2005.

Steinemann SG. Metal implants and surface reactions. Injury. 27, Supplement 3(0):S/C16-S/C22. 1996.

Sundararaj SC, Thomas MV, Peyyala R, Dziubla TD, Puleo DA. Design of a multiple drug delivery system directed at periodontitis. Biomaterials. 2013.

Sundararaj SK, Cieply RD, Gupta G, Milbrandt TA, Puleo DA. Treatment of growth plate injury using IGF-I-loaded PLGA scaffolds. J Tissue Eng Regen Med. 2012.

Tabata Y. The importance of drug delivery systems in tissue engineering. Pharm Sci Technol To. 3(3):80-9. 2000.

Tabata Y, Takebayashi Y, Ueda T, Ikada Y. A formulation method using D, L-lactic acid oligomer for protein release with reduced initial burst. J Controlled Release. 23(1):55-63. 1993.

Temenoff JS, Mikos AG. Review: tissue engineering for regeneration of articular cartilage. Biomaterials. 21(5):431-40. 2000.

Thomson RC, Yaszemski MJ, Powers JM, Mikos AG. Fabrication of biodegradable polymer scaffolds to engineer trabecular bone. J Biomater Sci Polym Ed. 7(1):23-38. 1996.

Tiţa D, Fuliaş A, Tiţa B. Thermal stability of ketoprofen—active substance and tablets. J Therm Anal Calorim. 105(2):501-8. 2011.

Tobita M, Ochi M, Uchio Y, Mori R, Iwasa J, Katsube K, Motomura T. Treatment of growth plate injury with autogenous chondrocytes: a study in rabbits. Acta Orthop Scand. 73(3):352-8. 2002.

Törmälä P, Pohjonen T, Rokkanen P. Bioabsorbable polymers: materials technology and surgical applications. Proc Inst Mech Eng H J Eng Med. 212(2):101-11. 1998.

Tracy MA, Ward KL, Firouzabadian L, Wang Y, Dong N, Qian R, Zhang Y. Factors affecting the degradation rate of poly(lactide-co-glycolide) microspheres in vivo and in vitro. Biomaterials. 20(11):1057-62. 1999.

Uematsu K, Hattori K, Ishimoto Y, Yamauchi J, Habata T, Takakura Y, Ohgushi H, Fukuchi T, Sato M. Cartilage regeneration using mesenchymal stem cells and a three-dimensional poly-lactic-glycolic acid (PLGA) scaffold. Biomaterials. 26(20):4273-9. 2005.

Uhrich KE, Cannizzaro SM, Langer RS, Shakesheff KM. Polymeric systems for controlled drug release. Chem Rev. 99(11):3181-98. 1999.

Van de Witte P, Dijkstra P, Van den Berg J, Feijen J. Phase separation processes in polymer solutions in relation to membrane formation. J Membr Sci. 117(1):1-31. 1996.

114

Van der Kraan P, Buma P, Van Kuppevelt T, Van den Berg W. Interaction of chondrocytes, extracellular matrix and growth factors: relevance for articular cartilage tissue engineering. Osteoarthritis Cartilage. 10(8):631-7. 2002.

Van Tienen TG, Heijkants RG, Buma P, de Groot JH, Pennings AJ, Veth RP. Tissue ingrowth and degradation of two biodegradable porous polymers with different porosities and pore sizes. Biomaterials. 23(8):1731-8. 2002.

Veilleux N, Spector M. Effects of FGF-2 and IGF-1 on adult canine articular chondrocytes in type II collagen–glycosaminoglycan scaffolds in vitro. Osteoarthr Cartilage. 13(4):278-86. 2005.

Vreven J, Lieberherr M, Vaes G. The acid and alkaline phosphatases, inorganic pyrophosphatases and phosphoprotein phosphatase of bone. II. Distribution in subcellular fractions of bone tissue homogenates and structure-linked latency. Biochim Biophys Acta. 293(1):170-7. 1973.

Wake MC, Gupta PK, Mikos AG. Fabrication of pliable biodegradable polymer foams to engineer soft tissues. Cell Transplant. 5(4):465-73. 1996.

Wang EA, Rosen V, D'Alessandro JS, Bauduy M, Cordes P, Harada T, Israel DI, Hewick RM, Kerns KM, LaPan P. Recombinant human bone morphogenetic protein induces bone formation. Proc Natl Acad Sci. 87(6):2220-4. 1990.

Wang L, Zhang X, Guo Y, Chen X, Li R, Liu L, Shi C, Guo C, Zhang Y. Involvement of BMPs/Smad signaling pathway in mechanical response in osteoblasts. Cell Physiol Biochem. 26(6):1093-102. 2011.

Wattenbarger JM, Gruber HE, Phieffer LS. Physeal fractures, part I: histologic features of bone, cartilage, and bar formation in a small animal model. J Pediatr Orthop. 22(6):703-9. 2002.

Weinreb M, Shinar D, Rodan GA. Different pattern of alkaline phosphatase, osteopontin, and osteocalcin expression in developing rat bone visualized by in situ hybridization. Journal of bone and mineral research : the official journal of the American Society for Bone and Mineral Research. 5(8):831-42. 1990.

Weng CY, Kothary PC, Verkade AJ, Reed DM, Del Monte MA. MAP kinase pathway is involved in IGF-1-stimulated proliferation of human retinal pigment epithelial cells (hRPE). Curr Eye Res. 34(10):867-76. 2009.

Westra A, Dewey WC. Variation in Sensitivity to Heat Shock during the Cell-cycle of Chinese Hamster Cells in Vitro. Int J Radiat Biol. 19(5):467-77. 1971.

Whang K, Thomas C, Healy K, Nuber G. A novel method to fabricate bioabsorbable scaffolds. Polymer. 36(4):837-42. 1995.

Whang K, Tsai D, Nam E, Aitken M, Sprague S, Patel P, Healy K. Ectopic bone formation via rhBMP‐2 delivery from porous bioabsorbable polymer scaffolds. J Biomed Mater Res. 42(4):491-9. 1998.

Willie BM, Petersen A, Schmidt-Bleek K, Cipitria A, Mehta M, Strube P, Lienau J, Wildemann B, Fratzl P, Duda G. Designing biomimetic scaffolds for bone regeneration: why aim for a copy of mature tissue properties if nature uses a different approach? Soft Matter. 6(20):4976-87. 2010.

Winkler L, Müller R, Wiemann M. Heat-treated BMP-2 depots release BMP-2 in its bioactive form. Materialwiss Werkst. 37(6):436-40. 2006.

Wu L, Ding J. In vitro degradation of three-dimensional porous poly(d,l-lactide-co-glycolide) scaffolds for tissue engineering. Biomaterials. 25(27):5821-30. 2004.

Wu L, Zhang J, Jing D, Ding J. "Wet-state" mechanical properties of three-dimensional polyester porous scaffolds. J Biomed Mater Res A. 76A(2):264-71. 2006.

Wu XS, Wang N. Synthesis, characterization, biodegradation, and drug delivery application of biodegradable lactic/glycolic acid polymers. Part II: Biodegradation. J Biomater Sci Polym Ed. 12(1):21-34. 2001.

Xian CJ, Zhou FH, McCarty RC, Foster BK. Intramembranous ossification mechanism for bone bridge formation at the growth plate cartilage injury site. J Orthop Res. 22(2):417-26. 2004.

Yadav JK, Prakash V. Thermal Atability of Alpha-Amylase in Aqueous Cosolvent Systems. J Biosci. 34(3):377-87. 2009.

Yang Y, Tang G, Zhang H, Zhao Y, Yuan X, Wang M, Yuan X. Controllable dual-release of dexamethasone and bovine serum albumin from PLGA/beta-tricalcium phosphate composite scaffolds. J Biomed Mater Res B Appl Biomater. 96(1):139-51. 2011.

Yang Y-Y, Chia H-H, Chung T-S. Effect of preparation temperature on the characteristics and release profiles of PLGA microspheres containing protein fabricated by double-emulsion solvent extraction/evaporation method. J Controlled Release. 69(1):81-96. 2000.

Yang Y-Y, Chung T-S, Ping Ng N. Morphology, drug distribution, and in vitro release profiles of biodegradable polymeric microspheres containing protein fabricated by double-emulsion solvent extraction/evaporation method. Biomaterials. 22(3):231-41. 2001.

Yannas I. Tissue regeneration by use of collagen-glycosaminoglycan copolymers. Clin Mater. 9(3):179-87. 1992.

Yeo Y, Baek N, Park K. Microencapsulation methods for delivery of protein drugs. Biotechnol Bioprocess Eng. 6(4):213-30. 2001.

Yoon SJ, Park KS, Kim MS, Rhee JM, Khang G, Lee HB. Repair of diaphyseal bone defects with calcitriol-loaded PLGA scaffolds and marrow stromal cells. Tissue Eng. 13(5):1125-33. 2007.

Yun Z, Y., Zhang H, P., Cai X, Z., Wang A, P., Zhang L, B. Kinetic and thermodynamic studies on the thermal denaturation of bovine milk insulin-like growth factor-I in model systems. Lait. 87(2):139-48. 2007.

Zeiter S, Lezuo P, Ito K. Effect of TGF β1, BMP-2 and hydraulic pressure on chondrogenic differentiation of bovine bone marrow mesenchymal stromal cells. Biorheology. 46(1):45-55. 2009.

Zhang Y, Chan HF, Leong KW. Advanced materials and processing for drug delivery: The past and the future. Adv Drug Delivery Rev. 65(1):104-20. 2013.

Zhang Y, Zhang M. Synthesis and characterization of macroporous chitosan/calcium phosphate composite scaffolds for tissue engineering. J Biomed Mater Res. 55(3):304-12. 2001.

Zolnik BS, Burgess DJ. Evaluation of in vivo in vitro release of dexamethasone from PLGA microspheres. J Controlled Release. 127(2):137-45. 2008.

116

PERSONAL INFORMATION

Place of Birth: Denver, Colorado, United States of America

EDUCATION

Rochester Institute of Technology, Rochester, New York, May 2008

B.S. Mechanical Engineering

RESEARCH EXPERIENCE

National Science Foundation IGERT Graduate Trainee

University of Kentucky, Lexington, KY, June 2009 – present

Advisors: Dr. D. A. Puleo, Department of Biomedical Engineering, Dr. J. Z. Hilt, Chemical & Materials Engineering

AWARDS AND HONORS

- NSF-IGERT Fellow (June 2009 – present)
- Society for Biomaterials Orthopaedic Biomaterials Special Interest Group (ORT SIG) award of merit poster presentation (April 2013)

PRESENTATIONS

- A. Clark, Z. Hilt, D. Puleo, "Comparison of degradation, modulus and pore size of poly(lactic-co-glycolic acid)", Society for Biomaterials Conference, San Antonio (April 2009)- Poster presentation.
- A. Clark, Z. Hilt, D. Puleo, "Tailoring Properties of Microsphere-Based Poly(lactic-co-glycolic acid) Scaffolds", Society for Biomaterials Conference, Seattle, WA (April 2010)- Poster presentation.
- A. Clark, Z. Hilt, D. Puleo, "Tailoring Properties of Microsphere-based Poly(lactic-co-glycolic acid) Scaffolds", Biomaterials Day, Cleveland, OH (November 2010). Oral presentation.

117

- A. Clark, Z. Hilt, D. Puleo, "Effect of Processing Temperature on Poly(lactic-co-glycolic acid) Scaffold Properties and Bioactivity of Insulin-like Growth Factor I", Society for Biomaterials Conference, Orlando, FL (April 2011)- Poster presentation.

- A. Clark, Z. Hilt, D. Puleo, "Effect of Processing Temperature on Poly(lactic-co-glycolic acid) Scaffold Properties and Bioactivity of Insulin-like Growth Factor I", Biomaterials Day, Purdue University (October 2011). Poster presentation.

- A. Clark, Z. Hilt, D. Puleo, "Effect of Processing Temperature on Poly(lactic-co-glycolic acid) Scaffold Properties and Bioactivity of Insulin-like Growth Factor I", Biomaterials Day, Memphis, TN (February 2012). Oral presentation.

- A. Clark, Z. Hilt, D. Puleo, "The Effect of Adding a Hydrogel Porogen into a Poly(lactic-co-glycolic acid) Scaffold", Society for Biomaterials Conference, Boston, MA (April 2012)- Poster presentation.

- IGERT: 2012 Poster and Video Competition

- A. Clark, Z. Hilt, D. Puleo, "Sustained Release of Protein Loaded in a Biodegradable Polymeric Scaffolds for Growth Plate Regeneration", Controlled Release Society Conference, Honolulu, HI (July 2013)- Poster presentation.

PUBLICATIONS

- Amanda R. Clark, Todd A. Milbrandt, David A. Puleo, and J. Zach Hilt, Treatment to Regenerate the Proximal Tibia Growth Plate after Injury Using a Poly(lactic-co-glycolic acid) Based Scaffold. In preparation for submission.

- Amanda R. Clark, Todd A. Milbrandt, David A. Puleo, and J. Zach Hilt, Retention of Insulin-like Growth Factor I Bioactivity during Fabrication of Sintered Polymeric Scaffolds. Biomedical Materials. Submitted.

- Amanda R. Clark, Todd A. Milbrandt, David A. Puleo, and J. Zach Hilt, Mechanical Properties and Dual Drug Delivery Application of PLGA Scaffolds Fabricated with a Polyβ-amino ester) Porogen, Acta Biomaterialia, 2013. Submitted.

- Amanda R. Clark, Todd A. Milbrandt, David A. Puleo, and J. Zach Hilt, Tailoring properties of microsphere-based poly(lactic-*co*-glycolic acid) scaffolds. Journal of Biomedical Materials Research Part A, 2013.